gear
TECHNOLOGY®

MAR/APR
2018

HEAT TREATING

INDUCTION HARDENING
PUSHING BOUNDARIES
HOT NEWS

INTELLIGENT WORKHOLDING

www.geartechnology.com

THE JOURNAL OF GEAR MANUFACTURING


G 500 H
SAMPUTENSILI
SU

gear TECHNOLOGY®

contents

MAR/APR 2018

30

24

features

technical

Vol. 35, No. 2 GEAR TECHNOLOGY, The Journal of Gear Manufacturing (ISSN 0743-6858) is published monthly, except in February, April, October and December by Randall Publications LLC, 1840 Jarvis Avenue, Elk Grove Village, IL 60007, (847) 437-6604. Cover price $7.00 U.S. Periodical postage paid at Arlington Heights, IL, and at additional mailing office (USPS No. 749-290). Randall Publications makes every effort to ensure that the processes described in GEAR TECHNOLOGY conform to sound engineering practice. Neither the authors nor the publisher can be held responsible for injuries sustained while following the procedures described. Postmaster: Send address changes to GEAR TECHNOLOGY, The Journal of Gear Manufacturing, 1840 Jarvis Avenue, Elk Grove Village, IL, 60007. Contents copyrighted ©2017 by RANDALL PUBLICATIONS LLC. No part of this publication may be reproduced or transmitted in any form or by any means, electronic or mechanical, including photocopying, recording, or by any information storage and retrieval system, without permission in writing from the publisher. Contents of ads are subject to Publisher's approval. Canadian Agreement No. 40038760.

Your future is already on your shop floor. Will you invest in them?


Joe Arvin, President
Arvin Global Solutions


Geoff Ashcroft
Gear Consulting Group
Manufacturing

In manufacturing, a workforce armed with deep technical knowledge is critical to success. But as the older generation leaves the workforce, their departure creates a knowledge gap. Helping you transform your most ambitious young talent into your future experts is what the **AGS Manufacturing Training Series** is all about.

Your best and brightest deserve nothing less than the finest in guidance and training. It is why we have assembled a coalition of the industry's top experts who want to share their knowledge with the next generation. Spanning a comprehensive range of technical disciplines, our experts will prepare your talent to be the experts of tomorrow. Sign up today to take advantage of these unique learning opportunities and gain access to decades of real-world experience. Your company's future stars deserve the best, and the **AGS Manufacturing Training Series** can deliver.

The AGS Manufacturing Training Series

NEW SEMINAR SCHEDULE

Spring 2018

May 1-3: Introduction to Gear Process Engineering

May 22-24: Advanced Methods and Best Practices for Gear Process Engineering

June 12: An In-Depth Study of the Causes and Prevention of Grinding Damage


Arvid Casler
Northstar Aerospace
Heat Treatment


Kevin Walsh
Overton Chicago Gear (Ret.)
Manufacturing


Ray Drago
Drive Systems Technology, Inc.
Gear System Consulting
& Forensic Analyses


Al Swiglo
Swiglo Metallurgical Consulting
Metallurgy

To learn more, please visit our Website at www.ArvinGlobalSolutions.com


Len Haas
Rolls Royce (Ret.)
Gearbox Design


The AGS Manufacturing Training Series Seminars are held at the Northern Illinois University Conference Center in Naperville, Illinois.


Mike Steele
Northstar Aerospace
NDT Specialist


Mark McVea
KBE+, Inc.
Gear Design


Rick Miller
Innovative Drive Solutions
Gearbox Design


Matt Mondek
Mondek Solutions
Manufacturing


Bruce Roberge
The Quote Machine
Manufacturing


Chuck Schultz
Beyta Gear Service
Gearbox Design

The AGS
Manufacturing Training
Series

ARVIN
Global Solutions
Manufacturing Excellence for the World Market

www.ArvinGlobalSolutions.com

Contact@ArvinGlobalSolutions.com • 1808 Ogden Ave., Lisle, IL 60532 • 800-815-2303

gear TECHNOLOGY®
Vol. 35, No. 2

departments

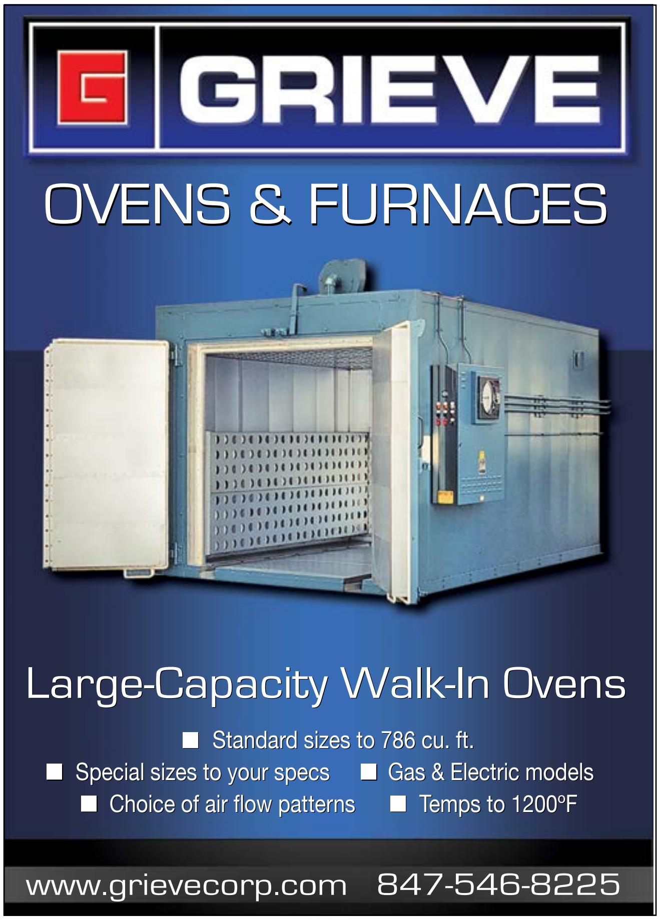

Cover image courtesy of Inductoheat

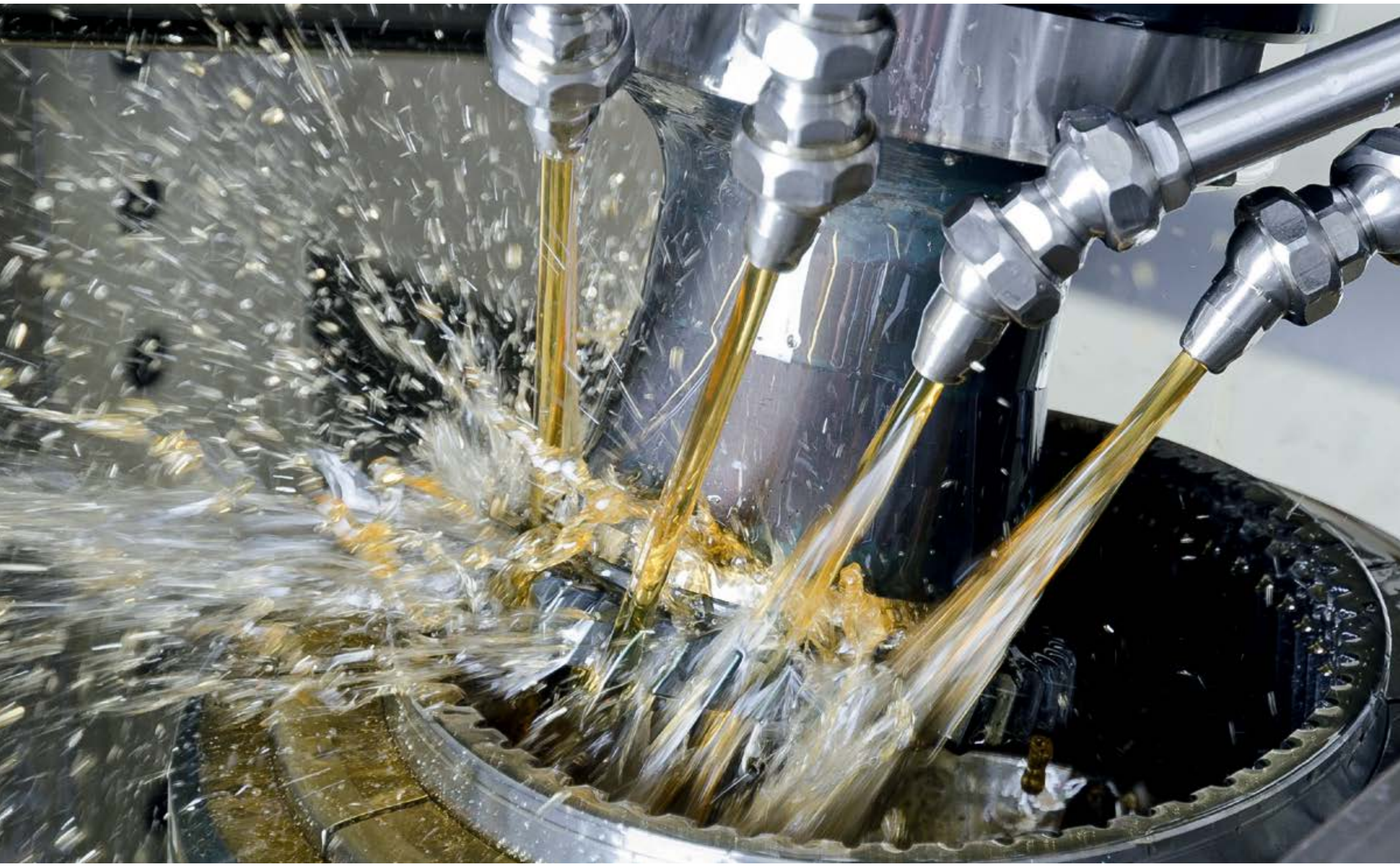

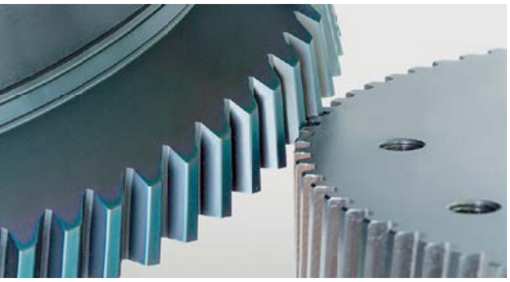

THE GEAR INDUSTRY'S INFORMATION SOURCE

www.geartechnology.com

Heimatec Spline Cutting

This video on spline cutting features Heimatec tooling with Hainbuch's TOPlus hexagonal collet chuck. Learn more at *www.geartechnology.com/videos/Heimatec-Spline-Cutting-/*

Gear Talk with Chuck

Charles Schultz looks at the basics in recent blog entries such as "Bevel Buzzwords" and "What About Worms?" Learn more at *www.geartechnology.com/blog/*.

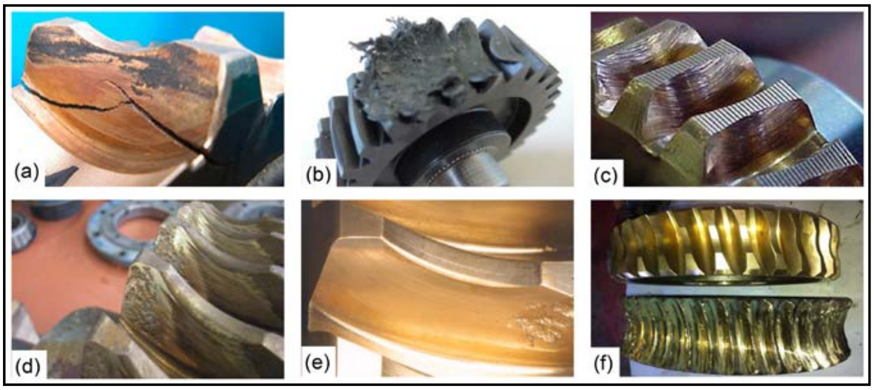

Event Spotlight: CTI Symposium USA

This event, organized by the German Car Training Institute (CTI), focuses on the latest technical innovations in automotive transmissions, hybrid and alternative drivetrains with experts and suppliers from the United States, Asia and Europe. Learn more at *www.geartechnology.com/news/8769/CTI_Symposium_USA/*.

Stay Connected

Join the *Gear Technology* Facebook group at *www.facebook.com/groups/210890932629794/*

Follow us on Twitter *twitter.com/#!/Gear_Technology*

Connect with us on LinkedIn *www.linkedin.com/groups/Gear-Technology-Magazine-3893880*

Subscribe Online *www.geartechnology.com/subscribe.htm*

gear TECHNOLOGY

RANDALL PUBLICATIONS LLC
1840 JARVIS AVENUE
ELK GROVE VILLAGE, IL 60007
(847) 437-6604
FAX: (847) 437-6618

EDITORIAL

Publisher & Editor-in-Chief
Michael Goldstein
publisher@geartechnology.com

Associate Publisher & Managing Editor
Randy Stott
wrs@geartechnology.com

Senior Editor
Jack McGuinn
jmcguinn@geartechnology.com

Senior Editor
Matthew Jaster
mjaster@geartechnology.com

Associate Editor
Alex Cannella
alex@geartechnology.com

Editorial Consultant
Paul R. Goldstein

Technical Editors
William (Bill) Bradley, Robert Errichello, Octave Labath, P.E., John Lange, Joseph Mihelick, Charles D. Schultz, P.E., Robert E. Smith, Mike Tennutti, Frank Uherek

DESIGN

Art Director
David Ropinski
dropinski@geartechnology.com

ADVERTISING

Associate Publisher & Advertising Sales Manager
Dave Friedman
dave@geartechnology.com

Materials Coordinator
Dorothy Fiandaca
dee@randallpublications.com

China Sales Agent
Eric Wu, Eastco Industry Co., Ltd.
Tel: (86)(21) 52305107
Fax: (86)(21) 52305106
Cell: (86) 13817160576
eric.wu@eastcotec.com

CIRCULATION

Circulation Manager
Carol Tratar
subscribe@geartechnology.com

Circulation Coordinator
Barbara Novak
bnovak@geartechnology.com

RANDALL STAFF

President
Michael Goldstein

Accounting
Luann Harrold

BPA WORLDWIDE℠ BUSINESS

The Reality of Having it all

Quality Production Without Compromise

Having it all should not be just a dream. With Mitsubishi's new for 2011 ZE40A gear grinding machine, it is a reality.

Mitsubishi has built a reputation for providing the job shops of America with flexible and accurate gear hobbing, shaping and shaving machines for finishing or roughing gears in their soft state. Now with the ZE40A, they introduce a flexible gear grinder that fulfills the needs of customers who require accurate gears in their hard state. The ZE40A delivers a complete and comprehensive package that requires little or no additional options.
The full circle of features include:

- **Single index form and Multi-Start Generating grinding of gears up to 400mm diameter**
- **Swing away tailstock arm for ease of loading heavy parts**
- **Integrated onboard inspection**
- **Integrated CNC dressing**
- **Integrated automatic meshing**
- **Integrated automatic wheel balancing**
- **Automatic bias adjustment**
- **Automatic pressure angle adjustment**
- **400mm axial travel for grinding shaft gears**

To personally experience the world-class performance of the Mitsubishi ZE40A visit **mitsubishigearcenter.com** or contact sales **248-669-6136**.

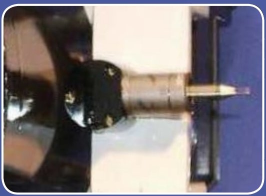
MEASURE

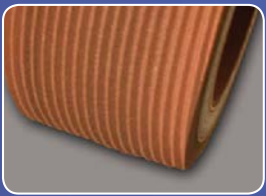
DRESS


GRIND

MITSUBISHI
HEAVY INDUSTRIES AMERICA, INC.

Machine Tool Division / Gear Technology Center • 46992 Liberty Drive • Wixom, MI 48393 • **mitsubishigearcenter.com**

Why Aren't You Training the Next Generation?

Publisher & Editor-in-Chief
Michael Goldstein

Last issue, when I went over the results from our annual State of the Gear Industry survey, I was being too nice. Sure, there's still a lot of optimism about the business climate. Gear manufacturers are mostly busy. For most, 2018 looks like it will be at least a little better than 2017. But there are dark clouds ahead, and they've been building for some time.

I'm talking about the skilled workforce crisis.

This is a problem that isn't going away. If anything, the rumblings keep getting louder and louder. By far, the single most important issue our survey highlighted was the gear industry's overwhelming need for trained workers.

Every year, the gripe is the same: we need skilled labor.

But the surprising thing is how few of you are actually doing something about it. According to our survey, more than half of you work at companies that don't take advantage of the gear-related training that's available.

More than half? Can this be true? Something doesn't add up. You're all suffering from the same problem. There aren't enough qualified people to do the work you need. But if there aren't enough people with the right skills, don't you need to figure out a way to train them?

The alternative is for your companies to slowly die.

There are a lot of options out there. The AGMA continues to expand its educational mission, offering more types of training and more ways to take advantage of it. They've added two new courses this year and have plans to add more next year, so no matter what type of training you need, chances are, they have it. Recently, they've also announced that AGMA's education programs are now accredited with the IACET – meaning that all AGMA classes now offer continuing education credits that count toward professional engineer and other certification programs. Please visit *www.agma.org* to see what's available.

Last issue, I also mentioned the seminars being offered by Arvin Global Solutions. Most of you feel that practical, hands-on manufacturing training is what you need most. Well, that's the whole idea behind what AGS is doing. Their seminars focus on process engineering and manufacturing best practices. Their instructors have decades of industry experience, and their goal is to transfer some of that well-earned experience to your employees. If you want your employees to understand the decision making processes that take place on a gear manufacturing plant floor, then take a look at the AGS ad on page 3 for a schedule of upcoming seminars and a roster of their experts.

As the publisher of the industry's leading trade publication, I feel an obligation to find out why you're not taking advantage of these services.

Are they too expensive? Is it because you don't want to travel? Are the options being offered not what you need? Are you unwilling to invest in an employee who might take that training and go somewhere else? Do you simply not have employees with enough promise to invest in?

I'm done being nice. I want answers to those questions. Please send them to *publisher@geartechnology.com*. It's time for all of us to stop moaning and do something about the problem.

Oh, and there's one other thing you can do. Make sure your employees are signed up to receive *Gear Technology* magazine. It's a free subscription, and we provide education every issue. There's really no excuse not to.

www.geartechnology.com/subscribe.htm

Michael Goldstein

Michael Goldstein,
Publisher & Editor-in-Chief

P.S.: Our technical editor and resident blogger, Chuck Schultz, has been writing a lot about gear basics lately. If you want to get someone started just learning about gears, gear design and gear manufacturing, it's not a bad place to start: *www.geartechnology.com/blog/*.

FRENCO REANY

GEAR INSPECTION SOFTWARE MELDS DATA FROM MULTIPLE SOURCES

What is REANY?

REANY is software for the evaluation of gears and splines that have been measured completely on all teeth. It is suited to both quality assessment and analyzing the causes for deviations. *REANY* is short for Reality Analysis.

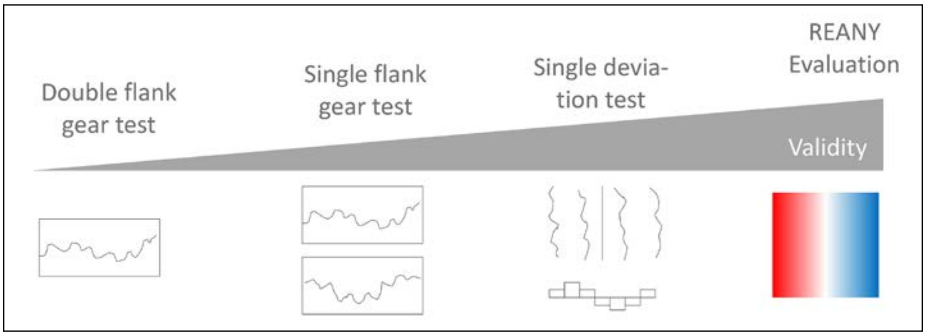

Figure 1

Table 1

Method	Data	Duration	Notice
Frenco Gear Flank Analyzing	Profile tracks in approx. 11–15 planes	7–13 minutes	For large batches only due to required master gear
Measurement of all teeth	Profile tracks at any number of planes, lead tracks at any number of diameters, combination of both possible	30–120 minutes	Almost all kinds of gears and splines measureable, though long duration
Focus variation	Point cloud; extraction of profile tracks at any number of planes	5–10 minutes	Profitable for micro gearings only

What is REANY's Use?

Various measurement methods have become prevalent during the past few decades. As a quick and simple test, double flank gear inspection looms large in the gear production area. One single curve represents the quality of the whole gear. The measurement result is not a special individual form deviation, but a summation of individual form deviations. The same applies to a single flank gear inspection. However, two curves are given out — one for the left and one for the right flanks. Since electronics are stringently required here, it is less popular than the double flank gear inspection.

Single deviation checks provide concrete information about profile, helix and pitch. To save time, profile and helix deviations are measured randomly at only four teeth. Pitch and runout deviations are calculated from a single point per tooth flank.

In some cases, information about the topology of all tooth flanks is desirable, especially when it comes to primary forming methods such as injection molding or sintering. The tooth flanks are refinished individually, which does not necessarily lead to a good result as the corrections are based on a random check. For classical machining methods, information about the whole gearing is interesting as well. Relations between the deviations and its causes in the manufacturing process can be established.

How Does It Work?

The evaluation is based on profile tracks of all teeth determined on several planes. Thereupon, the topology of every single tooth flank is generated by interpolating the measured data. The position of the flanks can be traced back to one point of origin. All measured values are related to each other, which is the main difference to standard plots. This data is the basis for the *REANY* evaluation.

The deviations from the nominal contour are displayed in colors. Like on a map, "hills" and "valleys" become visible. The view "Total Gear Geometry" shows all tooth flanks sorted and lined up.

So far, there are only a few methods to perform such measurements.

Focus variation is an optical measuring method providing a point cloud of the specimen's surface. Before reading the data, the desired number of transverse sections are extracted from the point cloud. Those can be loaded by

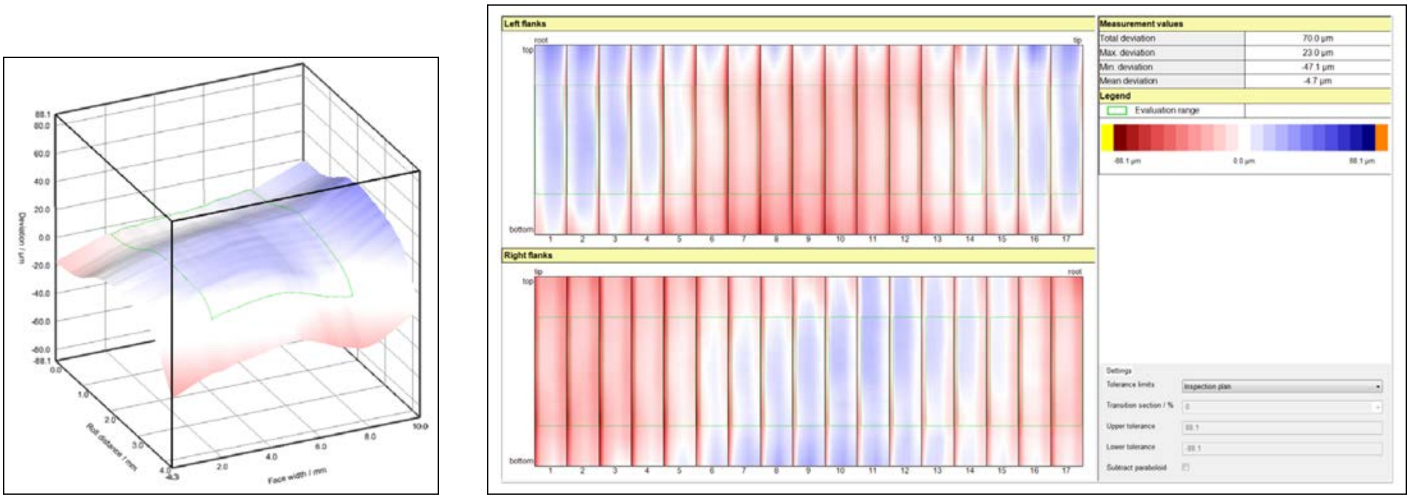

Measurement values

Total deviation	70.0 µm
Max. deviation	23.0 µm
Min. deviation	-47.1 µm
Mean deviation	-4.7 µm

Settings

Tolerance limits: Inspection plan

Transition section / %: 0

Upper tolerance: 88.1

Lower tolerance: -88.1

Subtract paraboloid ☐

Figure 2 Left: topology of a single flank; Right: View "Total Gear Geometry" with all flanks being related to each other.


BEVEL GEARS


WORMS


CAMSHAFTS


GEAR CUTTING TOOLS


CYLINDRICAL WORM GEARS

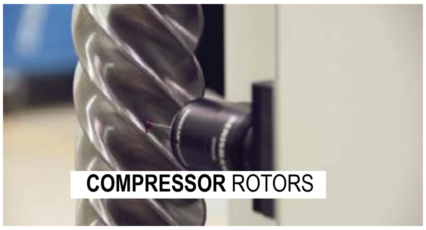
COMPRESSOR ROTORS


WENZEL
WGT 850
WENZEL
The company of µ

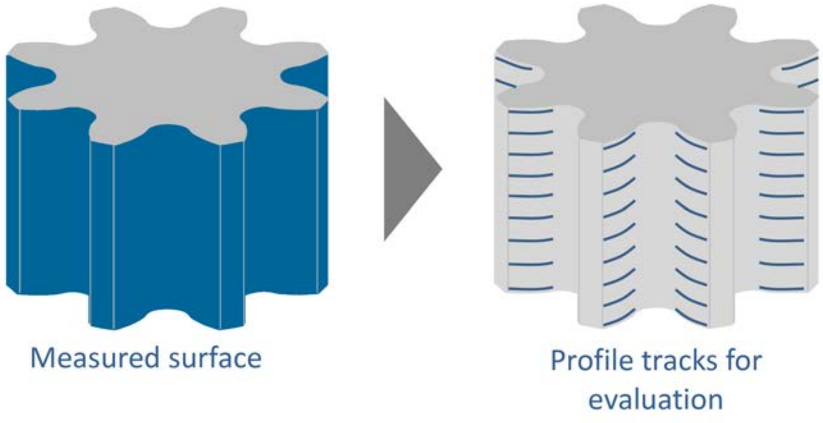

Figure 3

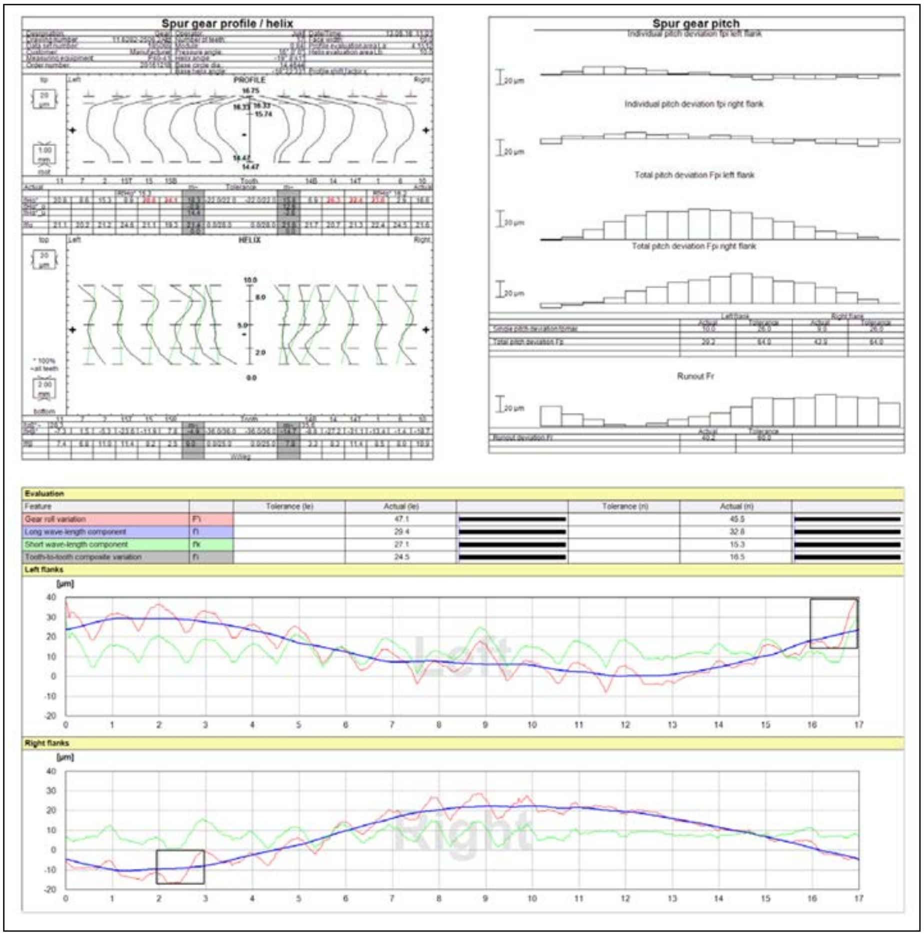

Evaluation

Feature		Tolerance (le)	Actual (le)		Tolerance (ri)	Actual (ri)	
Gear roll variation	F'i		47.1			45.5	
Long wave-length component	f'l		29.4			32.8	
Short wave-length component	f'k		27.1			15.3	
Tooth-to-tooth composite variation	f'i		24.5			16.5	

Figure 4 Top: Measuring plot including single deviations; Bottom: Curve of simulated single flank inspection.

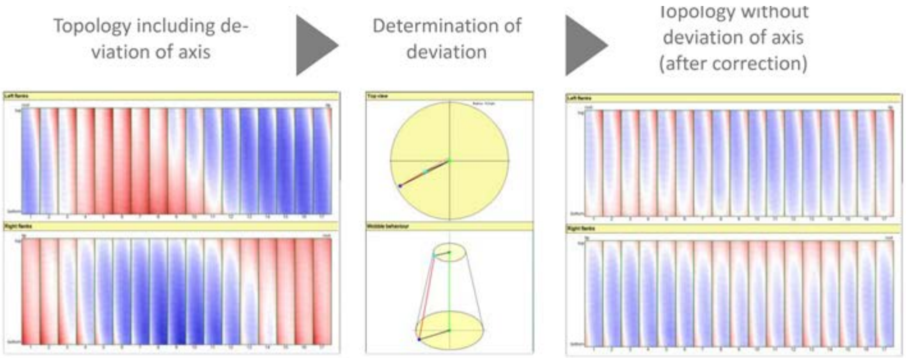

Figure 5

REANY software. Point clouds of other optical methods can be treated equally. Needless to say, direct processing without cutting the surface into pieces is on the to-do list as well.

What results Does REANY Provide?

Quality assessment according to standards

Primarily, the standard evaluation for quality assessment is included. The curves for profile, lead, pitch and runout are shown in the prevailing way. Furthermore, it is possible to simulate a single flank gear inspection due to the fact that all tooth flanks are available in their entirety. Associated, the FFT-Analysis of the roll curve is calculated to estimate noise emission.

Searching for deviation causes

The topology of tooth flanks available reflects the superposition of all deviations in the gearing. *REANY's* aspiration is to make systematic deviations visible. Systematic deviations are those that correlate with a cause in the production process and thus can ideally be corrected. The typical example is the deviation of the axis. Whenever the gearing's axis does not align to its reference axis (e.g. the bearing points), the whole topology is sinus-shaped. In case of a pure eccentricity, the sine's amplitude remains the same from top to bottom. In case of a wobble, the amplitude changes linearly along the face width. Both cases have an impact on any values calculated afterwards. The pitch curve will be sine-shaped, even if the pitch deviation as such might be okay. Profile slope and total deviations vary sinusoidally over one full rotation. In short, a deviation of axis casts a cloud over any other deviations, such as one coming from a tool error, for instance. Against this backdrop, *REANY* facilitates an automated correction of the axis. The correction affects the whole tooth flank topology and cached deviations appear.

REANY contains figures that display the pitch deviation, referring to the complete gearing. Pitch deviations are color-coded and shown from top to bottom. Before correcting the deviation of axis, the figure outlines the compliance with tolerances along the face width.

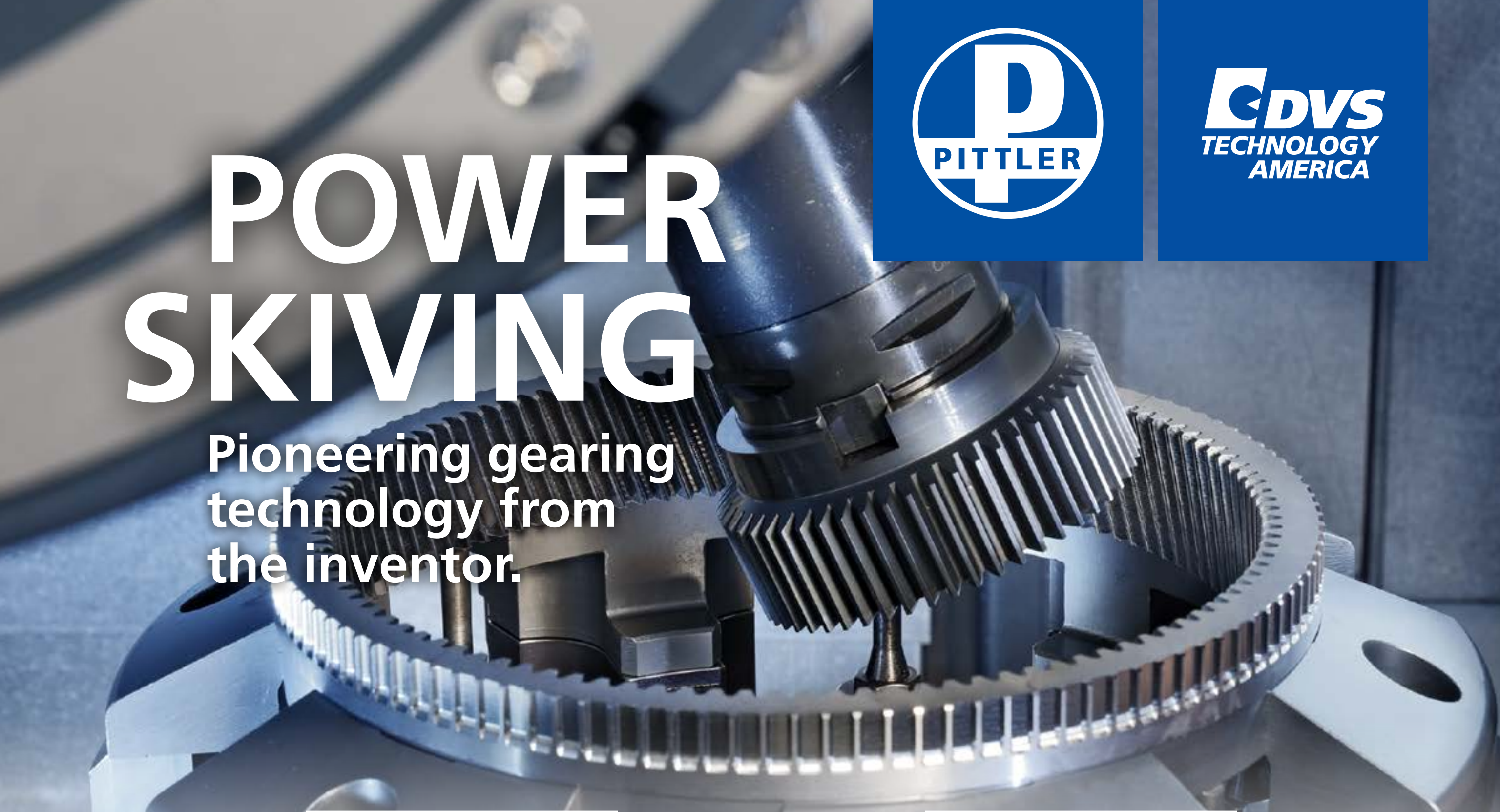

POWER SKIVING

Pioneering gearing technology from the inventor.

Turning

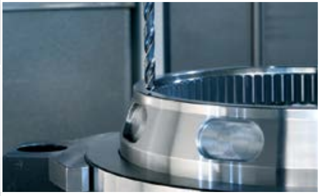

Drilling

Milling

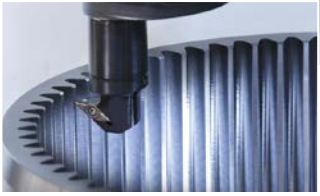

Deburring

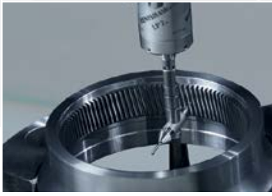

Measuring

Invented by their founder already in 1910, **PITTLER T&S** today offers the Power Skiving process in conjunction with complete machining. With highest precision green and hardened gears can be machined in one single clamping.

As a system supplier **PITTLER** designs, manufactures and re-conditions skiving tools as part of their all-in-one tool service.

PITTLER PV315

- Power Skiving for inner and outer gearings
- Integrated tool magazine for complete machining
- Single clamping operation for highest precision

CONTACT US:

DVS Technology America Inc.
☎ 734-656-2080 ✉ sales.america@dvs-technology.com
www.pittler.de | www.dvs-technology.com

Correcting the axis's deviation gives the possibility to search for systematic pitch deviations.

Since every pitch consists of a tooth and a gap, the pitch deviation is closely intertwined with tooth and space widths. While there is a tolerance for the tooth thickness, either directly or indirectly (e.g. dimension over pins), and thus it is evaluated, the space widths are usually disregarded. But it is worth a glance, as conventional production methods primarily produce the space widths, which result in tooth width and pitch deviations, depending on the gap's positions and sizes. The sizes of tooth and space widths are displayed in Figure 7.

The angular positions of teeth and gaps are shown by Figure 8. The positions are defined by their middles along the circumference. An output of +10 µm, for example, indicates an offset to the nominal position of the tooth or the gap in counting direction of 10 µm along the circumference. When profile grinding, a deviation of the encoder, for instance, results in a sine-sharped variation of the space middles. Subtracting

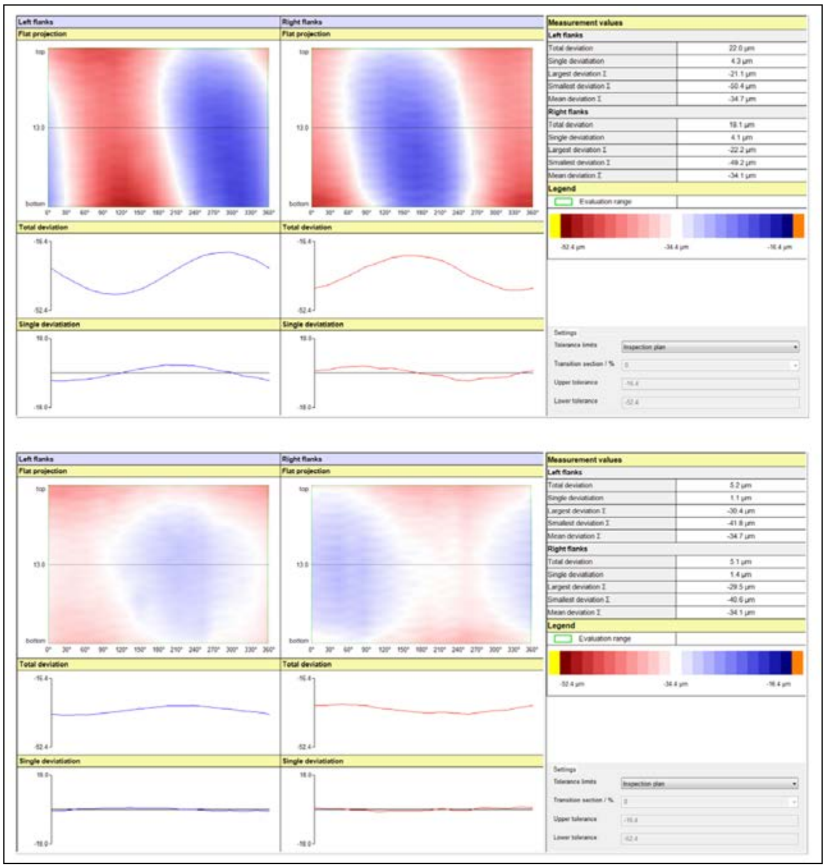

Measurement values	
Left flanks	
Total deviation	22.0 µm
Single deviatiation	4.3 µm
Largest deviation Σ	-21.1 µm
Smallest deviation Σ	-50.4 µm
Mean deviation Σ	-34.7 µm
Right flanks	
Total deviation	18.1 µm
Single deviatiation	4.1 µm
Largest deviation Σ	-22.2 µm
Smallest deviation Σ	-49.2 µm
Mean deviation Σ	-34.1 µm

Settings
Tolerance limits: Inspection plan
Transition section / %: 0
Upper tolerance: -16.4
Lower tolerance: -52.4

Measurement values	
Left flanks	
Total deviation	5.2 µm
Single deviatiation	1.1 µm
Largest deviation Σ	-30.4 µm
Smallest deviation Σ	-41.8 µm
Mean deviation Σ	-34.7 µm
Right flanks	
Total deviation	5.1 µm
Single deviatiation	1.4 µm
Largest deviation Σ	-29.5 µm
Smallest deviation Σ	-40.6 µm
Mean deviation Σ	-34.1 µm

Settings
Tolerance limits: Inspection plan
Transition section / %: 0
Upper tolerance: -16.4
Lower tolerance: -52.4

Figure 6 **Pitch deviation of left and right flanks along face width. Above: quality assessment before correction of axis; Below: remaining pitch deviations after correction of axis.**


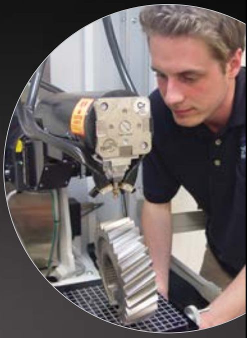

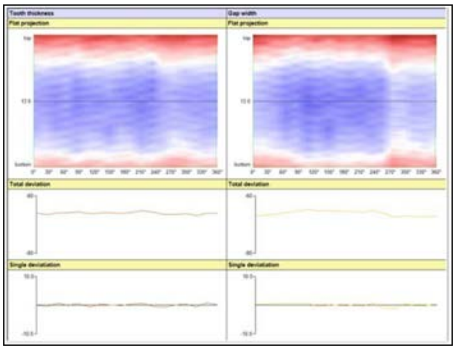

Figure 7 **Tooth widths (left) and space widths (right) equal the size of tooth and space widths**

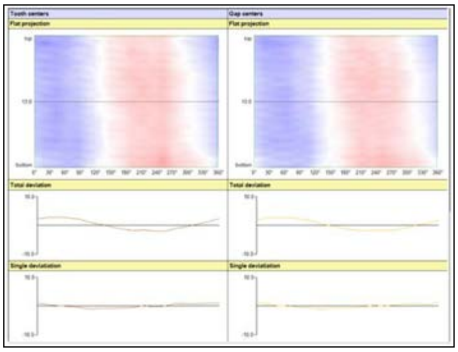

Figure 8 **Tooth middles (left) and gap middles (right) equal the angular position of tooth and space widths**

this systematic error from the topology makes pure form deviations visible.

REANY offers several figures to assess the form deviations in the whole gear. As with pitch deviations, the profile deviations of all teeth from top to bottom are marked in color. Before the correction of axis, the tolerance limit exceedance can be seen at a glance. After the correction, systematic deviations can be detected easily. For instance, when profile slope deviations show up solely the color red, a systematic tool error is the likely cause.

Correspondingly, the helix slope deviations are shown from root to tip. After the correction of the axis a systematic change of color appears, coming from a twist.

Another method to evaluate the form is to regard the individual tooth flanks as paraboloids. Every paraboloid consists of:

- Profile crowning
- Helix crowning
- Twist
- Profile slope
- Helix slope
- Offset (single pitch deviation)

On one hand this method allows the evaluation of intended modifications.

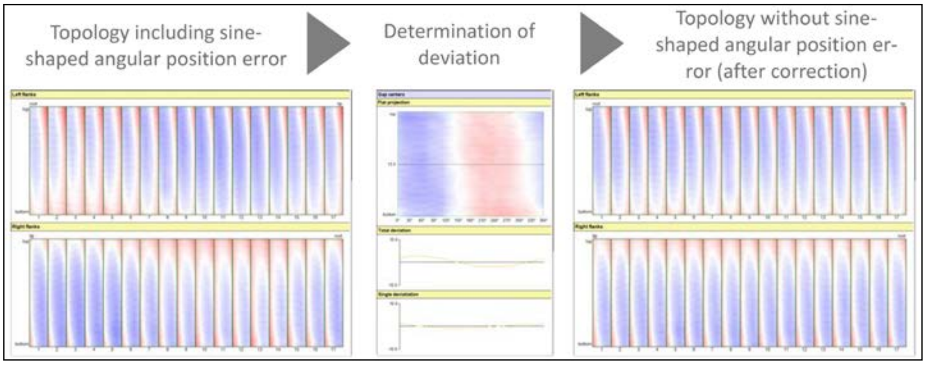

Figure 9

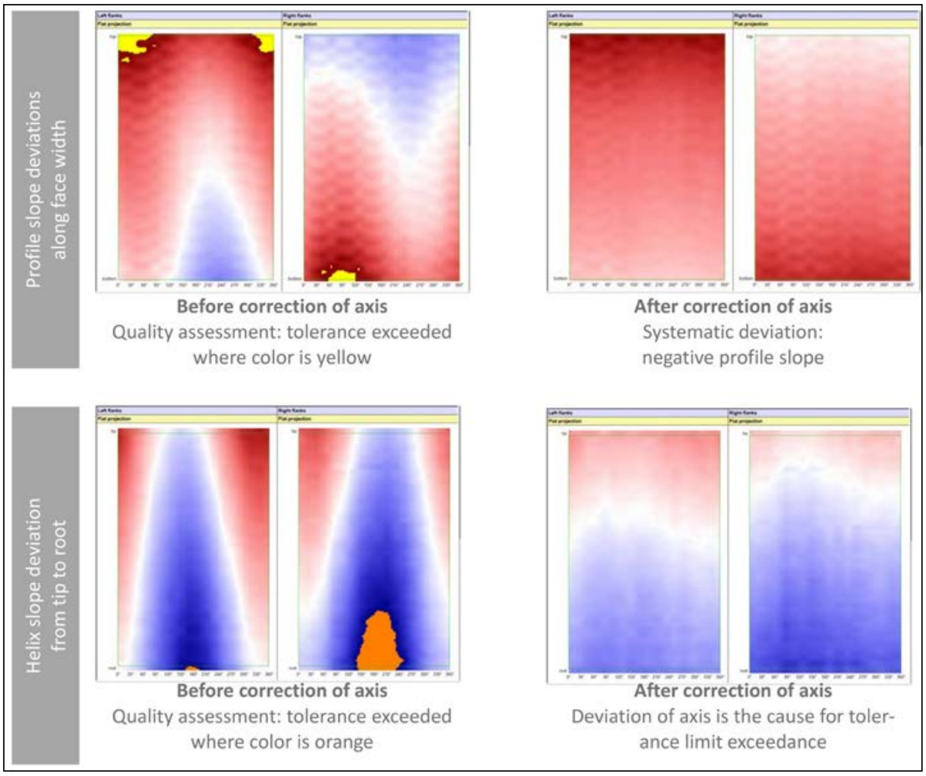

Figure 10

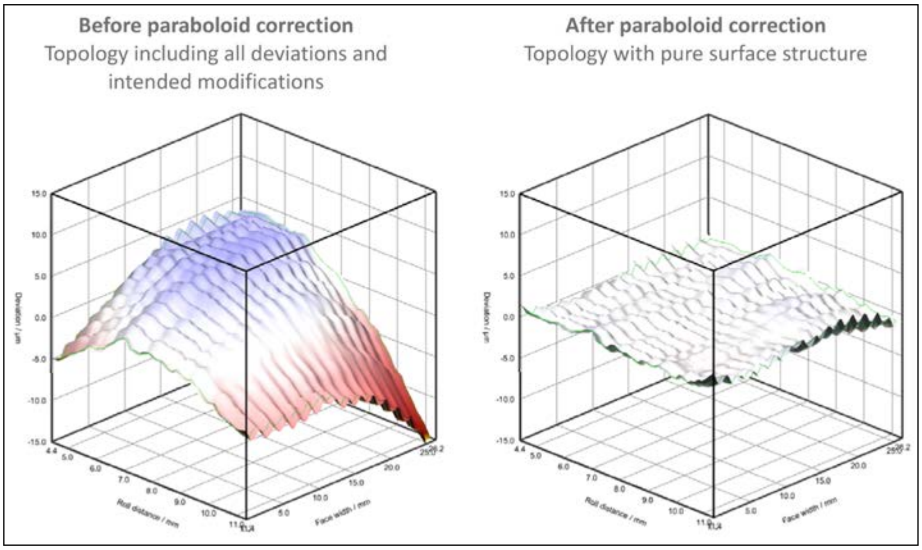

Figure 11

On the other, averaged corrections, concerning the whole tooth flank topology, can be defined to improve production. To estimate the influence of these corrections on the measurement results, computational corrections are possible. An output of 4 µm averaged profile slope deviation, for example, can be eliminated from the topology to simulate an associated tool-correction and see the effect on the quality.

Finally, it is interesting to look at the pure form deviations. For that, the paraboloid of each individual tooth flank is subtracted from the topology. This correction of the basic form deviations enables a precise evaluation of the surface structure.

The development of *REANY* is far from over. Cause studies require a deep knowledge of the production process and experts to brood about a solution. For now, *REANY* just supports the brood development. However, Frenco envisions a program, fed with the principal parameters, that tells the operator exactly what to do when a problem occurs. What about the long duration of the measurement? Well, Frenco believes that optical measurements, providing point clouds, will sooner or later take on in-line checks. That will be quick and certainly requires new evaluation methods, beyond those we know today. That's for sure.

For more information:
Frenco
Phone: +49 9187-9522-0
www.frenco.de

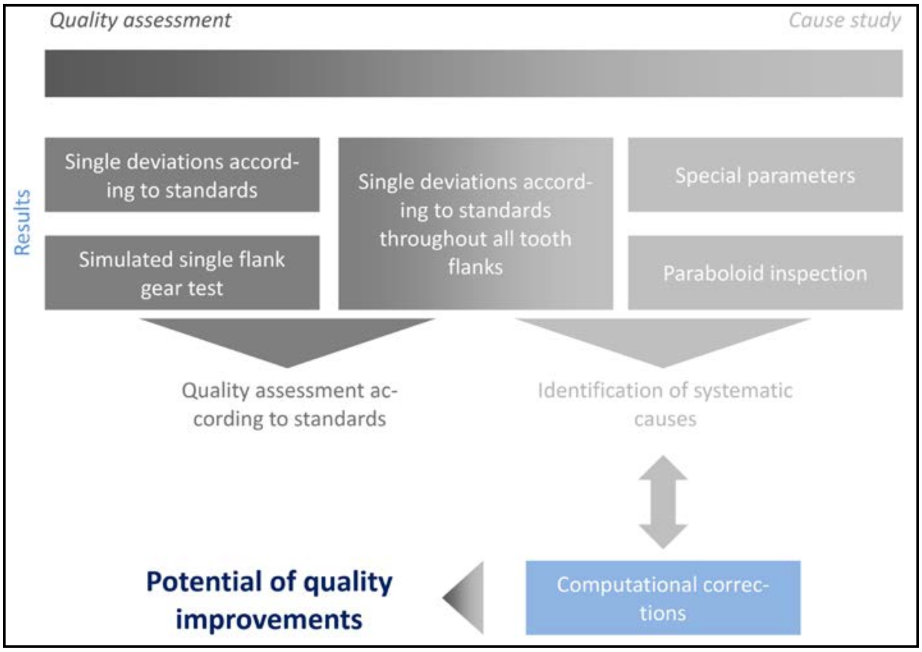

Figure 12

The New Blue

Gleason's new Segmented Collets give workholding maximum wear life; with sizes and an expansion range covering the bore clamping requirements of the most common cylindrical (and some bevel) gear types and sizes.

www.gleason.com/newblue

Total Gear Solutions **Gleason**

Houghton International

INTRODUCES TECHNOLOGY FOR AUTOMOTIVE MACHINING AND GRINDING

Houghton International has developed a new versatile soluble oil metal removal fluid for the manufacture of automotive parts including engine and transmission components. This technology measurably improves machining and grinding operations, delivering higher product quality and lower operating costs.

HOCUT 8750 is the first 8000 series product built from the ground up using Design of Experiment (DoE) Methodology to optimize critical performance parameters. It is designed for the machining and grinding of engine components, including blocks, crankshafts, cylinder heads, connecting rods, and pistons; transmission components such as gears, shafts, and bearings, aluminum wheels, braking systems and more. Extensive field testing has demonstrated significant performance improvements on a broad range of metals including high and low carbon steel, stainless and alloyed steel, cast nodular and gray iron, wrought and cast aluminum, powdered metal and carbon particle composites.

Designed to improve operational efficiency, part quality and surface finish, HOCUT 8750, with built-in detergency, runs clean and provides excellent wetting which reduces consumption due to drag out, lowering fluid costs. HOCUT 8750 also has superior dispersibility, improving chip removal and minimizing downtime. It has excellent emulsion stability and low foaming characteristics, resulting in consistent lubrication and heat transfer performance. HOCUT 8750 is also biostable, a hallmark of Houghton expertise, extending sump life and eliminating the need for costly sump-side additives.

For more information:

Houghton International
Phone: (800) 666-4684
www.houghtonintl.com

Dillon

DIAMETER JAW BORING RINGS PROVIDE UNIFORM PRESSURE

Dillon Chuck Jaws introduces an 18 diameter boring ring. Its relatively light weight allows customers the same ease boring out 18 diameter blank top jaws as is had when forming smaller diameters using the smaller sized boring rings.

Dillon jaw boring rings are easy-to-use tools that allow soft jaws to be machined precisely and thus grip the intended workpiece more firmly. These jaw rings provide uniform pressure on all jaws, for a consistent bore.

Available in adjustable or chuck-diameter-specific styles, both with no-tools attachment. The Dillon jaw boring ring compensates for jaw lift, even in worn chucks, which results in better parts concentricity. Use of this device will provide a jaw surface true to the machine centerline, reduce set-up times, and increase up-times for running machined parts.

Jaw boring rings are available for 5", 6", 8", 10", 12",15", and 18" chucks, or in adjustable versions for 5"–8", 6"–10", and 8"–12" chucks. Self-centering action provides equal pressure on all jaws.

For more information:
Dillon Manufacturing, Inc.
Phone: (800) 428-1133
www.dillonmfg.com

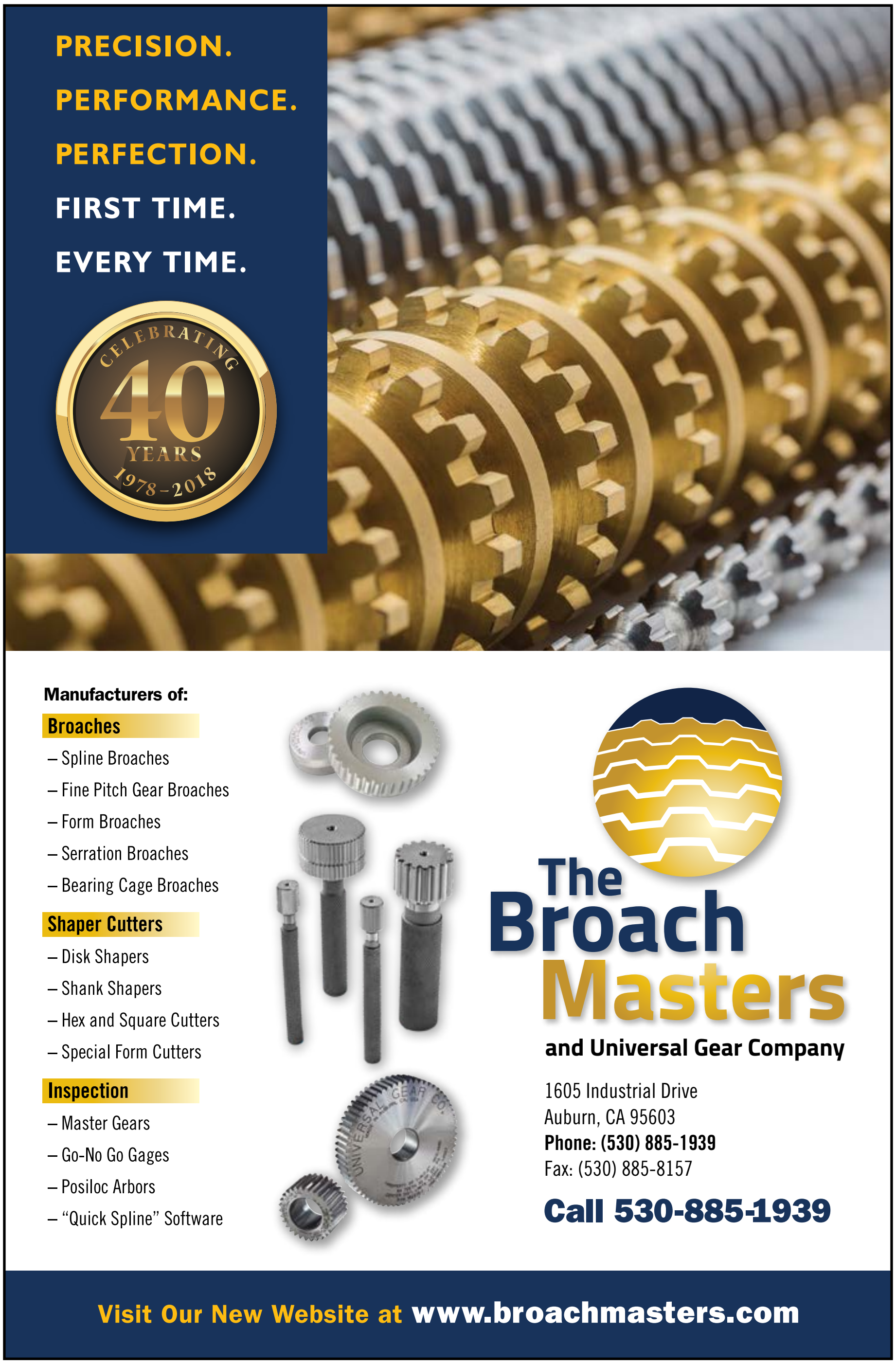

Open Mind Technologies

ENHANCES CAM SOFTWARE WITH VIRTUAL MACHINING SIMULATION AND MORE

Open Mind Technologies AG, a developer of CAM software solutions worldwide, has introduced *hyperMILL 2018.1*, a new version of its advanced, comprehensive CAM software. *HyperMILL 2018.1* has a range of new features and enhancements including greater blending capabilities, 3D-optimized roughing, global fitting, rotational abilities for CAD electrode applications and totally new to the industry - virtual machining simulation.

"*HyperMILL 2018.1* demonstrates our commitment to innovation when providing CAM users with the tools they need to be successful," said Alan Levine, managing director of Open Mind Technologies USA, Inc. "We continue to advance functionality in the *hyperMILL* suite to keep it at the forefront of CAM technology."

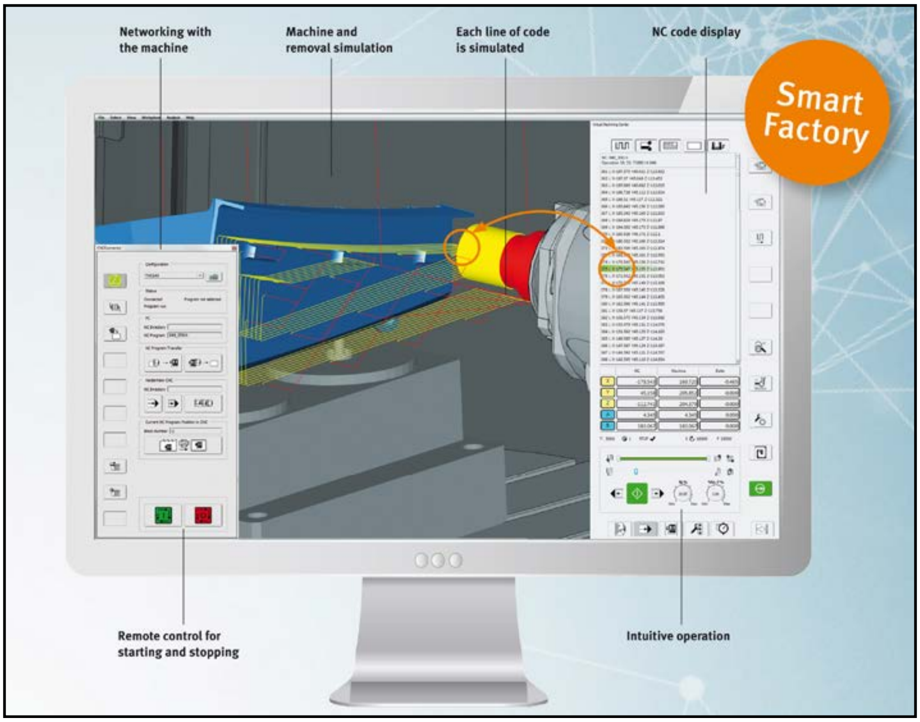

All The Gear Cutting Tools You Will Ever Need Are Right Here

DTR is one of the world's largest producers.

DTR. Your best choice for high quality gear cutting tools.

DTR is a world class supplier of the finest high performance long-life gear manufacturing tools, for small and large gear cutting applications. Established in 1976, we are one of the world's largest producers of cutting tools, shipping to over 20 countries.

DTR offers a full line of gear cutting tools including:
- Hobs
- Carbide Hobs
- Shaper Cutters
- Milling Cutters
- Chamfering and Deburring Tools
- Broaches
- Master Gears

We can produce virtually any tool you need for auto, aerospace, wind, mining, construction and other industrial gears.

Every tool is precision-made utilizing high speed steel, premium powder metal or carbide and the latest in coatings, to achieve superior cutting and long life. DTR uses top of the line equipment including Reischauer CNC grinders and Klingelnberg CNC sharpeners and inspection equipment.

Learn more about our outstanding quality tools at www.dtrtool.com.
Call us at **847-375-8892** for your local sales representative or
Email **alex@dtrtool.com** for a quotation.

DTR

PERFECTION MOVES US

(formerly Dragon Precision Tools)

WWW.DTRTOOL.COM

DTR has sales territories available. Call for more information.

U.S. Office Location **(Chicago) Email inquiries to: alex@dtrtool.com.**
1865 Hicks Road, Suite A, Rolling Meadows, IL 60008
PHONE: **847-375-8892** Fax: **224-220-1311**

Headquarters
85, Namdong-daero 370beon-gil, Namdong-gu, Incheon, Korea, 21635
PHONE: **+82.32.814.1540**
FAX: **+82.32.814.5381**

Smooth Transitions

New *hyperMILL 2018.1* functionality includes an enhancement to the "soft overlap" feature for blending machining marks found between steep and flat areas, or located at the boundaries of rest machining regions. Using this enhanced feature, the milling tool is briefly lifted to blend milling paths into another, preventing visible transitions from being generated, resulting in better surface quality.

3D-Optimized Roughing

In *hyperMILL 2018.1*, the 3D-optimized roughing cycle has been enhanced for applications with high feed cutters. The step-over distance can be calculated from the scallop height measured against the high feed cutter geometry. A special tool path movement removes rest material from corners when there is a very large step-over. Intelligent cut division and optimized toolpaths provide greater process safety for the remaining thin ridges.

Global Fitting

A new "global fitting" feature can simplify the definition of complex surfaces or patches of surfaces. Many *hyperMILL CAM* strategies will recognize and follow the ISO u-v orientation of the surface patch. *HyperMILL MAXX* Machining finishing is one technique that benefits from having a simplified surface definition.

Rotational Electrode

HyperCAD-S Electrode automates the construction and manufacturing of electrodes for die-sinking. Users can simply choose their electrodes from the face to be die-sunk within the component geometry, with no special expertise required. To save users time during milling and eroding, *hyperCAD-S* in *hyperMILL 2018.1* includes an easy-to-use "rotational electrode" feature which facilitates the circular placement of multiple electrode geometries with different spark gaps on a holder.

Virtual Machining

Developed with Industry 4.0 in mind, an early release of *hyperMILL VIRTUAL Machining* simulation is available in version 2018.1, which enables constant real time bi-directional communication between the machine tool controller and a remote *hyperMILL VIRTUAL Machining* simulation, significantly improving manufacturing workflow. Machining operations can be reliably evaluated, checked and optimized before running a job by using process networking and virtual mapping found in *hyperMILL VIRTUAL Machining*. The *hyperMILL VIRTUAL Machining* NC Optimizer can enhance computed NC instructions to optimize available workspace, manage limited axes and select the best approach for asymmetric machine heads. Safety, reliability, speed and process control optimization from CAD/CAM to machine are all improved with *hyperMILL VIRTUAL Machining*.

For more information:

Open Technologies
Phone: (339) 225-4557
www.openmind-tech.com

Mitutoyo America Corporation

RELEASES MICAT PLANNER VERSION 1.5

Mitutoyo America Corporation recently announced the release of MiCAT Planner v1.5 for the company's coordinate measuring machines. In as little as one click, MiCAT Planner automates the generation of measurement programs based on CAD models containing Geometric Dimensioning and Tolerancing (GD&T) information, as well as your Dimensional Measuring Equipment (DME). When no GD&T information exists, it can easily be added.

Functions include the support of multiple CAD coordinate systems and the creation of multiple part coordinate systems. These features can be created from the Plan View or the 3D View, a connection feature support that has been expanded to include connection lines and planes, mid-point, mid-line and mid-plane constructed features that can be set as datums, used in an alignment plan and as referenced features for other constructed features and more.

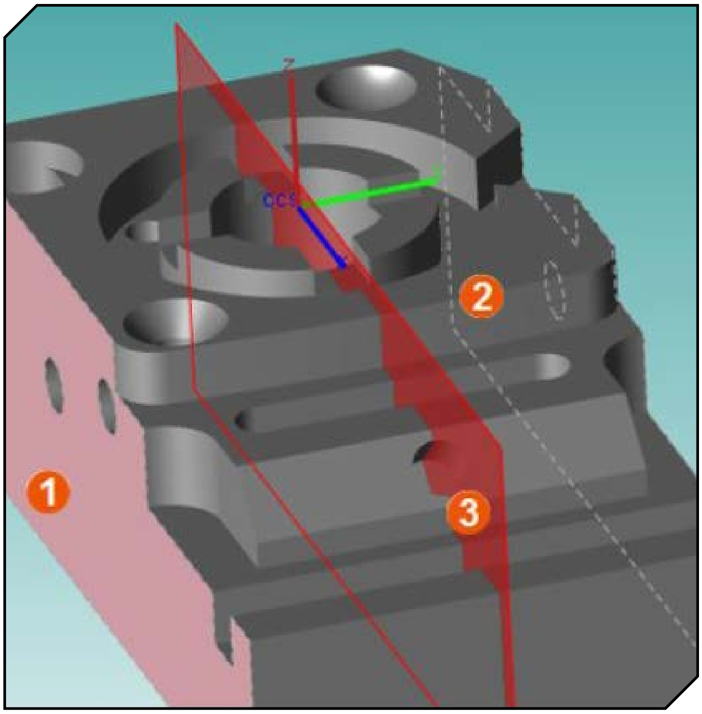

For more information:
Mitutoyo America Corporation
Phone: (630) 820-9666
www.mitutoyo.com


Sightia™

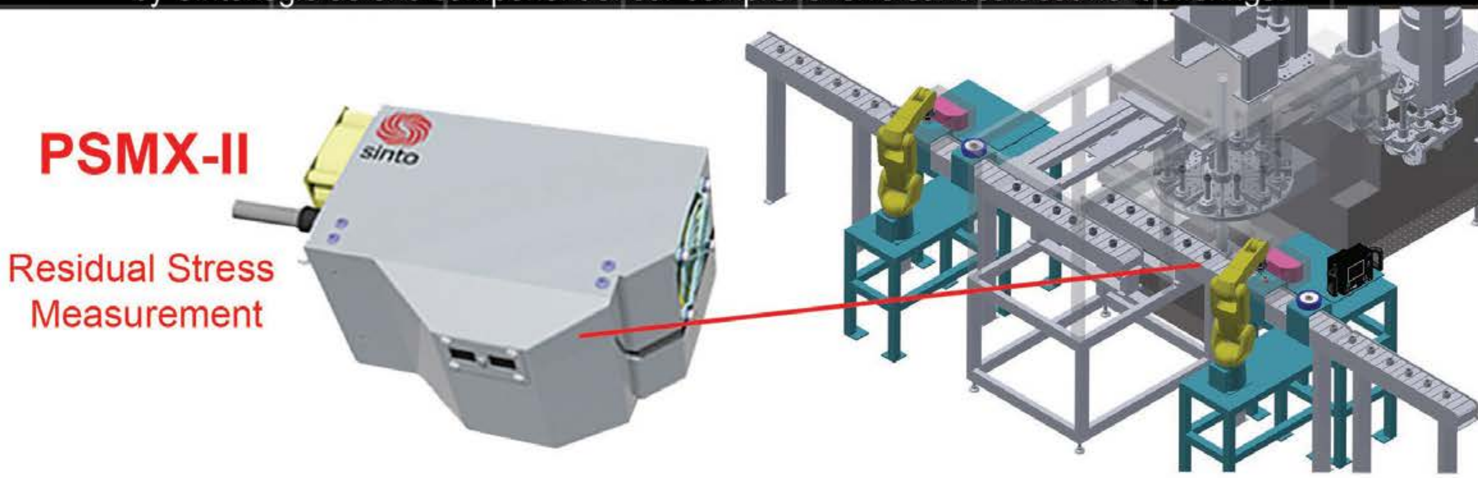
PSMX-II
Residual Stress Measurement
sinto

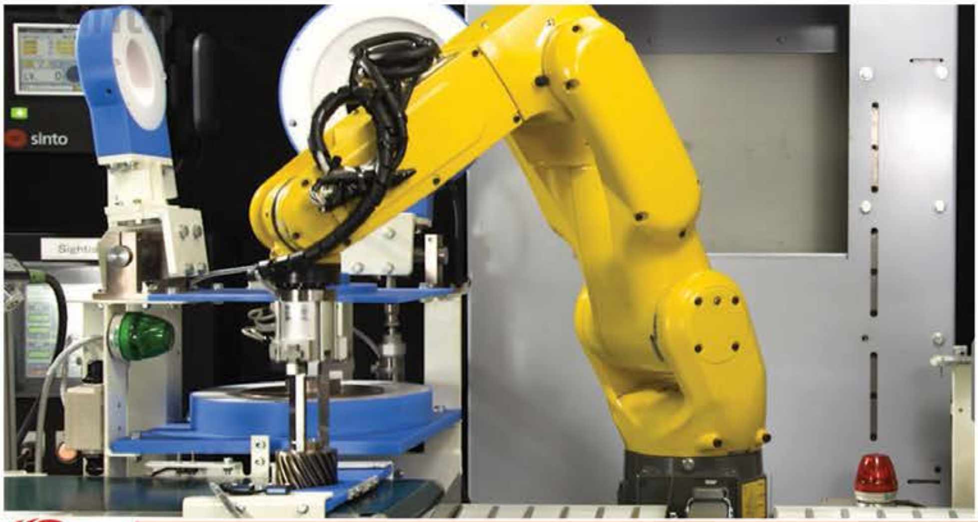

Pushing Boundaries

Induction hardening is becoming an increasingly popular alternative to thermochemical diffusion processes such as carburizing, and as it does so, manufacturers are on a never-ending quest to expand the scope of what's possible with the technology.

Alex Cannella, Associate Editor

Dr. Valery Rudnev, director of science and technology at Inductoheat, has been doing a lot of travelling the past few years. Known as "Professor Induction," he's one of the leading experts in the field of induction hardening, and his expertise regularly sees him touring facilities and giving seminars on the latest in the induction hardening industry. Needless to say, during his travels across Europe and the U.S., Rudnev has personally witnessed how a broad swath of the industry is getting along, and he's noticed a few trends.

The most notable one is an attempt to shift away from thermochemical diffusion processes such as carburizing in favor of induction hardening. Manufacturers' reasons for doing so are always different, but everywhere Rudnev has gone, the hottest button topic that always comes up is whether a heat treater can replace thermochemical diffusion processes like carburizing or not.

"Question number one I'm asked: 'Can you replace our thermochemical diffusion processes with induction?'" Rudnev said. "And the answer is sometimes yes, sometimes no, it depends on the gear."

There are a few reasons why the question has become so common. Some of the primary reasons are induction hardening's ability to produce increased compressive residual stresses compared to vacuum carburizing, low distortion and piece-by-piece processing capability with individual component traceability. According to Rudnev, single frequency induction hardening can achieve levels of 400-550 megapascals. And if using simultaneous dual-frequency, heat treaters can achieve 600-700 megapascals.

Induction hardening is also starting to see some promise for use on 7" to 9" hypoid ring gears, with Rudnev having seen some "extremely positive tests." In the future, it may become a widely accepted way to harden those gears.

In Europe, especially, induction hardening is gaining popularity off a wave of environmental-mindedness. The current political climate in Europe is motivating many heat treaters to consider shifting their production processes from vacuum carburizing to induction hardening, which is a more environmentally friendly process. Some, according to Rudnev, don't even feel there's room left for consideration, and that carburizing isn't an option anymore.

But as Rudnev said, induction hardening isn't a silver bullet solution for gear heat treatment. The process has difficulty, for example, with complexly shaped gears such as double helical or herringbone gears. The more complex a gear's shape, the more difficult it is to develop a uniform case hardened pattern, and eventually, the complexity can reach a point where induction hardening simply cannot evenly austenitize a tooth surface, leading to varying case depths on different parts of the gear and potentially producing some undesirable metallurgical structures. In these cases, Rudnev still recommends that heat treaters vacuum carburize or nitride their gears instead, whichever is more suitable.

Similarly, sharp corners on a gear or workpiece can lead to subpar heat treatment. Sharp corners sometimes get excessively heated compared to the rest of the teeth, which leads to grain coarsening and in some instances, even grain boundary liquation (incipient melting). Thus, appropriate chamfering and rounding of sharp edges is always welcomed by induction professionals.


Induction hardening's popularity is rising alongside its flexibility; manufacturers are finding new ways to expand the range of workpieces the technique can be utilized on.

Induction hardening also often requires using different steel grades to start with. Thermochemical diffusion processes (e.g. carburizing or nitriding) alter the actual chemical makeup of the material, thus hardening it. But one critical difference between these processes and induction hardening is that the latter does not alter the chemical composition of the material, which in turn means you need a stronger base material with sufficient carbon content to form the required amount of martensite at a gear's working surface in order to provide sufficient strength and wear properties.

Thanks to surface hardening capabilities of electromagnetic induction, a gear tooth's core remains relatively cool, which allows it to act as a shape stabilizer for the heated surface and in turn lessens the distortion caused by the heat treating process while also making that distortion more predictable.


UniCase Master
UniCase Master
SINGLE PIECE LPC

"Even more important is not just to reduce distortion, but to have predictable distortion," Rudnev said. "Because if the distortion is predictable and repeatable, then this type of distortion can be relatively easily compensated for."

It should be recognized that depending on the size of the gear, tooth geometry and gear working conditions, different techniques can be used to induction heat treat gears. This includes tooth-by-tooth hardening and spin hardening using encircling coils. Single frequency induction systems, as well as sequential or simultaneous dual frequency systems, have been developeed by several induction manufacturers, including Inductoheat.

One gear market segment that has been relatively soft in the last 5-8 years is heat treatment of large gears such as those that go into windmills. According to Rudnev, demand for induction hardening of those gears is quite low amongst large gear manufacturers in the U.S., in part because a lot of the field has been outsourced abroad.

One difficulty large gear manufacturers sometimes run into is actually finding a heat treater that can handle the sheer scale of gears that stretch to multiple meters in diameter, but according to Rudnev, scale isn't a concern for tooth-by-tooth induction hardening. In fact, that's one of the method's strong points.

"Even though that some distortion inevitably occurs when tooth-by-tooth induction hardening large gears and pinions, its magnitude is not nearly as large as compared to carburized gears," Rudnev said. "Carburizing requires soaking of gears for many hours at temperatures exceeding 1500°F. At these temperatures, the large masses of metal expand to a much greater extent compared to the case when only the tooth working surface layer is austenized by electromagnetic induction. The expansion of large masses during prolonged heating during carburizing and the contraction during quenching "move" the metal to a much greater degree, causing considerable gear distortion.

"Furthermore, heavy gears weighing several thousand pounds and being held at austenite phase temperatures for

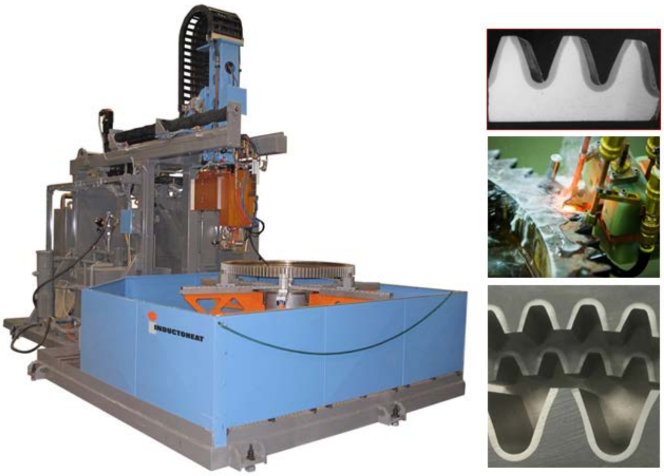

Figure 1 Tooth-by-tooth hardening of large gears. (Photo courtesy of Inductoheat Inc.)

many hours have little rigidity and can sag following their supporting structures. With induction hardening, areas unaffected by heat as well as areas with temperatures corresponding to the elastic deformation range serve as shape stabilizers resulting in not only reduced distortion but also making it more predictable. Induction hardening for those applications is the best process (Figure 1)."

Rudnev also frequently gets questions about shot peening, namely if heat treaters can avoid having to use it after induction spin hardening of small and medium size gears. The answer, again, is that it really depends on your requirements.

"Many times, when induction hardening gets used for a gear treatment, we don't use shot peening," Rudnev said. "But if the performance of the gear requires residual compressive stresses of considerable magnitude being in the range of 900-1,000 megapascals, then most likely, it will be required to have shot peening after induction gear hardening."

But most often, the focus is on the technology's competencies themselves; what it can handle, what it can't, and most importantly, how its compares to vacuum carburizing.

The answer to that question becomes a little more nuanced every year, however, as induction hardening is an evolving field, and the scope of what can be accomplished with the process is always widening. Rudnev's company, Inductoheat, for example, has developed a new power supply called the Statipower IFP (Independent Frequency and Power Control). The idea behind the patented IFP Technology is to fill a gap that the induction hardening industry as a whole currently has between cheaper, less flexible conventional single-frequency induction systems and expensive but effective dual frequency processes in an attempt to capture the selling points of both while minimizing some of their weaknesses (Figure 2).

"IFP Technology is a good compromise between simultaneous dual frequency, which has good results but high capital cost, and

Figure 2 **Statipower IFP Technology enables instant and independent adjustment of frequency within 5 to 60 kilohertz range in a preprogrammed manner during the heating cycle. (Photo courtesy of Inductoheat Inc.)**

conventional single frequency systems which are less costly but the quality of hardening of certain types of gears might not always be the best," Rudnev said.

Which isn't to say that IFP is the end-all be-all system that you should be immediately leaping to your feet to buy. As Rudnev notes, there are still plenty of gears that single frequency systems can already handle just fine. And on the other hand, some gears require a level of metallurgical quality and hardness pattern contouring only achievable with simultaneous dual frequency.

"It's not cure-all medicine," Rudnev said. "There are some limitations associated with IFP Technology. For example, at this point, IFP inverters enable instant and independent adjustment of frequency within a 5 to 60 range kilohertz in a preprogrammed manner during the heating cycle optimizing electromagnetic, thermal and metallurgical characteristics."

But Inductoheat has positioned IFP as a happy middle ground, giving induction hardening professionals a gradient of options instead of just two choices. And more importantly, the IFP is flexible, which according to Rudnev, has made it appealing to heat treat other components for automotive suppliers.

"Suppliers need to have flexibility. If tomorrow one automotive [company] comes to them and then, a day after tomorrow, another one with a different requirement, suppliers would like to process those parts using the same equipment," Rudnev said. "Obviously in induction, the coil would be different, being dedicated to a particular part, but the cost of the induction coil is relatively small compared to the cost of the entire system and in particular an inverter...Therefore, if the power supply will provide them greater flexibility, that's a big deal in our highly competitive world. Parts suppliers would not have to buy a new power source all the time to process different gearbox or powertrain components while still assuring high metallurgical quality of heat treated parts. Instead, now they can utilize universal inverters with flexible yet highly accurately controlled output frequency, which will extend horizons and the applicability of their induction equipment. Needless to say that such equipment can also be moved from one plant to another plant, optimizing overall cost savings."

The IFP Technology, couples with an advanced signature process monitoring system, is targeted towards automotive, aerospace, agriculture and off-highway industries and is best suited for heat treating gearbox components, as well as shafts, sprockets and splines of almost every variety. It's also particularly beneficial when tooth-by-tooth hardening a variety of large-sized gears. And the breadth of projects that can be undertaken with Inductoheat's IFP Technology is widening as the company works to introduce new models that expand coverage of different ranges of frequencies and maximum powers.

Inductoheat is, of course, not the only company innovating in the induction hardening space. Eldec has also been pursuing new technologies that expand

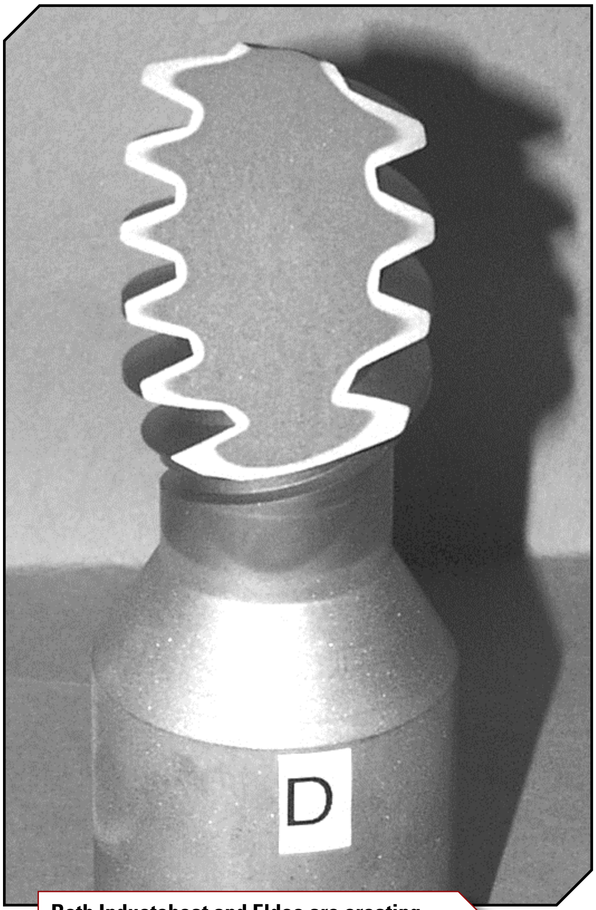

Both Inductoheat and Eldec are creating new induction hardening products capable of handling new shapes of gears.

the scope of the process's usefulness. In particular, they've been working with pushing the cutting edge of what can be done with simultaneous dual frequencies.

One of their most recent developments is a coil specifically designed to work with helical gears, a move meant to appeal to gearbox manufacturers. It's a bit of a leap of faith on Eldec's part, as gearboxes are still firmly vacuum carburizing territory, and getting customers onboard requires a lot more than just buying a new coil; it requires a complete changeover of their processes, and affects more than just the heat treatment. You have to consider materials and your chip making process, for example.

Eldec's coil certainly has merits to warrant the switch, however. All the previously discussed advantages that induction hardening has over vacuum carburizing still hold true here. But one of the process's biggest weaknesses, complex gear shapes, also remains. There are still difficulties with gears with a helix angle of more than 15–20 degrees, but Eldec has established a toe-hold that can be built upon, and that may change in the future.

In addition, Eldec has designed their induction hardening machines to work as part of a production line. Instead of having to take parts off the line to divert to a furnace before going back to the line, Eldec's machines can be incorporated directly into the workflow. And if you do ultimately decide to make the leap, Eldec has a full force of consultants to help make the transition as painless as possible.

According to Managing Director of Eldec, Thomas Rank, however, the best advice he can give those looking to incorporate induction hardening into their production line is to take stock of their entire process chain.

"Look at the whole process chain before you do that step," Rank said. "Investigate in all the process steps before and after hardening in order to have a result that doesn't surprise you in terms of cost."

Another frontier that Eldec is braving is that of IIoT technology. Whether you call it the Industrial Internet of Things or Industry 4.0, it's worked its way into almost every manufacturing process known to man, and induction hardening is no different.

Eldec's introduced a software suite dubbed Eldec Quality Control (EQC) for use with its induction coils that uses RFID tags to constantly monitor more than 20 different parameters in an induction hardening machine. EQC studies everything from energy, water temperature and the voltage of the coil during the process to even how many workpieces the coil has heat treated during its lifetime.

The benefits of this are the same as in other industries: having access to an unprecedented level of data means that engineers can not only better understand and control how their coils are functioning, but they can also use that information to predict when a coil looks like it will fail and preemptively replace it before it halts production. EQC also automatically shuts down a machine if any of its parameters go over previously designated levels, preventing catastrophic damage that might otherwise put a machine out of commission.

One unusual twist that is different from other industries, however, is that Eldec had to design around the electromagnetic field when developing EQC. In particular, the field could wreak havoc with EQC's RFID tags, but Eldec found a solution by monitoring the field itself.

There are numerous other advances also coming out of Eldec — 3D printed induction coils chief among them — but every advance shares a single goal: to expand the scope of what's possible with induction hardening. That similarly rings true for Inductoheat. And between them, the technology gains new footholds each year, and with those footholds, broader appeal.

For more information:

Eldec LLC
Phone: (248) 364-4750
www.eldec.net

Inductoheat
Phone: (800) 624-6297
www.inductoheat.com

What's the Latest in Heat Treating?

The following article highlights some of the new heat treat products, technologies and industry news articles recently featured on *www.geartechnology.com*.

Solar Atmospheres California

COMPLETES FACILITY EXPANSION

Solar Atmospheres of California (SCA) has announced the completion of its most recent facility expansion. The new expansion allows SCA to double its current heat treating capacity on the west coast while continually striving to meet the needs of an ever growing customer base.

Project expansion began taking shape in July 2016 with ground breaking for a new 25,000 sq. ft. building. Upon completion of building construction in July 2017 and, applying the lessons learned from SCA's initial facility build in 2010–11, SCA immediately began the design, fabrication and installation of all required support systems including water and gas delivery.

In preparation for the added growth, SCA has procured an additional four vacuum furnaces from sister company Solar Manufacturing (SMI) based in Souderton, PA.

Additional state-of-the-art vacuum heat treating equipment includes an SMI Model HFL-5748-10IQ-VC "High Pressure Vacuum Gas Carburizing Furnace." The furnace features a rigid graphite hot zone design measuring 36"W × 36"H × 48"D, 35" Varian diffusion pump for sustained high vacuum processing, low pressure vacuum carburizing capability, operating range of 600 °F–2,200 °F (maximum temperature 2750 °F), maximum cooling pressure of 10 Bar (135 psig) with 300HP gas blower and maximum loading capacity of 7,000 lbs.

Another new furnace is the SMI Model HFL-7472-10IQ-VC "High Pressure Vacuum Gas Carburizing Furnace" The furnace features a rigid graphite hot zone design measuring 48"W × 48"H × 72"D, 35" Varian diffusion pump for sustained high vacuum processing, low pressure vacuum carburizing capability, operating range of 600 °F–2,200 °F (Maximum Temperature 2,750 °F), a maximum cooling pressure of 10 Bar (135 psig) with 300HP gas blower and a maximum loading capacity of 15,000 lbs.

The third furnace is an SMI Model HFL-7472-2EQ "All Metal Hot Zone with Isolated Gas Quench System," featuring a 6-layer all moly hot zone design measuring 48"W × 48"H × 72"D, 35" Varian diffusion pump with "isolated" external gas quench system for optimized sustained high vacuum processing of sensitive materials, an operating range of 600 °F–2,400 °F (maximum temperature 2,800 °F), and a maximum loading capacity of 15,000 lbs.

The final furnace is an SMI Model HCB-120288-2EQ "120"DIA × 288" Long Horizontal Car-Bottom Furnace," featuring a rigid graphite hot zone design measuring 96"W × 96"H × 288"D, multiple 35" Varian diffusion pumps for sustained high vacuum processing, an operating range of 600 °F–2200 °F (maximum temperature 2,600 °F) and a maximum loading capacity of 150,000 lbs.

All Solar Manufacturing furnaces are designed for high performance, low maintenance and energy efficient results.

"We are very thankful for the opportunity to grow our facility," states Derek Dennis, president, Solar Atmospheres of California. "Every SCA employee appreciates the trust and confidence that our customers have placed in our abilities to service their Vacuum Heat Treating, Brazing and Carburizing requirements. Our focus remains on providing the highest quality product with unsurpassed customer service on-time, everytime in the safest, most efficient and environmentally friendly manner. The last 6+ years of providing vacuum processing services in Southern California have proven to be both challenging and rewarding. We look forward to working with our current customer base along with new customers in solving their heat treat challenges. SCA understands the importance we play in our customers' supply chain, especially where delivery and quality are expected. These new facility expansions well help us meet these expectations." (*www.solaratm.com*)

Seco/Warwick

PROVIDES RETECH FURNACE FOR PRODUCING LARGE COMPONENTS

Seco/Warwick Group recently provided a Retech Consumable Electrode Casting Furnace to AMRC Castings (AMRCC), capable of delivering up to 1,000 kg of molten titanium, which has just produced the heaviest ever ceramic shell casting in this material from a single pour in Europe. The achievement was unveiled by the Castings Group of the Advanced Manufacturing Research Center (AMRC), a world-class center for research into advanced manufacturing technologies used in the aerospace, automotive, medical and other high-value manufacturing sectors.

Working with U.K. SME pump manufacturer Amarinth, the component, an industrial centrifugal pump housing for highly corrosive applications in the chemical and petrochemical sectors, was produced from a 680 kg melt with a finished part weight in excess of 200 kg. The furnace is equipped with four interchangeable crucibles which form an integral part of a manufacturing cell capable of producing castings up to 500 kg in weight and 2,000 mm in diameter by 2,500 mm in length.

“Last year we were part of creating the first European recycling and refining plant for titanium alloys; now we are proud to announce our joint development with AMRCC, opening new business opportunities for Britain. By staying focused on our clients and their successes, we work together to deliver quantifiable results, enabling our partners to gain competitive advantage in their

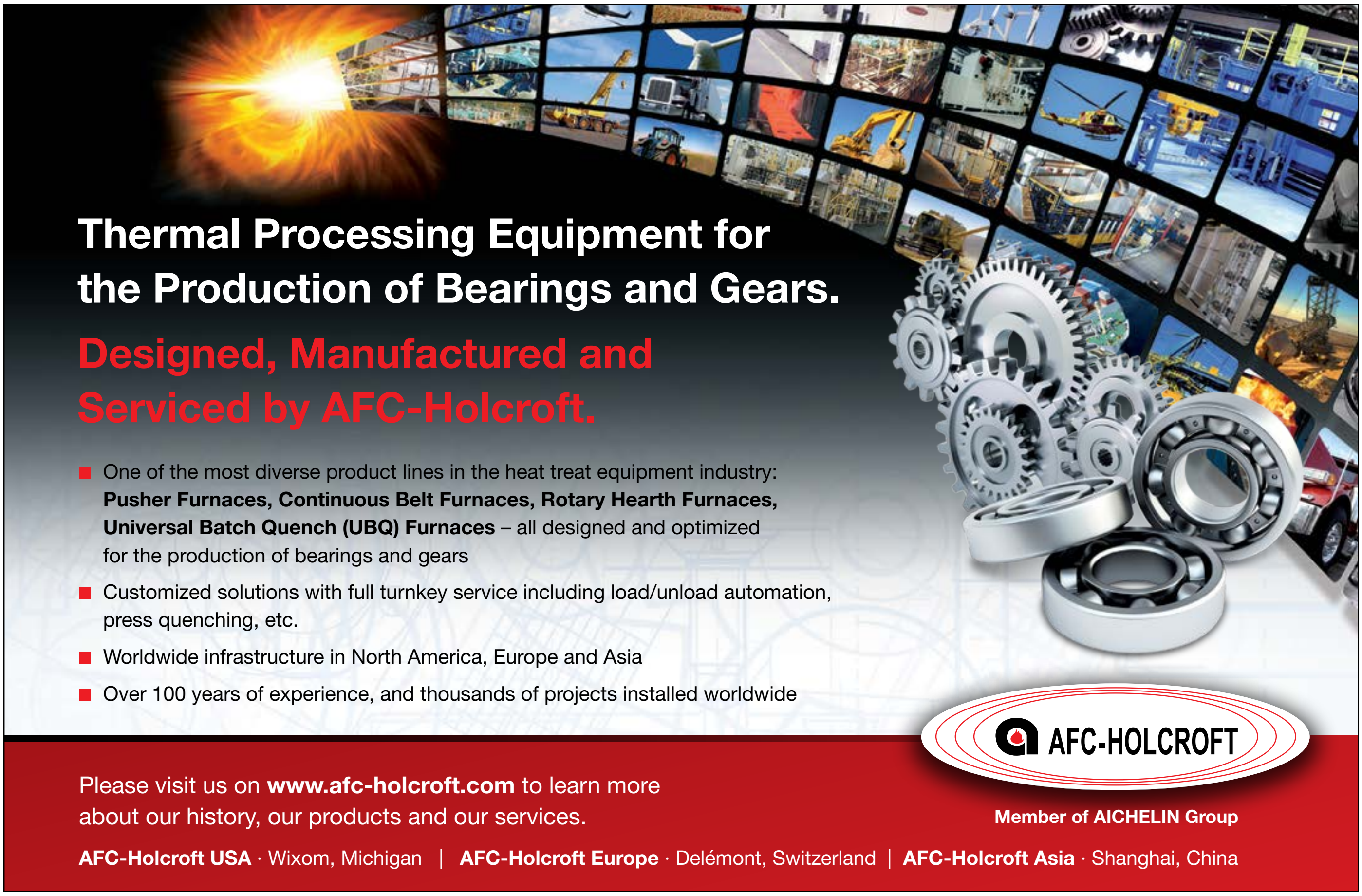

sector," said Earl Good, managing director, Retech Systems.

The Castings Group of the Advanced Manufacturing Research Center, the only U.K. titanium equiax casting facility, is already working towards a new goal — to pour over 1,000 kg of titanium, producing two centrispun parts each weighing in excess of 250 kg, fully testing the design parameters of their Retech consumable electrode castings furnace. The group's new milestone is planned for May 2018.

"AMRCC is dedicated to working with manufacturing businesses operating in the global supply chain, ranging from multi-national aerospace giants to local SMEs. We decided to cooperate with Retech, a global leader in the supply of metallurgical processing equipment, and thanks to their technology we achieved a record casting at the first attempt; a significant step forward for us and the U.K. as a whole," said AMRCC's General Manager, Richard Cook. (*www.secowarwick.com*)

Applied Process

OPENS NEW ARKANSAS PLANT

Applied Process, Inc. will expand with a new multi-million-dollar heat treatment plant in Fort Smith, Ark. The 51,000-square-foot plant will house six furnaces and add at least 30 jobs. The plant is expected to be fully operational in the 3rd quarter and will serve customers in the Midwest and South.

"We are very excited to announce our expansion in Fort Smith," said Chief Executive Officer Harold Karp. "Record sales performance in 2016 and 2017, combined with a strong new product forecast, make this the right time to expand."

Applied Process plants in Livonia, Mich., and Oshkosh, Wis., will remain in operation, serving the automotive, agriculture, aerospace, heavy truck, railroad, mining industries, as well as the military. The Oshkosh facility houses the world's largest integral quench batch austempering furnace which is capable of austempering parts up to 20,000 lbs. in weight.

"The additional capacity in Fort Smith will allow us to continue to offer industry-leading levels of customer service, quality and turn time," said Steve Metz, vice president of sales and marketing. "The new facility will allow us to expand into new markets and serve a broader geographic customer base."

Rusty Rainbolt, who has been with Applied Process for three years on the sales team, will be plant manager. Rainbolt holds bachelor's degrees in engineering and marketing from Oklahoma State University. "Rusty's engineering, sales and product experience, along with a strong, experienced leadership team, will ensure a smooth start-up of the new facility," Karp said.

(*www.appliedprocess.com*)

Messe Stuttgart

PRESENTS NEW CASTINGS AND FORGINGS TRADE SHOW IN 2018

CastForge is a new trade fair for castings and forgings as well as machining. Messe Stuttgart recently presented the concept of CastForge to interested companies within the framework of several rounds of talks. There was good feedback from the participants who unanimously welcomed the concept, date and venue. The event will take place June 5–7 2018 at the Stuttgart Trade Fair Center.

"The presentations gave the event organizers lots of valuable ideas," said Gunnar Mey, department director for industrial solutions at Messe Stuttgart.

"In our opinion, there has not been such a specific trade fair which addresses our products and services. We expect to meet a customer base which is specifically looking for our services and wants to establish new contacts in the industry," said Timo Richter, head of sales and marketing at Richter Formteile GmbH.

Hermann Bayer from RILE Management und Vertriebs GmbH also spoke in favor of the new trade fair. "As subcontractors we serve diverse industries, making it very difficult to find a suitable trade fair at which we can permanently exhibit. Several good contacts and requests from interested parties who we do not yet know will help us moving forward," Bayer said.

Bernard Hauffmann from ArcelorMittal Ringmill S.A. added: "As far as we know, CastForge is the first trade fair which specifically addresses this industry. First and foremost, we want to meet potential customers and partners here who are interested in our product as the trade fair is aimed at cast and forged products."

With CastForge, Messe Stuttgart gives the industry for castings and forgings as well as their machining its own platform. It showcases the entire value-added chain from the cast or forging blank to machining through to the final component and for the first time offers manufacturers an opportunity to present their range of cast iron, grey cast iron and

spheroidal graphite iron as well as non-ferrous castings and forgings to a wide audience.

For Ulrich Kromer von Baerle, president of Messe Stuttgart, the validation from the industry is not surprising: "With CastForge we have launched a trade fair topic at the right time which strikes a chord with companies. For many companies there was only the opportunity to showcase products and services within the framework of industry and user trade fairs. Now for the first time their castings and forgings as well as their skills as processors take center stage at a trade fair." (*www.messe-stuttgart.de/castforge*)

Ipsen

DESIGNS VERTICAL, HIGH-PRESSURE QUENCHING FURNACE

Ipsen recently designed and built a vertical, high-pressure quenching furnace, complete with twin cooling systems and a work volume of 350 cubic feet. During the testing phase, the furnace quenched with 1,000 horsepower (.75 megawatts)—a remarkable achievement that began as an idea just months prior. As is typical with a custom build, the customer came to Ipsen with specific requirements: they needed a large furnace with a very aggressive cooling rate. During the design phase, Ipsen's Engineering Team determined that twin cooling systems to provide 1,000 horsepower quenching capability were the right solution due to the customer's process requirements and the geometry and cross-section of parts.

Ipsen Engineers, alongside the customer, looked on during the testing phase. "We saw the furnace backfill and then go into quench," said Craig Moller, chief engineer. "It took us a minute to realize we were experiencing a groundbreaking design and test, with cooling curves that we've never seen for a furnace of this size." (*www.ipsenusa.com*)

For Related Articles Search
heat treating
at www.geartechnology.com

FOR UNSURPASSED QUALITY, PERFORMANCE AND VARIETY IN GEAR OILS....

LOOK TO LUBRIPLATE®

GEAR OILS

Lubriplate's complete line of premium-quality gear oils has been formulated to deliver unsurpassed performance in a wide range of gear reducers. They meet and exceed the performance specifications of most gearbox manufacturers and interchange directly with most OEM oils. Available products include...

SYN LUBE SERIES 150 - 1000
100% SYNTHETIC PAO-BASED GEAR OILS

- High-performance, 100% synthetic, polyalphaolefin (PAO)-based gear oils.
- Compatible with petroleum-based oils and most seals for easy conversion.
- Available in ISO viscosity grades 150, 220, 320, 460, 680 and 1000.

SYN LUBE HD SERIES
HEAVY-DUTY, EXTREME PRESSURE (EP) 100% SYNTHETIC, PAO-BASED OILS

- Super heavy-duty, polyalphaolefin (PAO)-based synthetic gear lubricants.
- Formulated to meet AGMA EP (Extreme Pressure) requirements.
- For Heavy-duty, high load applications where an EP oil is required.

SPO SERIES
HIGH-PERFORMANCE, ANTI-WEAR FORTIFIED, PETROLEUM OIL-BASED, INDUSTRIAL GEAR OILS

- Petroleum oil-based anti-wear, rust & oxidation inhibited (R&O) gear oils.
- Can be used with silver alloy, copper, and copper alloy bearings.
- Premium quality, high-performance, petroleum oil-based gear oils.

SFGO ULTRA SERIES
NSF H1 REGISTERED FOOD GRADE 100% SYNTHETIC, PAO-BASED GEAR OILS

- NSF H1 registered and NSF ISO 21469 certified - food machinery grade.
- 100% synthetic, PAO-based fluids for food processing and bottling plants.
- Available in ISO viscosity grades 150, 220, 320, 460, 680 and 1000.
- Fortified with Lubriplate's proprietary anti-wear additive XTREMITY

PGO & PGO-FGL SERIES
ADVANCED 100% SYNTHETIC PAG-BASED GEAR OILS

- Ultra High-Performance, Polyalkylene Glycol (PAG)-Based, Gear Lubricants.
- ECO-friendly- Inherently biodegradable, provides long service life, energy conserving.
- PGO-FGL Series is NSF H1 registered and NSF/ISO 21469 certified food grade.

SYNTHETIC WORM GEAR LUBRICANT

- 100% Synthetic, ISO 460 grade, polyalphaolefin (PAO)-based worm gear oil.
- Formulated especially for worm gear applications.
- Provides excellent lubricity and oxidation resistance.

APG SERIES
HEAVY-DUTY PETROLEUM OIL-BASED EXTREME PRESSURE (EP) GEAR OILS

- High-quality, petroleum-oil based, extreme pressure (EP) gear oils.
- Meets military specification MIL-PRF-2105E and MIL-L-2105D.
- Conforms to API categories GL-3, GL-4, GL-5, MT-1.

KLING GEAR OILS
HEAVY-DUTY, TACKY RED, PETROLEUM OIL-BASED EXTREME PRESSURE (EP) GEAR OILS

- Heavy-duty, tacky, red, extreme pressure (EP) petroleum-based gear oils.
- These tacky, adhesive, extreme pressure oils cling tenaciously to gear teeth.
- Formulated for heavy equipment and heavy service industrial applications.
- Meets military specification MIL-PRF-2105E and API classification GL-5.

"It's the Film"® PREVENTS WEAR and CORROSION LUBRIPLATE SUPER-LUBRICATION

Lubriplate® Lubricants

Newark, NJ 07105 / Toledo, OH 43605 / 800-733-4755
To learn more visit us at www.lubriplate.com

Backed By: Lubriplate® ESP

Complimentary Extra Services Package

Plant Surveys / Tech Support / Training
Color Coded Lube Charts & Machine Tags
Lubrication Software / Follow-Up Oil Analysis

KAPP Tools

Excellence In Manufacturing

KAPP NILES

(303) 630-1792
tools-usa@kapp-niles.com

kapp-niles.com
kapp-usa.com

ORRIS DRIVE
INCORPORATED

INNOVATION EXCLUSIVELY YOURS

- Gear Cutting service
- Worm Grinding Service
- Customized products

orris.drive@msa.hinet.net

B2B.WORLDTRADE.ORG.TW/16697150
ESTABLISHED IN 1998 -OEM- ISO:9001:2015

Gear Research Institute

GET IN GEAR

GEAR RESEARCH AND TESTING SPECIALISTS

- Testing and evaluation of gear tooth:
  - Bending and contact fatigue properties
  - Impact strength
  - Scoring and scuffing resistance
- Friction loss in gear meshes
- Rolling contact fatigue testing
- "Loss of Lube" simulation and testing
- Custom test applications
- High cycle fatigue testing
- Steel cleanliness assessment
- Heat treatment evaluation

Gear Research Institute (GRI)
An ASME, AGMA Institute at Penn State
gearresearch.org

Aaron Isaacson
(p) 814-865-5832
(e) aci101@arl.psu.edu

Contact GRI about Corporate Membership today!

PennState
Applied Research Laboratory

Nordex®
INCORPORATED
turnkey solutions with a higher level of intelligence

sales@nordex.com
eng@nordex.com
(203) 775-4877

ISO Certified / ITAR Registered / Trace Certified

- Standard Components
- Made to Print Parts
- Design & Engineering
- Gears, Pulleys & Racks
- Assemblies

Nordex.com

SHAPING THE FUTURE OF INDUCTION

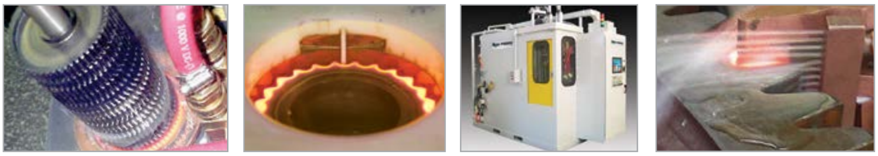

Your Global Source for Service, Support & Manufacturing

- Scanners
- Single Shot
- Lift & Rotate
- CHT
- Tooth by Tooth
- Part Development
- Power Supplies
- Parts & Service
- Installation & Construction

World Headquarters
1745 Overland Avenue
Warren, Ohio USA 44483
+1-330-372-8511

Ajax TOCCO Magnethermic

24 / 7 Customer Service: 800-547-1527

www.AjaxTocco.com

Sharpening Services

- Hobs
- Milling Cutters
- Shaper Cutters
- Shaving Cutters
- Broaches

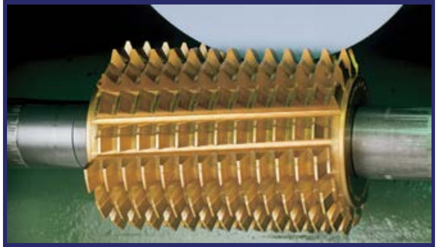

Service Centers

Hoffman Estates, IL
Phone: 847.649.1450
Fax: 847.649.0112

East Tawas, MI
Phone: 989.362.0414
Fax: 989.362.2720

Querétaro, Mexico
Phone: 52 442 217 34 45
Fax: 52 442 217 34 46

sales@star-su.com
www.star-su.com

oelheld
innovative fluid technology

Innovative grinding fluids
to get your production into gear.

Human Technology for man, environment and machines
HUTEC

oelheld U.S., Inc.
1100 Wesemann Dr
West Dundee, IL 60118
phone: +1–(847)–531-8501
fax: +1–(847)–531-8511
E-Mail: hutec-us@oelheld.com
www.oelheld.com

The Power of One²

Your Objective:
One face in perfect alignment with another. *For infinity.*

No problems. No distress. No delays.

That's the same objective you have for choosing your gear producer.
Circle Gear's objective is to engage with every customer's objectives.

- **One to 1000 gears**
- **Customer designed or reverse engineered**
- **Gearbox repair, rebuild or redesign**
- **OEM or end-users**
- **ISO 9001:2015 Certified**

1501 S. 55th Court, Cicero, IL 60804
(800) 637-9335
(708) 652-1000 / Fax: (708) 652-1100
sales@circlegear.com
www.circlegear.com

Circle Gear

Spiral and Straight Bevel Gears *(Cut, Ground or Lapped)* • Spur Gears • Helical Gears • Long Shafts • Herringbone Gears • Involute and Straight Sided Splines • Internal Gears • Worm and Worm Gears • Racks • Sprockets • ISO Certified

MADE IN ★ THE USA

Partnering with QualityReducer to provide Gearbox repair, rebuilding and reverse-engineering.

gear TECHNOLOGY
Power Transmission Engineering
HEAT TREATERS

A Look at Intelligent Workholding and Toolholding

New Solutions Aim at Reducing Changeover Times and Improving Reliability

Matthew Jaster, Senior Editor

The notion of smart workholding and toolholding is a bit redundant when you think about it. Sure, the marriage of information, technology, engineering and communication to change how products are manufactured can be called smart, but isn't it just workholding and toolholding in 2018?

We're simply at a point in manufacturing where robotics, automation, sensors and condition monitoring can be applied to everything from heat treating to inspection to gear grinding. Workholding and toolholding are just other areas in manufacturing that are getting "smarter" because the gear industry is demanding that mechatronics and digitalization play a significant role in the development of new products.

The "smart" designation won't last long because every process will be smart, every gear application integrated and every shop floor will be paying close attention to quality, efficiency and cost savings potential. Here's a few ways these concepts are being applied to workholding and toolholding today.

Röhm Takes on Challenges of Robotics in Workholding

Advanced turning machine chucks especially designed for gear production now provide quick-change capability. More importantly, they offer the repeatability and precision necessary for low-to-high-volume part production while simultaneously reducing changeover times. In a recent article by Matthew Mayer, CEO, Röhm Products of America, Mayer examined a shop that has benefitted from these innovative chucks: Global Gear & Machining.

The KZF-S collet chuck is designed specifically for surface face grinding and hard turning gears.

The quick-change capability of the KZF-S collet chuck is key to repeatability.

Global Gear is a Downers Grove, Illinois-based manufacturer serving Tier 1 and Tier 2 diesel engine OEMs and other engine manufacturers in the broad automotive and construction/agriculture industries. Their choice of workholding is the KZF-S collet chuck from Röhm, an external clamping chuck designed specifically for surface face grinding and hard turning gears.

In the past, Global Gear would dedicate seven operators to seven machines for a single gear family. Now, with the KZF-S chuck, a single operator can handle one cell with eight machines or multiple four-machine cells.

The key to quick-change workholding solutions is a BT-style collet that mounts to a machine in a manner similar to how a bayonet-style lens mounts to a camera body. The resulting collet is longer and supported by the back face and taper for parallelism and accuracy, respectively. To change from one collet to another with this system, including clamping down on the part and verifying its orientation, requires no more than 60 seconds in total.

A big part of the quick verification process comes from the fact that the system uses a gear tooth pattern and clamps on every point of a gear's diameter rather than only three or six points. By clamping onto every tooth, the chuck ensures the precision of the gear's diameter in relation to its pitch line. This approach delivers exceptional repeatability and gear cylindricity without arduous inspection processes as the chuck can simply take an average of all teeth locations to eliminate inspection errors.

Robots can present challenges when it comes to modern quick-change workholding. It was easy to integrate traditional pin-style collet systems into automation solutions, but chucks that clamp onto every tooth of a gear require more complex robot movements. The solution is a free-floating rotational axis.

Even helix-shaped gears can be mounted into these chucks by robots when programmers instruct them to utilize a free-floating rotational axis. While applying pressure toward the chuck, the part's free-floating state in the robot's gripper allows the gear to guide itself in, much the same way as when gears are loaded manually. Of course, every system is vulnerable to human error, whether it occurs when manually changing a chuck or programming a robot to do so. To avoid any issues, workholding OEMs equip quick-change chucks with air sensing that will detect improper part seating and warn the operator. Operators can load a gear, make an initial cut, inspect it and produce a perfect gear, all with the assurance that any mistake will be easily detected and corrected before it can slow down production. For Global Gear and other gear suppliers, products like Röhm's KZF-S chucks have made it possible to thrive in a globally competitive market. The quick-change capability is what ties together every aspect of their production cells – as long as the chuck's location is established, perfect repeatability can easily be maintained from one collet to the next. As the automotive industry continues to transform transportation, suppliers and the manufacturing system OEMs they rely on have succeeded in matching their pace and creating innovative solutions that will help build the future automakers envision.

Intelligent Clamping with Hainbuch

Hainbuch's TOPlus chuck is just one example of a product that hints at the possibilities of the future of workholding. The TOPlus chuck offers more holding power and higher output due to its pyramid arrangement of guide surfaces. The clamping head rests with full-surface contact in the chuck body—even with large workpiece tolerances. This geometry ensures that TOPlus is less sensitive to contamination. The chuck is suitable for raw material, cast and forged parts as well as fine-particle non-ferrous metals such as brass.

Additionally, it offers integrated sensor technology that permanently measures the actual clamping force applied to the workpiece. Using contactless transmission of both data and energy, measurement results are sent directly to the machine´s control system for processing. The control system performs a comparison with the target values and then outputs messages or makes adjustments as required. In-line checking of the

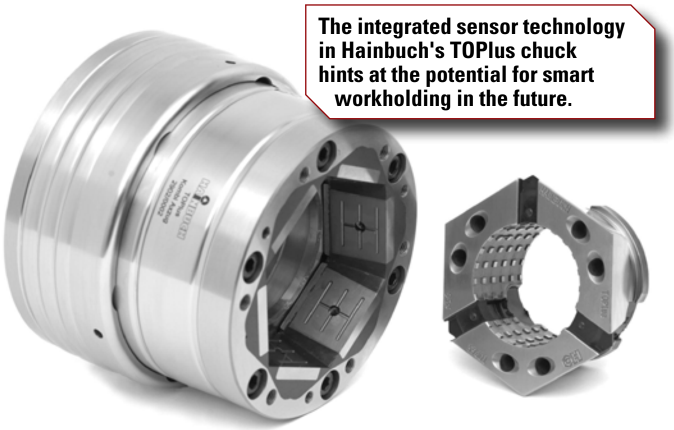
The integrated sensor technology in Hainbuch's TOPlus chuck hints at the potential for smart workholding in the future.

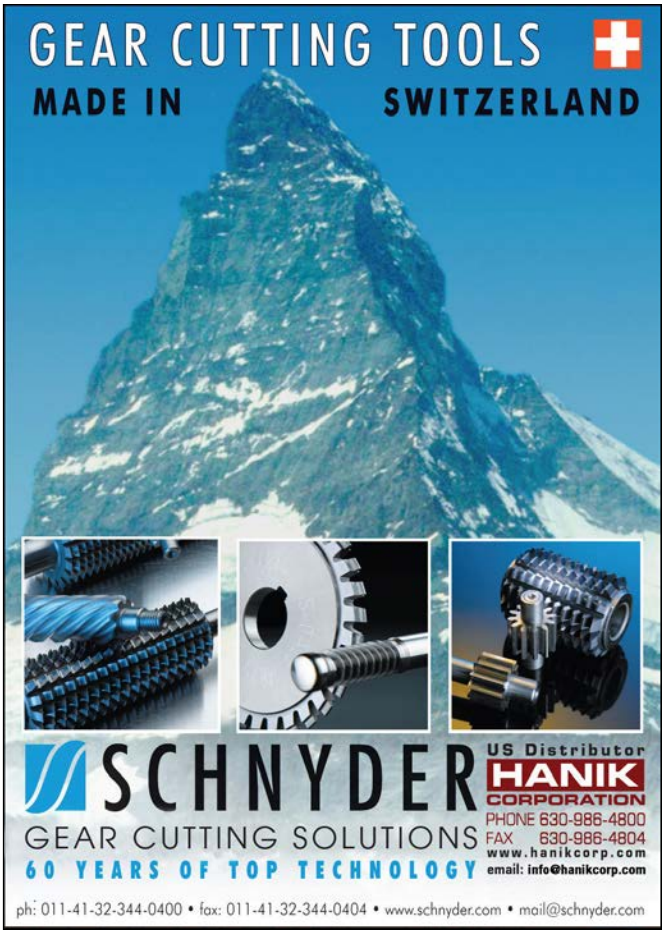

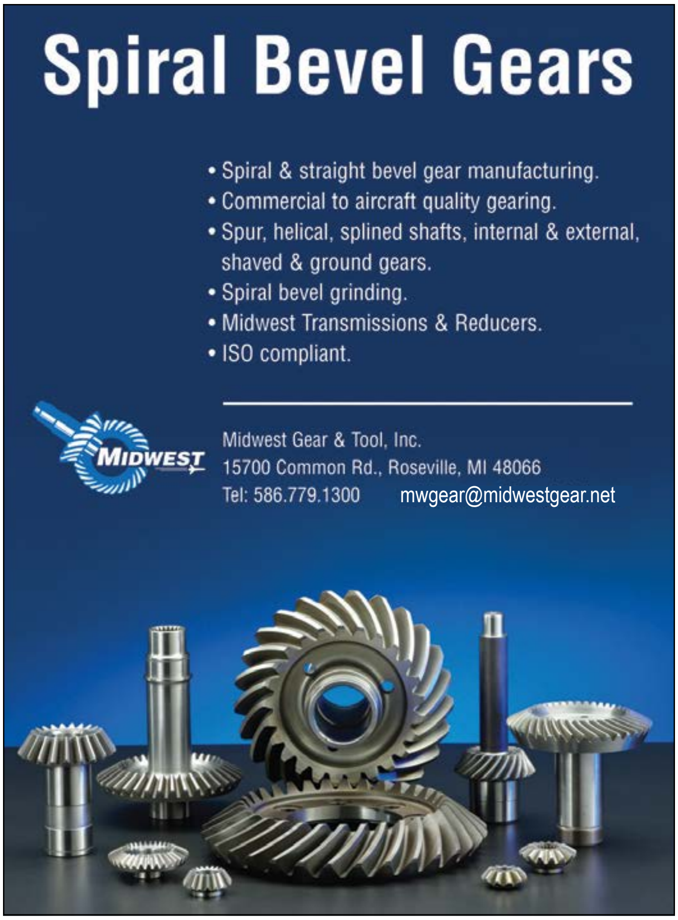

dimensions of each workpiece when it is clamped can even be performed directly using an integrated system of measurement sensors. The temperature near to the workpiece is also monitored to allow temperature compensation.

Using the data harvested by the control system, it is possible to perform condition monitoring for both safety and machine efficiency. This is a mandatory prerequisite for need-oriented and status-oriented preventive maintenance and servicing. However, many modern condition monitoring systems put very tough requirements on the sensor systems, data capture and automated measurement data processing, as well as system specific knowledge.

But the cost savings potential is noteworthy because the expected working life of critical machine parts can be exploited while any required maintenance interventions can simultaneously be planned to mesh with production schedules. This makes it possible to prevent unnecessary downtime which in turn increases machine availability and reduces production shortfalls.

Essentially, the chuck can detect reject parts. If a workpiece breaks, it is discarded and the value-adding process is interrupted. This improves quality and reduces personnel costs. As a result, employees can focus more on proactive tasks. Permanent monitoring reduces the risk of workpiece loss and the resulting damage to man and machine.

The chuck has even won accolades as an innovative intelligent clamping solution. First from the Baden-Württemberg Industry 4.0 Alliance and then again at the AMB trade fair in Stuttgart.

Smart Gripping with Schunk at Hannover

In the years to come, digitalization, mechatronization and automation of production processes, will inspire the emergence of a new mindset in industrial production. The focus here is on three aspects: communication between all the components involved, maximum transparency on the system, component, control and company levels, and finally, flexible responses to external and internal events. Reduction in production costs and set-up times as well as providing efficient, intelligent, mechatronic components is Schunk's objective moving forward. Intelligent, compact, and easy to operate – that's how Schunk sees the gripping of tomorrow.

One of Schunk's latest innovations is the EGL 90 mechatronic parallel gripper. The EGL 90 offers variable gripping force between 50 and 600 N and was specifically developed for industrial applications.

Since the finger position, closing speed, and gripping force are freely programmable within a maximum stroke of 48 mm per finger, diverse components with a weight of up to 3 kg can be precisely handled in force-fit gripping. The gripper fingers can be prepositioned to reduce cycle times. The entire control and power electronics of the EGL are integrated to save space allowing decentralized operation and even mobile use due to the 24V DC operating voltage.

Standard Profibus DP and CAN-Bus interfaces allow fast and easy integration in higher level system controllers. The gripper also features a USB-port as a service interface. A brushless servo motor ensures continuous and reliable operation with no maintenance required. To maintain the position in the event of a power outage, the gripper features an electrically operated brake.

Since the EGL fulfills industrial standards and the basic version is connected only by means of industrial connectors, installation time is greatly reduced. The powerful mechatronic gripper is compatible with the world's most extensive standardized line of modules for gripper systems from Schunk. In combination with quick-change systems and other robot accessories, it can significantly increase the flexibility and efficiency of handling processes. It is ideal for diverse applications in the field of industrial assembly technology, mechanical engineering, and lab automation.

Schunk believes the collaboration between humans and robotics will play a significant role in the future. At Hannover Messe 2018, Schunk is exhibiting clever mechatronic components to visionaries as well as practical technicians. With their plug and play 24 V modular system, the gripper system specialist defines a new standard in assembly automation.

"Even though pneumatic components will continue to play an important role, the trend is clearly moving towards mechatronics," said Henrik A. Schunk, CEO of Schunk. "The digital transformation of industrial production requires a networked interaction between all components involved, especially in the field of handling and assembly. At Hannover, we'll show how broad the spectrum of mechatronic gripping is, how easy the intelligent modules are to use now, and what opportunities they offer for process monitoring closest to the part, i.e. directly on the workpiece."

Schunk will be focusing on the mechantronic aspects of workholding for the foreseeable future.

For more information:

Hainbuch America Corp.
Phone: (414) 358-9550
www.hainbuchamerica.com

Röhm Products of America
Phone: (770) 963-8440
www.rohm-products.com

Schunk
Phone: (919) 572-2705
www.schunk.com

For Related Articles Search
workholding
at www.geartechnology.com

Small Toolholding Changes Lead to Job Shop Milling Improvements

Despite the fact that more than 750,000 CNC mills were put into service in the past 15 years in the United States, CNC machining job shops often hover at the bottom of the totem pole where there's little room for error–as most bids are won by a 1-2 percent price variance. Most low-to-mid volume run production machine shops struggle in achieving their share of the 5-10 percent maximum profit margins typically realized on most jobs.

Given these constant challenges, along with changing consumer demands, overseas competition, a lack of skilled labor, and across-the-board changes in industry–the goal becomes how to improve efficiency, quality, and profits in every business phase. CNC machining job shops are essentially multi-stage process operations where there is potential for improvement at each stage. Consequently, achieving a shop's potential while expanding its business largely depends on how many of those improvements can be capitalized upon.

Ultimately, being better and faster keeps costs lower while raising the bar on potential profits. The ability to quickly adopt new machine tool technologies and cutting tool strategies becomes paramount to the overall success equation for today's machining job shop sector.

Vibration and chatter can result in added man hours for gear production. A complex gear must have flawless edges. If it doesn't, the manufacturer is forced to spend more time on finishing operations to get the component as precise as possible. While the future points at robotics, sensors and automation in workholding and toolholding, there's also an argument to be made that simple, efficient toolholding changes can effective for any job shop.

One of the quickest, simplest investments a job shop can make starts at the spindle with JM Performance Products, Inc. (JMPP) high torque retention knobs. The knobs overcome a key design flaw inherent in CNC v-flange tooling, eliminating the toolholder expansion responsible for costly and ongoing CNC milling and boring issues.

JMPP designed the knobs to be used in existing toolholders to eliminate the bulge at the small end of the holder, which stops it from making full contact with the taper of the spindle. By increasing contact with upwards of 70 percent more spindle surface, a wide range of CNC milling issues are overcome including: vibration and chatter, poor tolerances, non-repeatability, poor finishes, shortened tool life, excessive spindle wear and tear, run-out, and shallow depths of cuts.

According to JMPP President, John Stoneback, "Bridging this gap of missed productivity can conservatively help job shop operations achieve a 10-20 percent competitive advantage per hour via faster set-ups, better feed rates, and more rigid tools–reducing tooling cost by 20-50 percent or more. In essence, every tool on the machine works better and faster to make job shops more competitive and increase profit margins dramatically."

The fact is all U.S. manufacturers will have to bundle more technology in their products to compete–at home and globally. The power of combining lean manufacturing with modern technology is even more important to today's small-to-medium job shop where everyone is competing for the same work. The positive short-and-long term effects of optimizing production methods with JMPP's High Torque retention knobs can help shops realize their full potential with a low risk/high return ROI ratio.

According to JMPP Plant Manager, Craig Fischer, "A small advantage in labor hour savings alone can help impact a job shops' leverage in getting the job. With payroll hours reduced and machine hours freed up, the collective ability to get more work goes up. Additionally, everyone's tooling budget keeps going up as the cost of buying carbide from China increases. Factoring in a conservative savings on carbide tooling costs of even 5 percent when using our knobs is significant, as all of these value-added factors collectively add up in a job shop winning more work in today's competitive climate."

Key design elements of JMPP's patented High Torque Retention Knobs include: Longer than traditional retention knobs, with a precision pilot to increase rigidity, a relief below the flange forces threads into a deeper cross section of the toolholder. The knobs are hard turned to ensure precision fit, and are balanced by design with threads cut to start and finish 180 degrees from each other. ⚙

For more information:

JM Performance Products, Inc.
Phone: (440) 357-1234
www.jmperformanceproducts.com

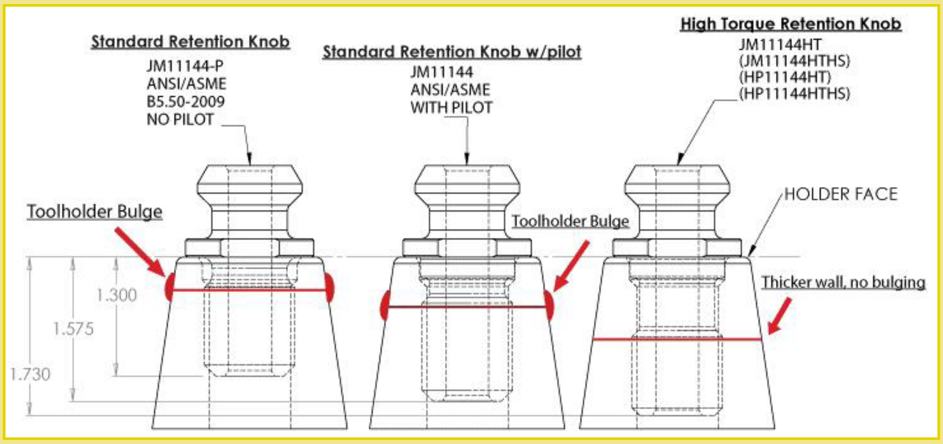


WE ARE

Effect of Non-Metallic Inclusions on Bending Fatigue Performance in High Strength 4140 Steel

Michael E. Burnett, Peter C. Glaws and Daniel K. Gynther

Introduction

The fatigue performance of three sets of quench and tempered 4140 steel samples, representing three distinctly different inclusion populations — low oxygen/low sulfur, high oxygen/low sulfur and low oxygen/high sulfur — were evaluated through a series of various bending fatigue tests. Three different bending fatigue tests with differing stress ratios were employed, including: rotating bending (−1); single-tooth bending (0.1); and modified Brugger (0.1). The inclusion populations for each of the three steel sample sets were characterized using both a SEM-based image analysis system, primarily for the micro-inclusions, and a high-resolution UT system for the macro inclusions. All three sample sets were evaluated using both longitudinal and transverse specimens in all the bending fatigue tests. The transverse samples displayed significantly lower fatigue performance (typically ~50% lower fatigue strength values) than the longitudinal samples. Furthermore, the high-sulfur sample set clearly had the lowest performance in the transverse orientation. While there was more scatter with the data on the longitudinal samples, the high-oxygen sample set had a lower fatigue strength and a higher percentage of the failures initiating at subsurface oxides than the other two sample sets.

In general terms, non-metallic inclusions can have a measureable impact on many steel properties. Perhaps most significant is the effect on fatigue properties. Previous studies, compiled and reviewed by Murakami (Ref. 1), have demonstrated that a linear correlation exists between bending and axial fatigue strength and the ultimate tensile strength (UTS) in low- and medium-strength steels. However, in high-strength steels (Hv > 400) (*Note: a strong correlation exists between UTS and hardness in these steels. Accordingly, Vickers hardness is often used as a proxy for UTS in many fatigue studies.*) the linear correlation fails, and there is significant scatter in the measured fatigue strength (Refs. 1-4). This deviation from linearity often has been attributed to the presence of non-metallic inclusions. In many cases, the fatigue origin, often clearly identifiable by a "fish-eye" pattern, is observed to be subsurface with a non-metallic inclusion located at the center (Fig. 1). The effect of individual inclusions on the fatigue performance, and in particular the fatigue strength, of a given steel will be a function of the inclusion type, size, morphology, and location/orientation with respect to the principle stresses from the applied cyclical load. The properties of the inclusion/matrix interface also can play a significant role.

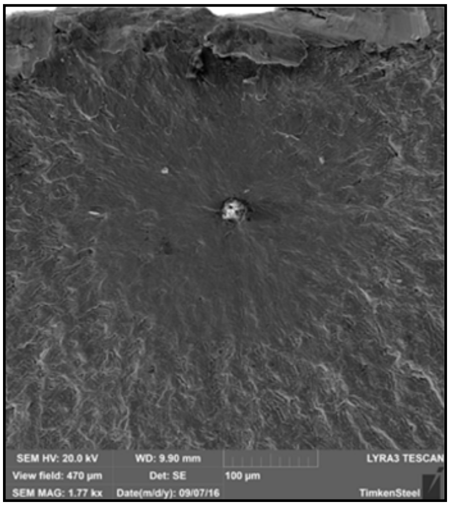

Figure 1 SEM image of subsurface fatigue initiation site showing common fish-eye pattern with globular oxide inclusion at the center.

The effect of non-metallic inclusions, especially oxides, on fatigue performance in bearings, gears, and other high-cyclic load applications has long been a subject of study. Our understanding of the relationship between inclusion content and fatigue performance has been enhanced with the continued improvement of tools and methods employed in steel cleanness measurement.

In the current study, single-gear tooth bending (STB), Brugger beam-type bending and rotating bending fatigue (RBF) tests were conducted on three sets of quenched and tempered 4140 steel samples, representing three distinctly different inclusion populations — low oxygen/low sulfur, high oxygen/low sulfur, and low oxygen/high sulfur. The inclusion populations for the three sample sets were characterized using both an advanced SEM-based image analysis system, primarily for the micro- inclusions, and a high-resolution UT system for the macro-inclusions.

Experimental

Materials. Three sets of 4140 steel samples of varying sulfur and total oxygen contents were employed in this study. Group A was low oxygen/low sulfur; Group B was high oxygen/low sulfur; and Group C was low oxygen/high sulfur. The compositions of each group are provided in Table 1.

The inclusion population of each sample group was fully characterized by SEM-based image analysis and

Table 1 Compositions of the 4140 steel sample groups used in the study

Sample Group	C	Mn	P	5	Si	Cr	Ni	Mo	Cu	Al	Ca*	O^*_{Tot}	N*
A Low O Low S	0.41	0.97	0.013	0.007	0.29	0.90	0.14	0.15	0.22	0.024	3	7	97
B High O Low S	0.41	0.96	0.014	0.008	0.29	0.90	0.14	0.15	0.22	0.022	4	15	97
C Low O High S	0.41	0.94	0.014	0.024	0.19	0.88	0.11	0.18	0.22	0.027	1	7	119

*Calcium, total oxygen, and nitrogen concentrations given in ppm.

Table 2A Measured oxide inclusion microcleanness and macrocleanness metrics for the three sample groups. Values in red are maximums.

Sample Group	Oxygen Content (ppm)	Total Oxide Area	Conc. $\sqrt{A} > 10$ µm $\sqrt{A} > 20$ µm	Oxide Stringer Length L > 100 µm L > 200 µm	SEV Oxide √Area (µm) Stringer Length (µm)	UT Metric (Oxides)	DIN 50602 (Oxide) OG+OA K1/K4
A	7	29.07	2.17 0.07	1.19 0.36	26.06 285	0.469	0.82/0.29
B	15	56.98	7.45 0.46	20.82 8.36	52.79 801	1.798	3.92/1.21
C	7	20.14	0.81 0.07	2.10 0.46	20.41 416	0.678	0.28/0.0

Table 2B Measured sulfide micro-cleanness metrics for the three sample groups; values in red are maximums.

Sample Group	Sulfur Content (wt. %)	Sulfide Area Total L > 100 µm	DIN 50602 (Sulfide) SS K1/K4
A	0.007	208.2 45.6	5.09/0.0
B	0.008	199.4 50.2	5.51/0.0
C	0.024	565.1 111.5	13.56/0.0

high-resolution ultrasonic testing. The key metrics for the oxide inclusion populations were total oxide area; area of large oxides; oxide stringer length; and area (all normalized by sample inspected area). Key metrics for sulfide inclusions included total sulfide area and area of large sulfides. Statistics of extreme values (SEV) analysis was also performed to provide additional information about the inclusion populations. To provide a description of the oxide and sulfide populations of the three sample groups in terms of an industry standard, the data from the SEM image analysis was configured to generate DIN 50602 values (K0 – K4). The measured values for inclusion population metrics are provided in Tables 2A and 2B. The respective DIN 50602 oxide (OG + OA) and sulfide (SS) plots are shown (Figs. 2A and 2B).

The inclusion evaluation showed that the relationship between total oxide area and oxygen content of the steel was approximately linear. Group B had about twice the total oxygen content, as well as about twice the total oxide area, as compared to Groups A and C. However, the concentration of large oxide inclusions (√Area > 10 or > 20 µm) was significantly higher in Group B, and was not proportional to oxygen content. For example, the concentration of oxides greater than 10 µm was about nine times higher in Group B, compared to Group C (Table 2A). This lack of proportionality was also illustrated by the DIN 50602 K0 – K4 cleanness (OA + OG) results (Fig. 2A). Furthermore, although Groups A and C had the same oxygen content (7 ppm), Group A had a higher concentration of large oxide inclusions and higher DIN 50602 K0–K4 cleanness (OA + OG) results. These results indicate that the concentration of large oxides does not necessarily depend on the oxygen content. Therefore, the oxygen content does not fully predict the nature of the oxide inclusion population.

In regard to sulfide inclusions, the total sulfide area, as well as the area of large sulfide inclusions, was linearly related to the sulfur content of the steel. Group C had a sulfur content that was three times higher than Groups A and B, and

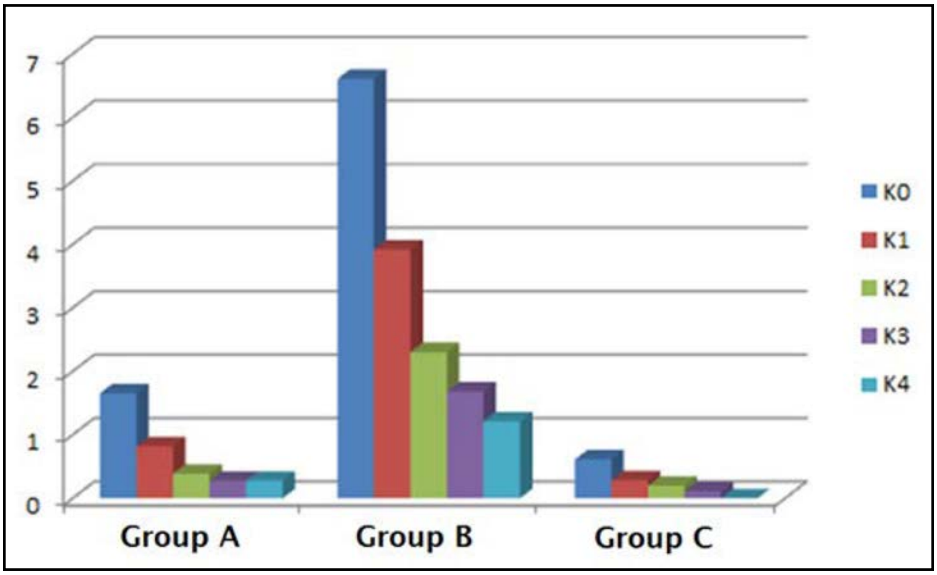

Figure 2A DIN 50602 K0—K4 cleanness (OA+OG) results for the three sample groups.

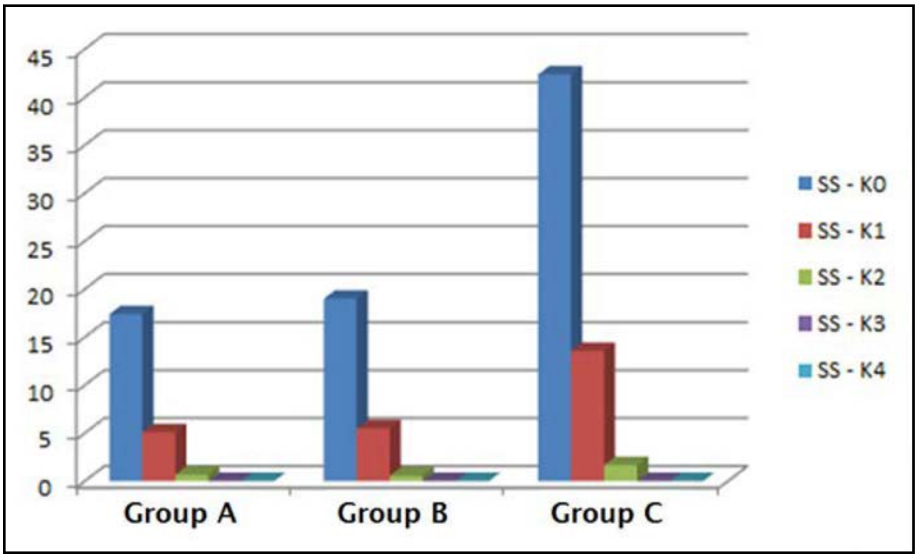

Figure 2B DIN 50602 K0—K4 sulfide cleanness (SS) results for the three sample groups.

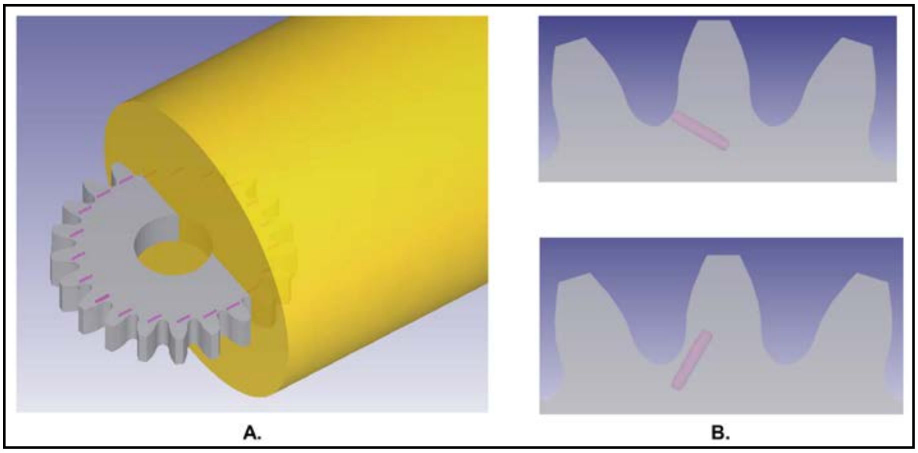

Figure 3 Orientation of spur gears machined from as-rolled bar stock (A), and the inclusion orientations (B), in the longitudinal test position (lower photo) and transverse position upper photo).

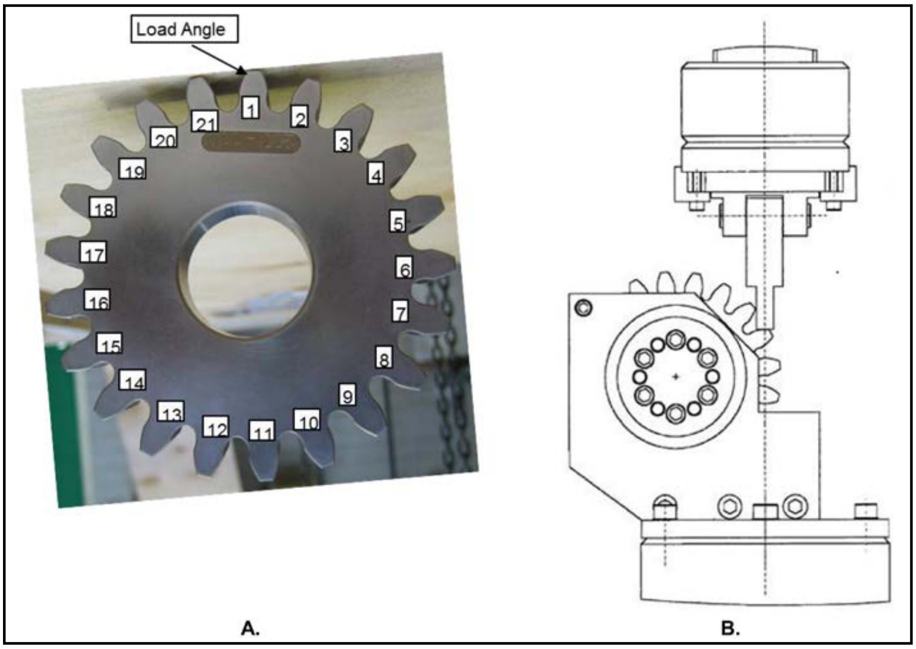

Figure 4 Machined spur gear with numbered teeth for testing showing the loading angle (A), and the testing fixture showing the loading gear tooth in the cyclic R = 0.1 loading condition (B).

all sulfide inclusion metrics were also approximately three times higher (Table 2B and Fig. 2B). It is important to note that the sulfide count and area metrics were significantly greater than the oxide count and area metrics in all sample groups. Even the high-oxygen/low-sulfur samples (Group B) showed that the concentration of the large sulfides (>100 μm^2) was more than four times greater than the concentration of the large oxides (>100 μm^2).

Fatigue Testing

Single tooth-bending fatigue. 4.2 modulus spur gears were manufactured from each steel condition (A, B, and C) and oriented such that both longitudinal and transverse orientations — with respect to inclusion orientation — were bending fatigue tested at the gear teeth root locations (Fig. 3). The gear steel blanks were through-hardened as follows: austenitized at 885 °C (1,625 °F) for 30 minutes at temperature, oil-quenched and tempered at 177 °C (350 °F) for one hour to an average hardness of 55 HRc (~595 Hv). Following heat treat, the gears were finish machined, followed by controlled, dual shot peening to maximize the near-surface compressive stress state in the tooth root area.

The 4140 spur gears were tested on a single tooth bending testing rig (Fig. 4) at one of five pre-selected loads with a load ratio of R = 0.1, until root bending fatigue failure occurred, or a run-out condition was met (10^7 cycles). Tests were repeated three times at each load for all steel conditions and orientations, and an average value for each test sequence was calculated to compare to one another. The generation of an endurance limit — or fatigue strength — based on various runout conditions was not a goal of this testing mode, as compared to the other two test types, and will not be compared to those tests in that method. The fractured gear teeth were examined under an FE-SEM to locate the initiation site(s), and in the case of inclusion origin failures, the type of the inclusion was documented.

Brugger bending fatigue. Modified Brugger bending fatigue specimens (Fig. 5) are designed to simulate a gear tooth root bending condition. The failures occur nearly perpendicular to the

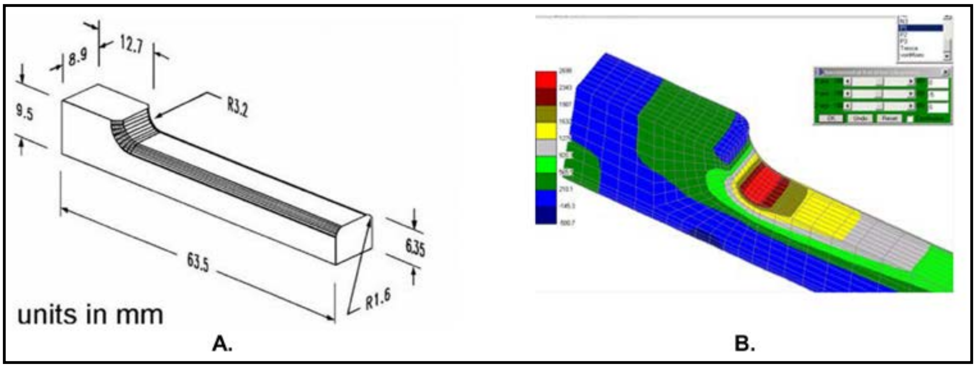

Figure 5 Brugger specimen print dimensions (A), and the maximum loading stress profile imposed by the cyclic R = 0.1 loading condition (B).

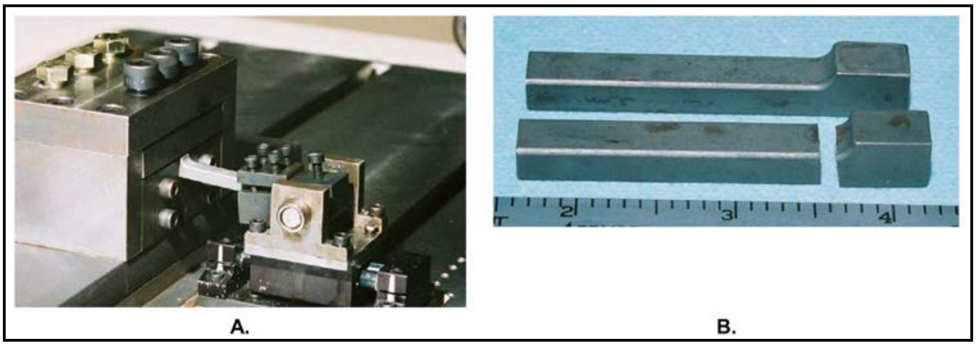

Figure 6 Brugger test machine setup (A) and as-manufactured-and-tested to failure specimens (B).

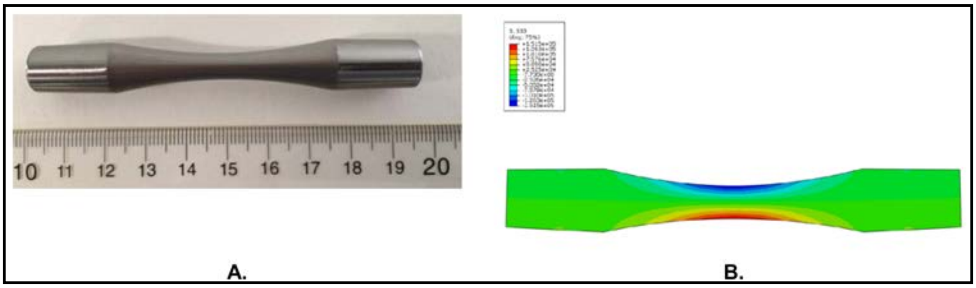

Figure 7 Image of the RBF test (RR Moore) specimen (scale shown in mm) (A), and a typical stress profile during loading (B).

length of the specimen (Fig. 6B) and, as such, longitudinal and transverse blanks were cut from as-rolled bar along the length and transverse to the length to represent these orientations. The Brugger specimens were machined from the blanks to a 16 micro-inch surface finish prior to heat treatment. The specimens were austenitized at 885 °C (1625 °F) for 30 minutes at temperature, oil-quenched and tempered at 177 °C (350 °F) for one hour to an average hardness of 55 HRc (~595 Hv). The finished specimens were then controlled dual shot peened to provide a near-surface compressive stress layer.

Testing was performed at various loads to a ratio of R = 0.1 until failure or a runout condition was met (10^7 cycles). Testing was performed until a complete S-N type fatigue curve was developed — including multiple runout failures at loads where no failures occurred — to determine an endurance limit for each steel condition and orientation. The fractured specimens were examined under an FE-SEM to locate the initiation site(s) and, in the case of inclusion origin failures, the type of the inclusion was documented.

Rotating bending fatigue (RBF). Longitudinal (i.e., parallel to the rolling direction) and transverse (i.e., perpendicular to the rolling direction) RBF specimens from the three sample groups (A, B, and C) were manufactured from the mid-radius portion of the representative bars. The test samples were austenitized at 885 °C (1,625 °F) for 30 minutes at temperature, oil-quenched and tempered at 177 °C (350 °F) for one hour to an average hardness of 55 HRc (~595 Hv). Following the heat treatment, the specimens were finish machined, ground, and polished along the specimen axis to an axial Ra < 2.5 µin (0.06 µm) and a circumferential Ra < 2.0 µin (0.05 µm). An image of the RBF test (RR Moore) specimen and a typical stress profile are shown (Fig. 7).

The 4140 samples from the A, B and C sample groups were fatigue tested in the fully reversing/rotating bending test rig (i.e., stress ratio; R = −1 and mean stress; $\sigma_m = 0$). A minimum of 12 (in most cases, 16 or more) test specimens from each of the three groups (×2 orientations) were run to generate comparative S-N curves. At least two specimens from each group were run at each loading condition. The selected suspension criteria (i.e., runout

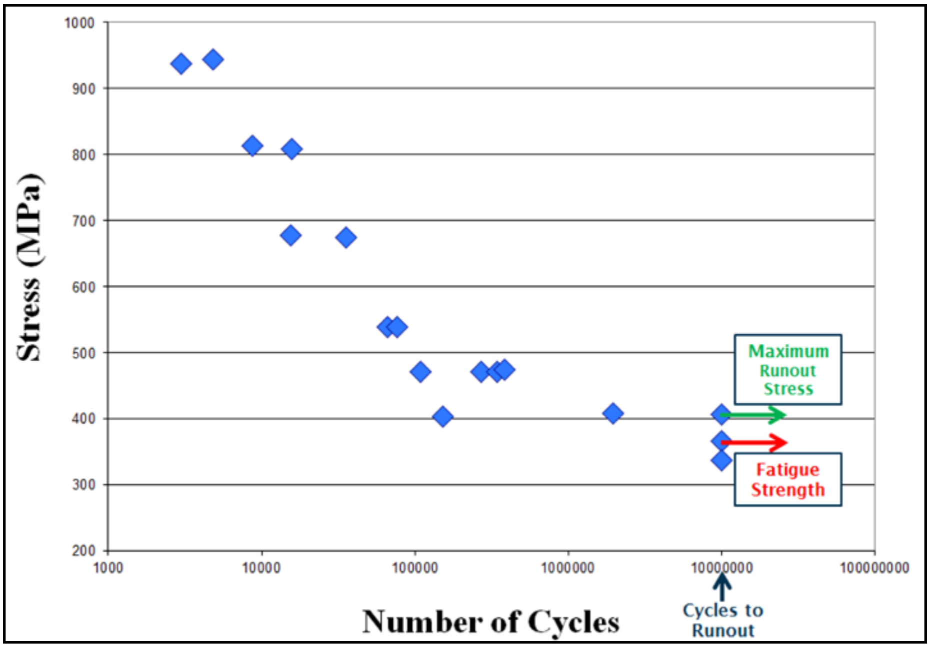

Figure 8 A depiction of how the key metrics were determined from the S-N type curve data.

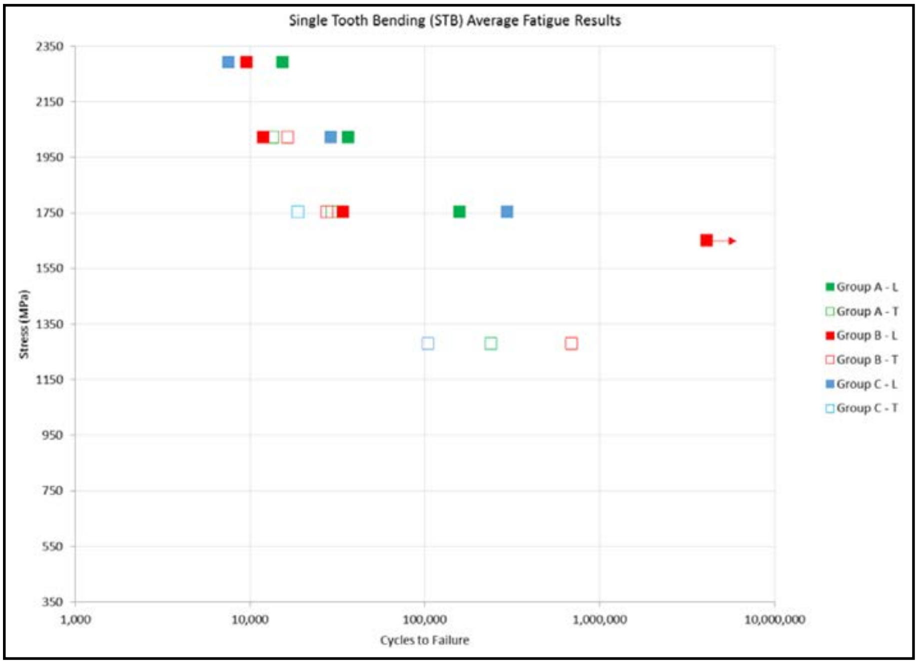

Figure 9A

bogey) was 10^7 cycles.

The fracture surface of failed test specimens was evaluated using an FE-SEM to determine the initiation point of the fatigue failure. If the fatigue crack initiated at an inclusion, the type was noted.

Two key fatigue metrics were measured for the Brugger and RBF tests. The maximum runout stress (MRS), as the name implies, was the highest stress level at which at least one specimen in a given test group reached the test suspension bogey. The second metric was fatigue strength (FS) (note that the fatigue strength is occasionally referred to as fatigue or endurance limit.), defined as the maximum stress level, at or below which no samples within a group failed. These two metrics are graphically displayed in one of the experimentally generated S-N curves (Group C – Transverse Orientation) shown in Figure 8.

Results

Fatigue results. The fatigue results generated from these three bending fatigue testing methods on the three steel cleanness conditions and two orientations are presented in Figures 9 A, B, and C. The fatigue strength and maximum runout stress for the Brugger and RBF tests for each sample group and orientation are listed in Table 3. These results essentially compare the testing methods, the steel conditions, and the orientation effects that were tested within this overall effort.

Test type comparison. Based on the test results in Figure 9 and Table 3, it is apparent that fatigue performance was highly dependent on the test type. STB testing consistently had the highest cycles to failure at a given stress level, followed by Brugger testing (~20% lower than STB), and RBF testing (30% to 50% lower than Brugger testing). Similarly, the Brugger test showed higher fatigue strengths and maximum runout stresses than the RBF test (Table 3). Only one runout was obtained for STB testing, for a longitudinal Group B sample tested at 1,650 MPa — well above the maximum runout results for either of the other test methods.

Both the STB and Brugger tests had a cyclic loading ratio (R value) of 0.1, while the RBF test had a cyclic loading ratio of −1. The test results were contrary to the expectation that the RBF test (R = −1) would produce the highest fatigue strength due to the lowest average stress (0). Both the STB and Brugger tests (R = 0.1) had a positive average stress. A possible explanation for the unexpected relationship between test type and fatigue performance will be explored in the discussion section of this paper.

Steel variant and orientation comparison. The fatigue test results showed that sample orientation had a significant effect on fatigue performance. In RBF testing the fatigue strength of the transverse samples was about one-half of the longitudinal samples, and in Brugger testing it was about one-half to two-thirds. A fatigue strength was not determined in STB testing; however, the transverse samples had fewer cycles-to-failure at a given stress level than the longitudinal samples.

In testing of longitudinal samples, Group B (high oxygen) generally had the lowest fatigue performance. Specifically, in longitudinal STB testing, Group B had significantly fewer cycles-to-failure at the stress levels of 1,753 MPa and 2,022 MPa. At 1,753 MPa, Group B had 78% and 88% fewer cycles than Groups A and C, and at 2,022 MPa, Group B had 67% and 59% fewer cycles, respectively. In longitudinal Brugger tests, the fatigue strength and maximum runout stress only varied by about 4% between the sample groups. This suggests that the inclusion population had a limited effect on the longitudinal Brugger test. However, in longitudinal RBF tests the high-oxygen steel (Group B) had 8–16% lower fatigue strength and maximum runout stress than the two low-oxygen steels. Due to the differences in performance between the low-oxygen steels, the fatigue results were also compared with respect to the concentration of large oxide inclusions. This analysis revealed that the fatigue performance showed a better correlation to the concentration of large oxide inclusions than to oxygen content (Fig. 10A).

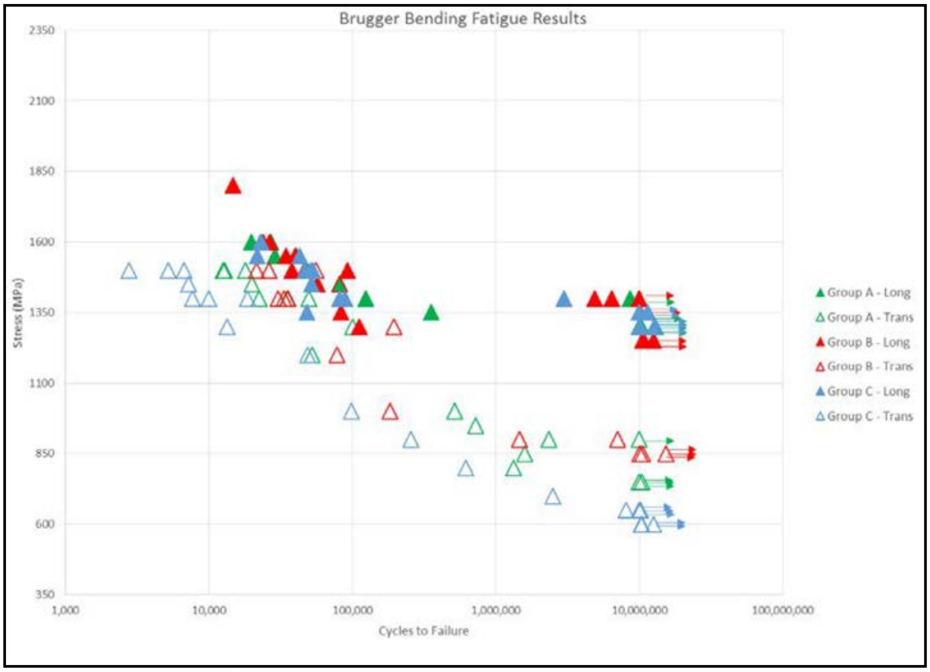

Figure 9B

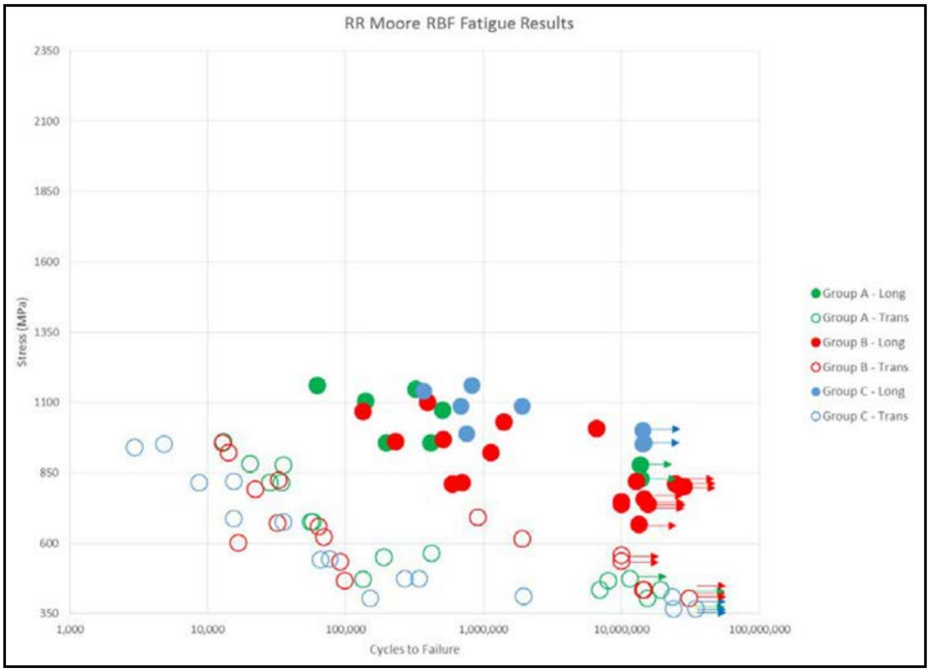

Figure 9C

Figure 9 Fatigue plots for the A—STB (each point is an average of 3 tests; B—Brugger and C—RBF plots for all steel groups.

Table 3 Fatigue strength values (FS) and maximum runout stress (MRS) for the Brugger and RR Moore RBF tests for each steel condition and orientation.

Sample Orientation	Longitudinal			Transverse		
Group	A	B	C	A	B	C
Oxygen Content (ppm)	7	15	7	7	15	7
Oxide Conc. $\sqrt{A} > 10$ µm	2.17	7.45	0.81	2.17	7.45	0.81
Sulfur Content (wt%)	0.007	0.008	0.024	0.007	0.008	0.024
Brugger FS (MPa)	1300	1250	1300	750	850	600
Brugger MRS (MPa)	1400	1400	1350	900	850	650
RBF FS (MPa)	877	804	955	412	402	366
RBF MRS (MPa)	967	882	999	527	533	407

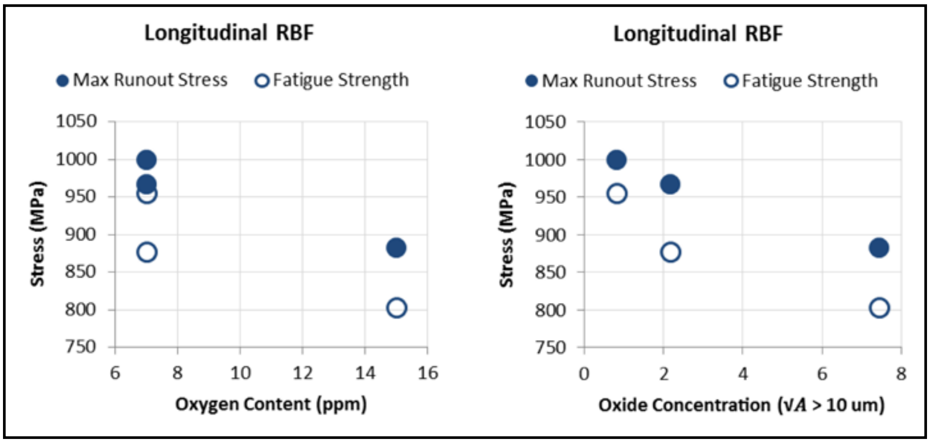

Figure 10A Plots showing RBF fatigue performance vs. oxygen content (left); and the concentration of large oxides (right).

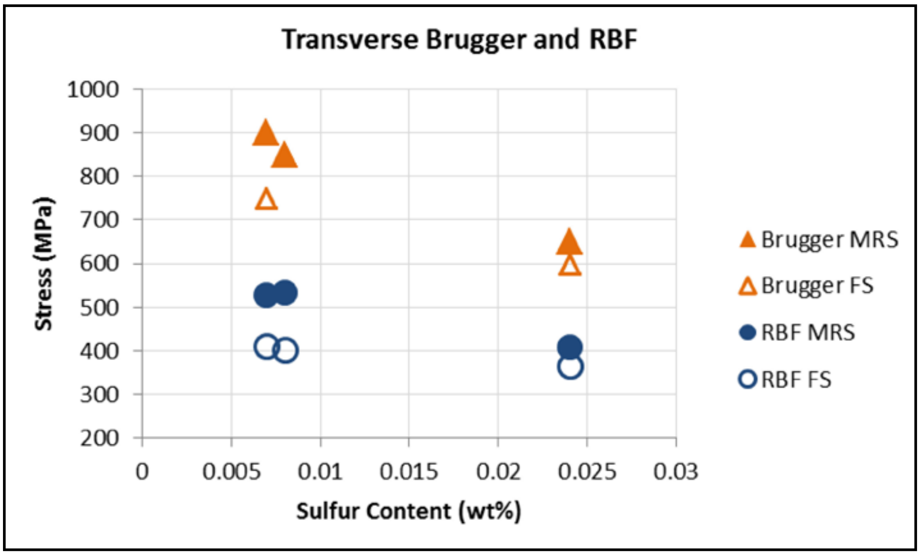

Figure 10B Plot showing transverse Brugger and RBF fatigue performance vs. sulfur content.

In testing of transverse samples, Group C (high sulfur) consistently had the lowest fatigue performance. In transverse STB testing, Group C had 57% and 85% fewer cycles at 1,281 MPa than Groups A and B, and 36% and 32% fewer cycles at 1,753 MPa, respectively. In transverse Brugger testing the fatigue strength of Group C was about 20–30% lower than groups A and B. In transverse RBF testing, Group C had a fatigue strength that was about 10% lower than both Groups A and B. The effect of sulfur content on fatigue strength and maximum runout stress in Brugger and RBF testing is illustrated in Figure 10B.

Fractography results. The fracture surface of a majority of the failed test specimens were examined by scanning electron microscopy (SEM) in order to locate and characterize the fracture initiation site(s). All fracture initiation sites were located either at a non-metallic inclusion or at the specimen surface with no inclusion present. In cases where fracture initiation occurred at a non-metallic inclusion, the initiation sites were further categorized by inclusion type (oxide, sulfide, etc.). The number of fracture initiation sites (single vs. multiple) was also noted. Examples of a surface, oxide, and sulfide initiation site are shown (Fig. 11).

Specimen orientation and sample group comparison. In Figure 12 the frequency of each fracture initiation type by sample group and orientation is shown for each test method. As illustrated in the figure, specimen orientation had a dramatic effect on fracture initiation type. Transverse specimen fractures were predominantly sulfide-initiated while longitudinal specimen fractures were largely surface-initiated or oxide

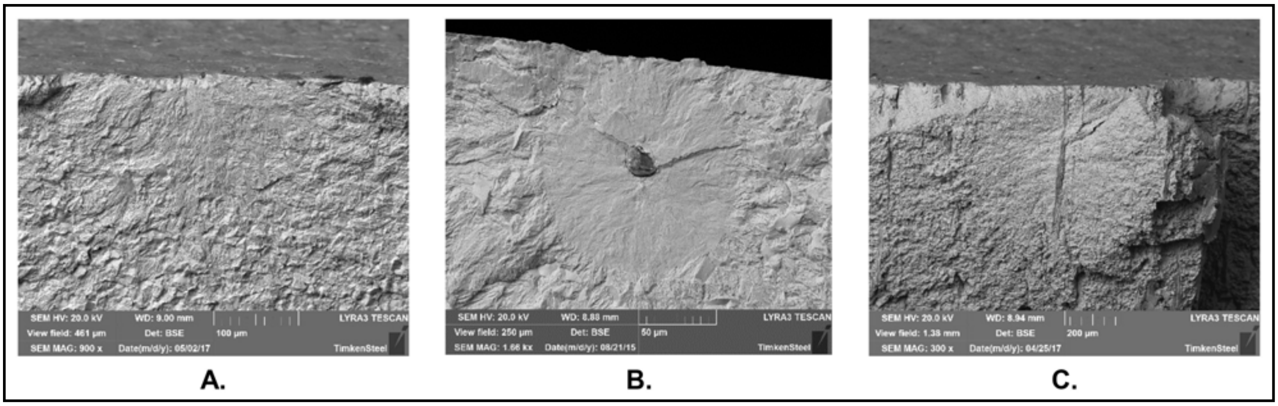

Figure 11 SEM images showing a surface initiation site with no inclusion (A); an oxide initiation site (B); and a sulfide initiation site (C).

inclusion-initiated. When data from all test methods and sample groups were combined, 88% of all transverse specimen fractures were sulfide-initiated, compared to just 1% of longitudinal specimens.

In Brugger and STB testing of longitudinal specimens, nearly all fractures were surface-initiated and little group-to-group variation was observed. It is worth noting that 52% of surface initiations in Brugger testing were located at the corner (surface transition from horizontal to the R1.6 radius) of the specimen. In RBF testing of longitudinal specimens a significantly higher rate of oxide inclusion initiation was observed in Group B (high concentration of large oxides) compared to Groups A and C. Oxide inclusions initiated 67% of longitudinal Group B failures, compared to 33% and 20% in Groups A and C, respectively.

In testing of transverse specimens, Group C (high sulfur) had the highest frequency of multiple sulfide initiation sites for all test methods. In RBF testing, 100% of transverse Group C specimens had multiple sulfide initiation sites, and in Brugger and STB testing, the frequency was approximately 50%.

Magnitude of applied Stress. In addition to sample orientation and sample group, the level of applied stress also had a significant effect on the fracture initiation type of longitudinal specimens. At stress levels where multiple failures were observed, inclusion-initiated failures increased in frequency with decreasing applied stress (Fig. 13). In RBF testing, the frequency of inclusion initiations was 80% at 900 to 1,000 MPa, 50% at 1,000 to 1,100 MPa, and 25% at 1,100 to 1,200 MPa. Similarly, in Brugger and STB testing, inclusion-initiated failures were only observed at the lowest level of applied stress at which multiple failures occurred.

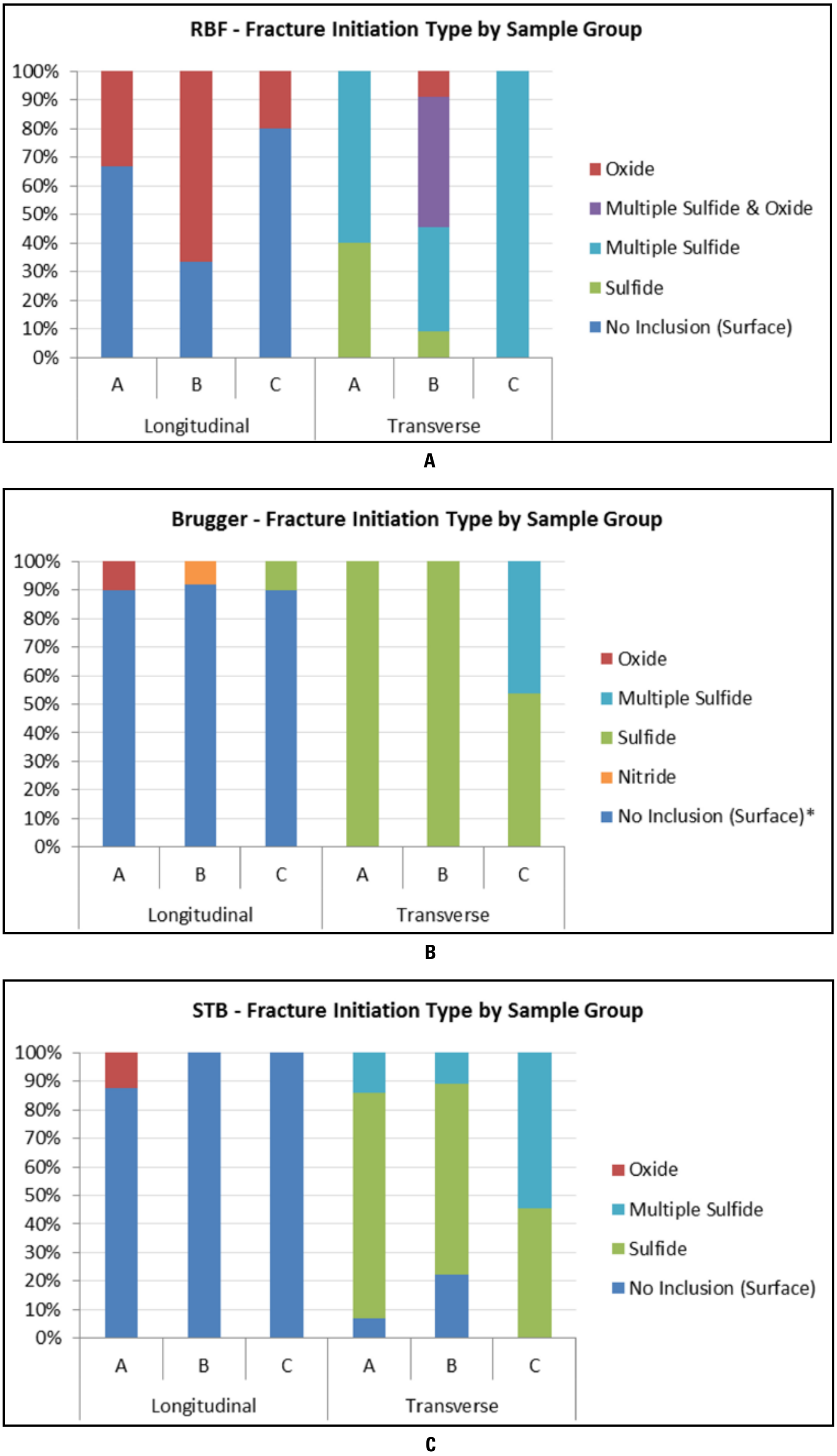

Figure 12 Plots showing the frequency of each fracture initiation type (oxide, sulfide, etc.) by sample group and orientation in RBF testing (A); Brugger testing (B); and STB testing (C).

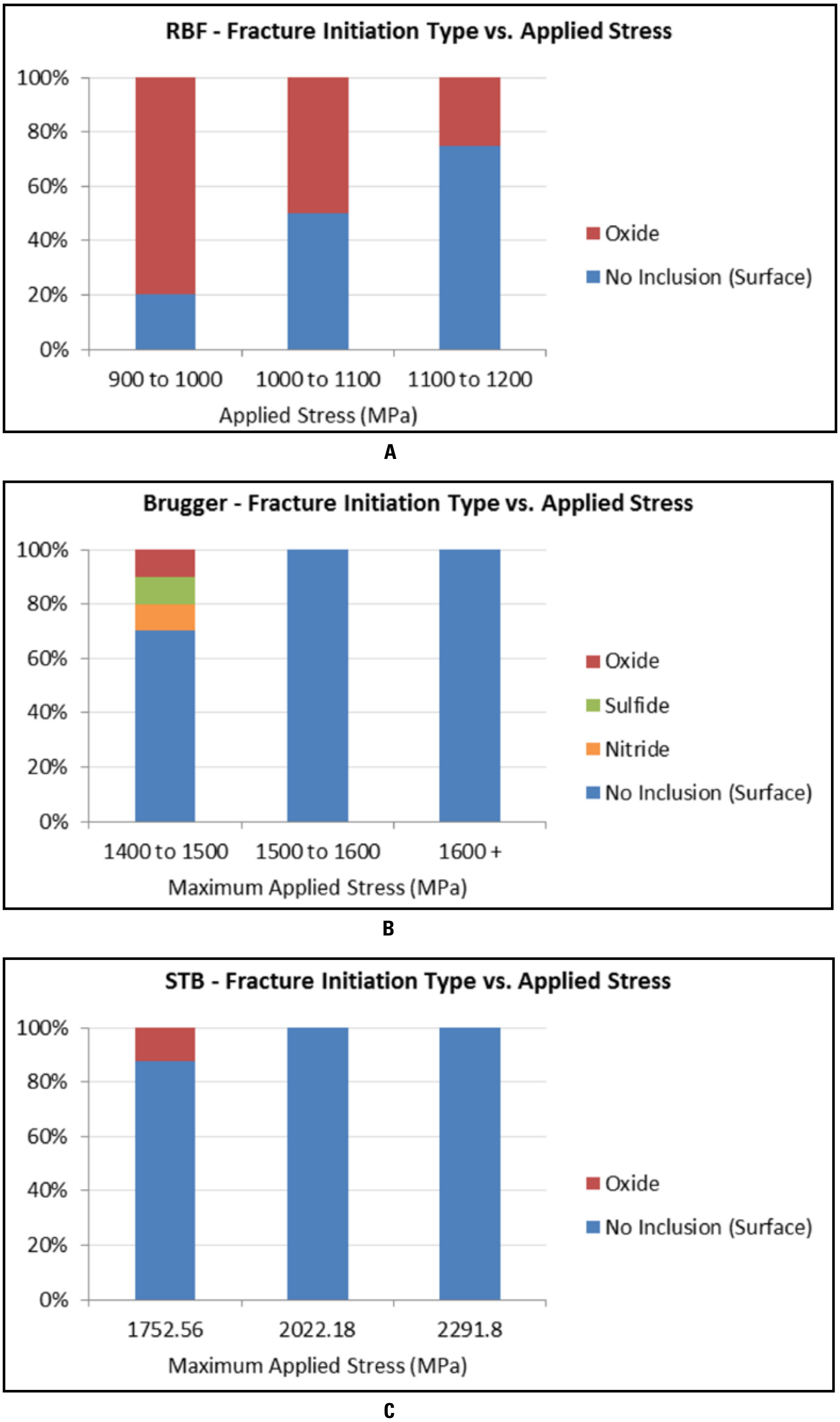

Figure 13 Plots showing the frequency of each fracture initiation type (oxide, sulfide, etc.) of longitudinal specimens vs. the maximum applied stress in RBF testing (A); Brugger testing (B); and STB testing (C).

Discussion

As noted previously, the RR Moore RBF results present some of the more interesting results in regard to the effects of inclusions on fatigue properties. As such, the primary test for discussion will be the RBF results and the impact of the inclusion population on the fatigue properties for this test mode. However, the discussion will begin by comparing the three different test types and the types of information obtained from each. It was noted that there was a large discrepancy in fatigue results between these tests, i.e. — on the order of nearly a factor of 2 between the highest and lowest test results for the same steel conditions.

Single-tooth bend test. The higher-stress/cycle results observed in the single-tooth bend test — as compared to the other tests for all steels and orientations — suggests a difference in this test method compared to the other methods. It is also apparent that the peened surface on these samples was not effective in preventing surface initiation and may have resulted in an overriding degradation of surface finish, which resulted in the high quantity of surface failures. Since most of the longitudinal tests were surface-initiated, while most transverse tests were inclusion-initiated, it is unlikely that the effect was due to a surface stress condition.

However, this test did in fact differentiate between the low and high oxide levels in the longitudinal orientation, showing lower cycles to failure for the higher-oxide group (showed similar results to transverse tests), indicating that the dirty steel condition resulted in a significant compromising of the STB fatigue results. This was true even though the initiation location of many of the longitudinal tests was at the surface rather than at a subsurface inclusion. The transverse test showed the general reduction in fatigue properties, as compared to longitudinal, and the cycles to failure tended to trend opposite the volume of inclusions present, with multiple initiation sites resulting in the lowest cycles to failure.

Brugger bending test. The Brugger stress/cycle results were intermediate, as compared to the other two tests, possibly for reasons, described later on, related to stressed volume factors. This test also suffered from a high quantity of surface

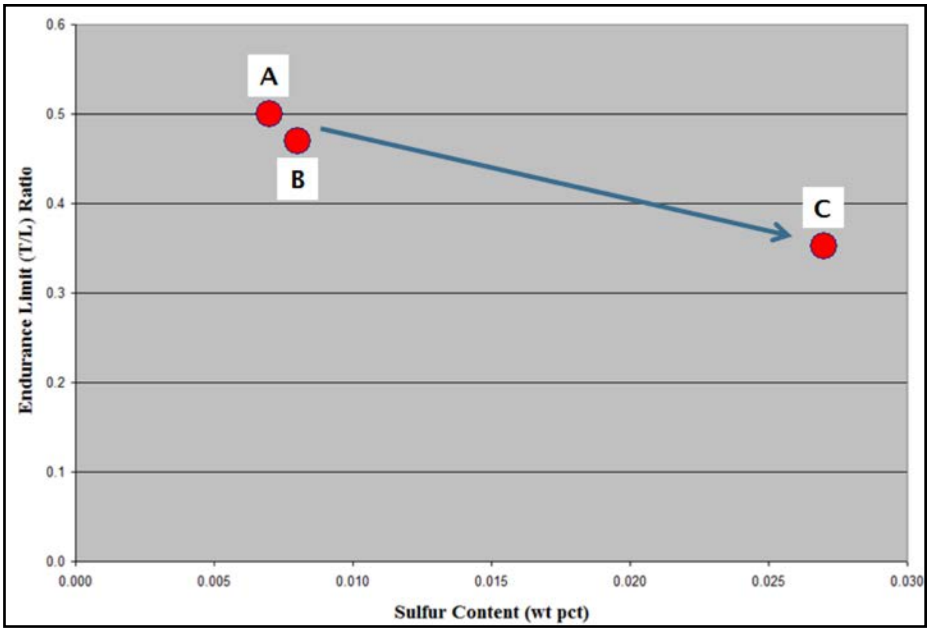

Figure 14 **Ratio of transverse to longitudinal fatigue strengths plotted as a function of sulfur content.**

failures in the longitudinal orientation, indicating that the compressive stresses on the peened surface may not have been effective at preventing surface-initiated failures. Furthermore, a large number of the surface initiation sites (52%) were located at the corner of the Brugger specimen, suggesting that a geometric stress concentration promoted fracture initiation at this location. As a result inclusions played a very limited role in failure of the longitudinal specimens, and the high-oxide variant had only 4% lower fatigue strength. The sulfides dominated the transverse fatigue origin sites for each steel variant and applied load, resulting in a relationship between sulfur level and fatigue strength. As such, this test was probably least sensitive to inclusion content, type, and orientation, requiring more macro shifts between the steel variants to affect the fatigue performance.

RR Moore rotating bending test. A number of observations can be extracted from the measured RBF fatigue data. Perhaps the most apparent information from the S-N data (Figs. 9 and 10; Table 3) is that the transverse samples from each sample group displayed significantly lower fatigue life at a given load, and about half the fatigue strength than found for the corresponding longitudinal samples. Experimental data from an early study by Sumita et al. (Ref. 5) revealed a corresponding difference in fatigue strength between longitudinal and transverse specimens in medium- and high-strength steels (Hv > 300), but no cause was assigned. The measured fatigue strength ratios from the current study are in reasonable accord with reported ratio values found in the literature (Ref. 6). Upon closer inspection of the data, the ratio of longitudinal- to transverse-measured fatigue strengths appears to be a function of sulfur content of the steel (Fig. 14). This may be expected, given that the measured total inclusion areas (oxides + sulfides, but dominated by sulfides) perpendicular to the applied stress for Group C were more than twice that of either Group A or B.

Further review of the fatigue data with regard to inclusion population metrics on the transverse specimen indicates that the high-sulfur sample group (C) displayed the poorest fatigue performance in this orientation. The measured fatigue strength of the C samples, containing 0.024% S, was about 10% below that measured on sample groups A and B, which contained about one-third the sulfur and, equivalently, had approximately one-third the measured sulfide area.

The S-N results on the longitudinal samples were more scattered than was found with the transverse samples. This may be due to the initiation location (both radially and axially) differences between these two orientations, as discussed later. Still, it is clear that the high-oxide sample group (B) had approximately a 10 to 15% lower MRS and FS than the two low-oxide sample groups. This result is in directional accord with findings reported in the literature (Refs. 7–9).

These effects in both sample orientations are clearly shown (Figs. 15A and 15B). The fatigue metric (MRS and FS) values for the longitudinal samples are plotted as a function of the oxide cleanness in terms of DIN 50602 (OG + OA) K1 values (Fig. 15A), while the fatigue metric values for the transverse samples are plotted as a function of the sulfide population, as defined by the measured DIN 50602 SS K1 values (Fig. 15B).

Another observation from this study was the reasonably consistent difference in the location of the fatigue fracture along the specimen axis between longitudinal and transverse test specimens.

Given the hour-glass geometry of the standard RBF test (RR Moore) specimen, the highest tensile stresses in the absence of internal defects (e.g., non-metallic inclusions) and surface imperfections occur at the surface of the mid-point of the sample. Accordingly, it may be expected that most of the test samples would fracture at or very near the mid-length of the specimen. As shown in Figure 16, the measured length difference of the mating halves of the failed test specimen indicated that average axial fracture location on the transverse samples was significantly and consistently closer to the mid-length point of the specimen than was found with the longitudinal samples.

This observation may be reflective of the following facts: the fatigue failures in the transverse samples were primarily associated with MnS stringers, which were significantly more abundant (and likely more uniformly distributed) than the oxide inclusions where most of the failures in the longitudinal samples occurred. Accordingly, there would be a greater probability that the highest stresses would occur closer to the mid-length position in the transverse samples. Whereas in the longitudinal inclusion-initiated samples the highest stresses would be a combination of the applied and local stresses located around the inclusion. This may also account for the higher level of scatter in the longitudinal data, as this combination of stresses would be dependent both on the applied load and the inclusion population present.

The results of the current study

demonstrate the adverse effect of oxide inclusions on the fatigue life in the axial orientation. While a 10 to 15% difference in fatigue strength between the high- and low-oxide sample sets is not particularly large, the difference has been shown to be statistically significant. Furthermore, this detrimental effect of oxide population is directionally consistent with results reported in much of the literature (Refs. 7–13).

One possible explanation for the smaller-than-expected effect on fatigue performance is related to stressed volume. As recently reported, axial fatigue studies by Furuya (Ref. 14) on SCM440 steel (similar to 4140) demonstrated the importance of relative stressed volume when evaluating the impact of steel cleanness (oxide population) on fatigue performance of two specimen sizes. The detrimental impact of cleanness on fatigue was observed with both specimen types. However, the single melt (higher oxygen) larger specimen that had a calculated stressed volume of 781 mm^3, showed 25% lower fatigue strength than the double-melt (low-oxygen) samples. While in the smaller specimen, with a stressed volume of only 33 mm^3, the difference was between 5 and 10%.

Interestingly, in the current study both the measured 10 to 15% difference in fatigue strength between the high- and low-oxygen sample groups and calculated stressed volume of the RBF specimen, about 23 mm^3, were both very similar to the results with the smaller specimen used in Furuya's work.

The size of the stressed volume may also offer a possible reason for the discrepancy in fatigue performance between

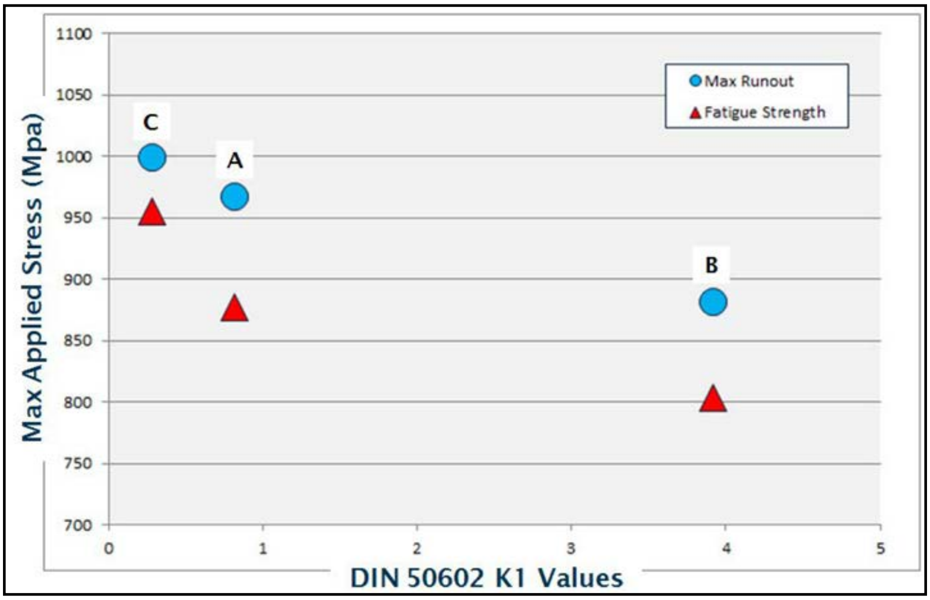

Figure 15A Fatigue metrics of longitudinal samples plotted as a function of oxide cleanness.

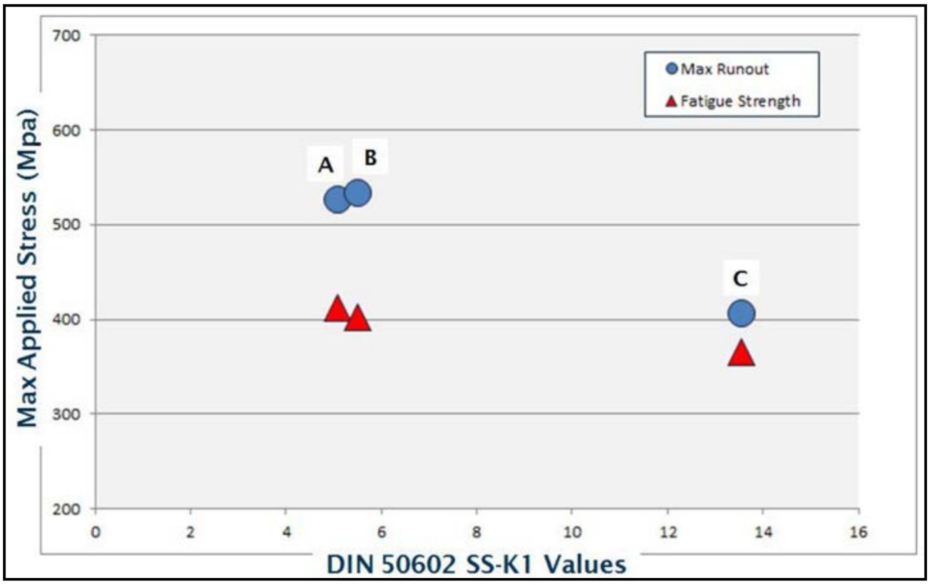

Figure 15B Fatigue metrics of transverse samples plotted as a function of sulfide cleanness.

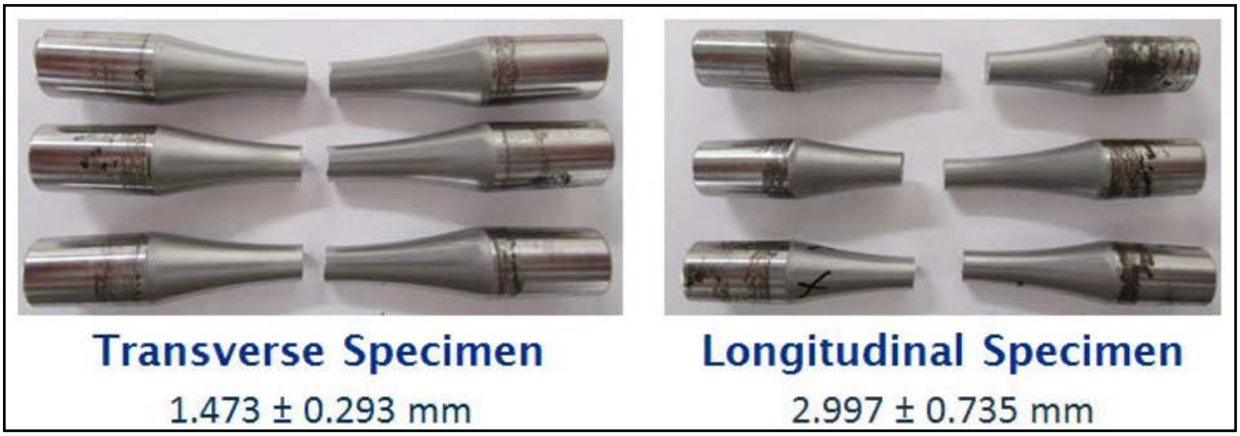

Figure 16 Images of typical transverse and longitudinal failed test specimens, illustrating the difference in axial failure location. The average axial distance of the fracture surface from the specimen mid-length (and corresponding standard deviation) are provided.

the three tests. The RBF specimen had the highest stressed volume (about 23 mm^3) and the lowest fatigue performance. The Brugger specimen had an intermediate stressed volume (about 5 mm^3) and an intermediate fatigue performance relative to the two other tests. Finally, the STB specimens had the smallest stressed volume (about 4 mm^3) and the highest fatigue performance.

Summary

Three sample sets of quenched and tempered 4140 steel, with varying levels of oxygen and sulfur, were submitted to a series of single-tooth bending, Brugger bending, and rotating bending fatigue tests. Test specimens were prepared in both longitudinal and transverse orientations.

Oxide and sulfide inclusion populations of all three sample sets were thoroughly characterized employing both SEM image analysis and high-resolution ultrasonic methods. The key cleanness metrics were in reasonable accord with the measured total oxygen and sulfur contents of the steel sample sets.

The following observations and conclusions can be drawn from this study:

The oxygen contents of the steels did not fully predict the nature of the oxide inclusion populations. Based on SEM-based image analysis, Group B had roughly twice the oxygen content of Group C, but the concentration of large oxides ($\sqrt{\text{Area}} > 10\ \mu\text{m}$) was about nine times greater. Furthermore, Groups A and C had the same oxygen content, yet the concentration of large oxides in Group A was three times greater than in Group C.

Sample orientation had a significant effect on the fatigue performance and failure modes in each of three test methods. In RBF testing the fatigue strength of the transverse samples was about one-half of the longitudinal samples; in the Brugger testing it was about one-half-to-two-thirds. In STB testing a fatigue strength was not determined; however, the transverse samples had fewer cycles to failure at a given stress level than the longitudinal samples. In each test method a large majority of transverse failures were sulfide inclusion-initiated, while very few longitudinal failures were sulfide-initiated.

The fatigue performance and failure mode of transverse samples was dependent on the sulfur content of the steel. The high-sulfur sample set (Group C) had approximately 10% lower fatigue strength in RBF testing, and approximately 20–30% lower in Brugger testing. In STB testing, Group C samples had consistently fewer cycles to failure. In all test methods, Group C had a high frequency of failures with multiple sulfide initiation sites (as opposed to a single initiation site).

The fatigue performance of longitudinal samples in RBF and STB testing was dependent on the concentration of large oxide inclusions. Furthermore, the concentration of large oxide inclusions provided a better prediction of fatigue performance than oxygen content. In RBF testing, Group B (highest concentration of large oxides) had a fatigue strength that was 8% lower than Group A and 16% lower than Group C. In STB testing, Group B samples had 59 to 88% fewer cycles to failure at a given stress level. In RBF testing, the failure mode of longitudinal samples was also dependent on the concentration of large oxides. Group B had the highest rate of oxide-initiated failures (67%), followed by Group A (33%) and Group C (20%).

References

1. Murakami, Y. "Metal Fatigue: Effects of Small Defects and Nonmetallic Inclusions," Elsevier, London, Ch. 6, 2000.
2. Erickson, M.A., M.F Garwood and H.H. Zurburg. "Interpretation of Tests and Correlation with Service, American Society of Metals," 1951.
3. Nishijima, S. "Statistical Analysis of Fatigue Test Data," *Journal of the Society of Material Science*, Japan, Vol 29, 1980, pp. 24–29.
4. Homma, H. and H. Nakazawa. "Fatigue Strength of Metals," Yokendo Ltd., Tokyo, pp. 25; 1992.
5. Araki, T., M. Sumita and I. Uchiyama. "The Effect of Inclusions on Fatigue Properties of Steel with Various Matrixes," Tetsu to Hagane, 57(2), pp. 298–334, 1971.
6. Boardman, B. *ASM Handbook: Properties and Selection: Irons, Steels and High-Performance Alloys*, ASM International, Vol. 1, p. 683, 1990.
7. Firth, P.H. "Fatigue Tests on Rolled Steel Made in Electric and Open-air Furnaces," *Journal of the Iron and Steel Institute*, Vol. 80, pp. 26–33, 1955.
8. Forrest, P.G. *Fatigue of Metals*, Pergamon Press, pp. 64–65, 1962.
9. Adachi, A., Y. Inoue, A. Kuwabara and H. Shoji. "Rotating Bending Fatigue Phenomenon of JIS SUJ2 Bearing Steel," *Elect. Furnace Steel*, Vol. 46, pp. 176–182, 1975.
10. Machida, H. *Technology of a Traction Drive CVT – Past, Present and Future*, D. Dowson, et al. (Eds), Elsevier B. V., 2005.
11. Rösch, S. and W. Trojahn. "Steel Cleanliness and Bearing Life," *Bearing Steel: Advances in Rolling Contact Fatigue Strength Testing and Related Substitute Technologies: STP 1548, ASTM*, pp. 102–113, 2012.
12. Gabelli, A., et al. "Rolling Bearing Material Quality Fatigue Testing — Material Quality Life Factors," *Bearing Steel Technology: STP 1419, ASTM.*
13. Adkinson, C.W., H.V Anderson, C.M. Sellars, G. Shi and J.R. Yates. "Fatigue Tolerant Design of Steel Components Based on the Size of Large Inclusions," *Fatigue Fracture Engineering of Material Structures*, Vol. 25, pp. 667–677, 2002.
14. Furuya, Y. "Gigacycle Fatigue Properties of Double Melted SCM440 and Size Effects," *ISIJ International*, 54(6), pp. 1436–1442, 2014.

For Related Articles Search
gear steel
at **www.geartechnology.com**

Michael Burnett, a technologist at the Timken Steel corporation, earned a Bachelor's degree from Purdue University and a Master's degree from the Colorado School of Mines — both in Metallurgical Engineering before joining the company 35 years ago. He has since worked primarily in a technical capacity developing and implementing advanced engineered steels and technologies for crankshafts, gears, bearings and other demanding applications, with an emphasis on improving both the manufacturing and performance characteristics.

Peter Glaws is a senior scientist-materials (since 2014) at Timken Corp, and has worked at Timken received his (BS) metallurgical engineering degree at Lafayette College in 1977. After four years (1977–1981) working in the steel industry, he returned to academia (1981–1985), moving on to Carnegie Mellon University where (1981–1985) he received his PhD in materials engineering. After two years (1985–1987) as a doctoral fellow at the University of Newcastle, NSW Australia, Glaws joined Timken Corp. (1987), where he has held various senior technical positions, including his present senior scientist position.

Daniel Gynther is a senior metallurgical development engineer at TimkenSteel Corporation. Since joining the company in 2010, his primary responsibilities have included performing failure analysis investigations and providing metallurgical support for product and process development efforts. Prior to joining TimkenSteel, he earned a Bachelor's degree in materials science & engineering from the University of Connecticut.

Reliability, Lifetime and Safety Factors

Dr. Stefan Beermann

(*The statements and opinions contained herein are those of the author and should not be construed as an official action or opinion of the American Gear Manufacturers Association.*)

Introduction

The most important criteria for the design of a gearbox is a sufficient strength of all components. There are, however, different ways to define this demand. The two most common ones are either defining minimum required safety factors for a given lifetime or prescribing a minimum likelihood to achieve a certain lifetime, often expressed in the reliability of a component within a given lifetime. This paper discusses the different approaches and the relationship between the safety factors and the calculation of the reliabilities. It will concentrate on ISO and AGMA standards for gears, shafts and bearings and will only discuss endurance calculations, no static calculations.

After an introduction to the concept of reliability calculation based on the book of Bernd Bertsche (Ref. 2), an example to show the difference between safety factor and reliability is given. After that, the built-in reliability coefficients of ISO 281 and AGMA 2001-D04 are compared to the general approach in Bertsche.

Symbols

Symbol	Notation	Unit
R	Reliability (of a single component)	-
t	Lifetime/number of load cycles (depends on context)	h/-
t_0	Number of load cycles without failure	-
T	Characteristic service life (in cycles) with 63.2% probability of failure(or 36.8% reliability)	-
b	Weibull form parameter	
f_{tB}	Factor according to Table 2	
L_p	Achievable service life of the component with a failure probability p	h
L_{10}	Achievable service life of the component with 0.1 (10%) probability of failure	h
p	Specific probability of failure	-
A_1	Reliability factor from ISO 281	-
K_R	Reliability factor from AGMA 2001	-

The Art of Designing a Gearbox

When challenged with the job of designing a new gearbox, the engineer has several suitable calculation methods available for the sizing of the components. Typically, these methods determine the maximum effective stress in the component and the permissible stress for the current case. The detail level of modelling can be very different, ranging from simple assumptions to sophisticated models. In most cases, the methods deliver a safety factor in the end, which is the quotient of permissible stress over effective stress.

Due to commercial demands (cost reduction and sales increase), the sizing process has a design lifetime as a required parameter in its center. Ideally, all components should fail at the same time. Since the failure of the first critical component normally determines the end of life of the complete gear box, each component that is designed for a longer lifetime is, in this sense, overdesigned and generates unnecessary costs. For consumer products, there might be additional requirements to reduce the lifetime of the product to sell replacements.

Inside the methods, the parameter lifetime influences the permissible stress by making it dependent on the number of load cycles. This follows the idea that the damage to a part is caused by the change in stress and leads to S-N curves for the selected materials. With this, the safety factor depends on the number of load cycles.

With this procedure at hand, everything seems well-defined, and indeed in practice, this approach has worked very well. However, expecting the components to fail at the exact number of load cycles defined for the lifetime means asking too much. The S-N curves for a specific material are based on tests conducted. In these tests, samples are exposed to alternating load and the number of load cycles until failure is recorded. Of course, the results show a certain variation. The final S-N curve is therefore a statistically extracted curve for a given failure probability. Several standards define the procedure on how to perform this extraction, for instance (Ref. 11).

For the sake of clarity, we will first define the central variables.

Design life, achievable life. In this paper, we are only looking at fatigue strength due to changing stresses. If there are changes in stress, there are also load cycles. Typically, there are a number of hours given, which is the planned lifetime for the component or the machine. Since questions might arise on how to interpret this number (percentage of up-time considered, changing speeds), it is a good idea to transfer the hours into load cycles. In this way we end up with a number of load cycles the machine is designed for — the design life. And we might determine the maximum number of load cycles until the machine fails with a certain likelihood — this is the achievable life.

Effective stress; permissible stress; safety factor. Due to the loads applied, there is a stress distribution inside the components. This stress is time-dependent, changing with the load cycles. Typically, the maximum stress is calculated with a constant part (mean value) and a transient part (amplitude). For endurance, only the amplitude of the stress is relevant. The stress used for the strength assessment is called "effective stress."

Printed with permission of the copyright holder, the American Gear Manufacturers Association, 1001 N. Fairfax Street, Fifth Floor, Alexandria, VA 22314-1587. Statements presented in this paper are those of the author(s) and may not represent the position or opinion of the American Gear Manufacturers Association.

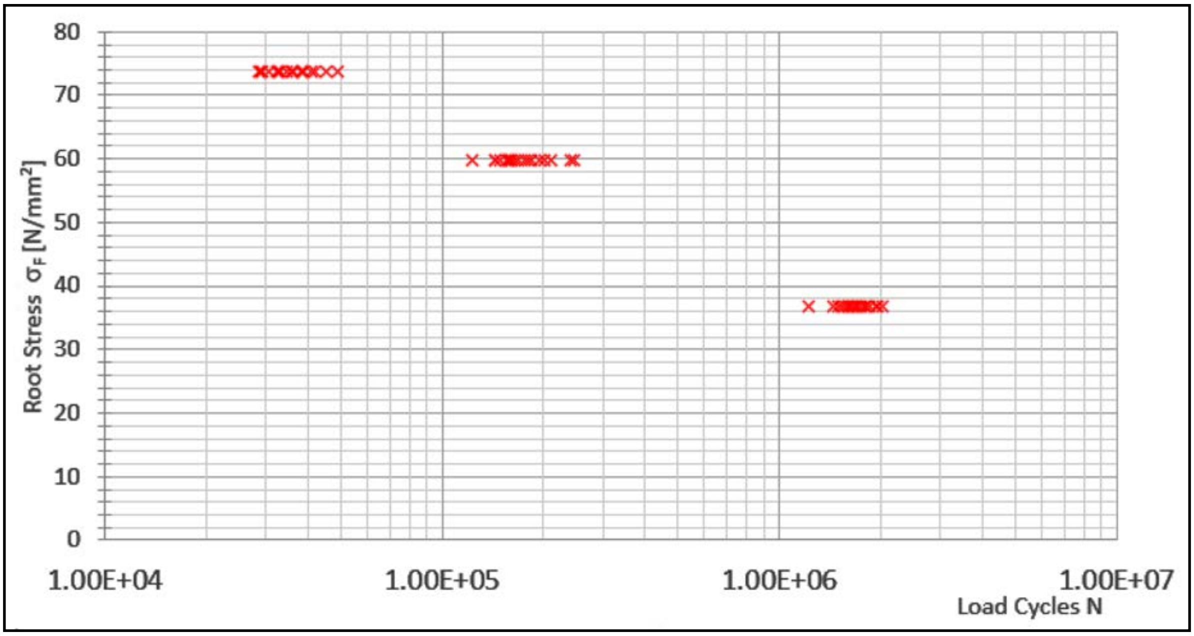

Figure 1 Series of gear tests for three different torque levels.

On the other hand, the material of the component can endure a maximum stress level for a given number of load cycles, i.e. — the "permissible stress." The quotient of permissible stress over effective stress gives the safety factor. This safety factor must be larger than a threshold value to fulfill the requirements. This threshold value is called the "required safety factor."

S-N curve. The basis of most methods is an S-N curve that defines the permissible stress limit over the number of load cycles. The name "S-N curve" simply comes from the fact that it shows a stress (S) over the number of load cycles (N).

The basis for this curve is a series of tests in which test specimens were subjected to load under standardized conditions until they failed. The number of load cycles until failure at a given load level is recorded and represents the result of one of these tests. However, if a test is repeated several times with the same load conditions, and all other environmental parameters fixed, still no one would expect all specimens to fail at the exact same number of load cycles. Rather, there will be some scattering of the results. So, some statistical evaluation needs to be done to produce an S-N curve. Figure 1 shows a typical result of a gear test with constant torque levels and the resulting scattering of load cycles until failure.

For bearings, the scattering can get quite extreme. Figure 2 shows a graph from Harris (Ref. 1). On the y-axis, the number of load cycles is found; on the x-axis is the percentage of failed bearings. The first bearing fails after about $30 \cdot 10^6$ revolutions, and the last one after $1{,}800 \cdot 10^6$ revolutions. The result is a factor of 60 from the first to the last! The L_{10} lifetime in this case — where 10% of the bearings failed and 90% are still working — would be about $120 \cdot 10^6$ revolutions. This is about 4 times more than the first failure and 15 times less than the last one.

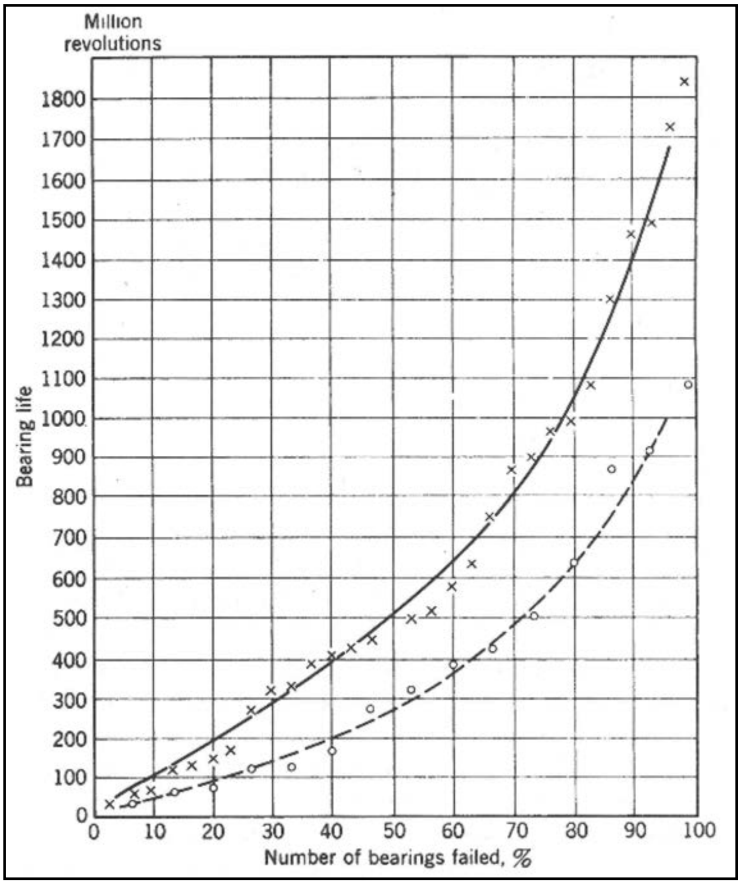

Figure 2 Results of bearing tests (Ref. 1).

Assuming an arbitrary number of tests were conducted to allow statistical evaluation, the combination of all tests at a specific load level requires the definition of a

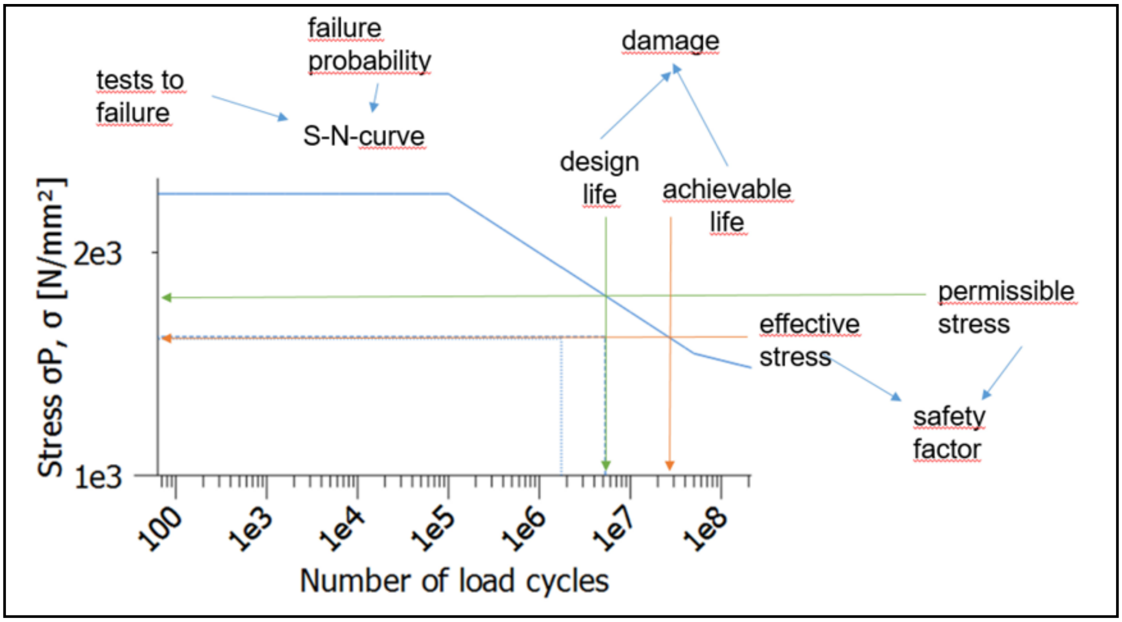

Figure 3 **Relationships between strength parameters.**

probability value. Changing the probability shifts the S-N curve horizontally.

Damage. The calculation methods discussed here all follow the concept of damage accumulation. This assumes that small cracks or failures in the material structure are enlarged due to the changing stress levels. The theory predicts the growth of the crack following a logarithmic law. The ratio of design life over achievable life is called "damage." The idea is that the same length on the load cycle's axis (which is scaled logarithmically) corresponds to the same amount of damage caused. The damage is usually expressed as a percentage, with the idea that reaching 100% damage means failure. Mathematically, damage larger than 100% is possible.

Relationships. Figure 3 shows the relationships between the terms described above. It starts with an appropriate number of tests, which in conjunction with a given failure probability, lead to an S-N-curve. The curve defines the permissible stress over the number of load cycles, so if we use the graph with a given number of load cycles (design life), we find the corresponding permissible stress (green arrows). On the other hand, if we have a given effective stress, then we can read the achievable life from the diagram (orange arrows). The quotient of permissible stress over effective stress gives the safety factor. And finally, the ratio of design life to achievable life defines the damage.

Methods to Dimension a Gearbox

There are different approaches used for designing a gearbox. The simplest one is to determine the stresses in the components and make sure to stay below a given threshold that comes from experience. This approach is not very sophisticated, since it blanks out many influences that affect the permissible stress. Still, it is commonly used, especially when FEMs (finite element methods) are applied, simply because an FEM can only calculate the effective stress — not the permissible.

An alternative is the application of a standardized method (or textbook method). The most common concept here is the determination of the effective stress by applying simplified models leading to analytical formulations. In a second step, the permissible stress is calculated (or read from a table) and compared to the effective stress by calculating the safety factor. Instead of a safety factor, some methods provide the exposure of the material. This is basically the same, only expressed in a different way. As a design requirement, a minimum safety factor (or maximum exposure) is given.

Some of the standardized methods for bearings calculation, like ISO 281 (Ref. 3), directly deliver an achievable life out of the loads. In the case of the bearings, the loads are the forces in radial and axial direction.

If load spectra are applied, a different approach is the calculation of damage. The advantage is that damage is more easily compared across different components than safety factors.

Failure Probability of Machine Elements

All the above methods have one major weakness in common: they are based on an intrinsic failure probability which differs from method to method (Table 1). Therefore if a shaft has a calculated safety factor of 1.2 and a gear root has a safety factor of 1.3, it is not clear which is the more critical component. As well, the calculated life of a bearing and of a gear are not directly

Table 1 **Probability of failure used by various calculation methods when determining material properties (Ref. 8)**

Calculation procedure	Probability of damage *p*	Comment
Shaft, DIN 743	2.5%	Assumed, not documented
Shaft, FKM guideline	2.5%	
Shaft, AGMA 6001	1%	If $k_c = 0.817$
Bearing, ISO 281	10%	If factor $a_1 = 1.0$
Tooth flank, ISO 6336; DIN 3990	1%	
Tooth bending, ISO 6336; DIN 3990	1%	
Tooth flank, AGMA 2001	1%	If reliability factor $K_R = 1$
Tooth bending, AGMA 2001	1%	If reliability factor $K_R = 1$

comparable.

A material strength value with a failure probability of 90% is higher than a material strength value with a failure probability of 99%. So if the 90% failure probability is applied, the safety factor is greater and the element has both a greater service life and a lower damage rate for its design life. Damage that is calculated using the methods prescribing different failure probabilities cannot be compared directly. A gear unit may fail because a part that is not considered to be critical breaks prematurely. This happens quite frequently in real life.

To overcome this problem, the reliability concept can be used. Here the result is a curve that shows the probability of failure of a component or a system over the lifetime. When statistical parameters such as the scatter of results in a standard distribution are determined on the basis of measurements on probes, a probability of failure as a function of time (or cycles) can be determined using a statistical approach. The opposite of the probability of failure is called "reliability." Therefore, since the reliability calculation takes into consideration the inherent failure probability (Table 1), the calculated reliability at design life of different parts can be compared effectively with each other. Also, at a given probability level the component with the smallest achievable life is the critical component of the system.

Probability distributions. In statistics, probability distributions are used to describe stochastic processes (see numerous textbooks, e.g. — Ref. 9). A probability distribution is a function that gives the likelihood of an event for a specific value of a probability variable. In our case the event is failure (or survival) and the probability variable is the number of load cycles.

The reliability function $R(t)$ gives the probability of survival until t load cycles. The values of $R(t)$ range between 0.0 and 1.0, often expressed in percent: $R(t)\cdot 100\%$. In principal, t is an integer value; however, due to the large number of load cycles (from several thousand to billions), we can treat it like a real value and use the existing theories.

For the definition of a probability distribution, the first derivative $R'(t)$ is defined, i.e. — the so-called density. The density is a function that defines the probability of the event happening at a given number of load cycles.

The most common distribution for general purposes is the normal distribution. This distribution is defined by the mean value μ and the standard deviation σ. The density of the normal distribution is symmetric to μ. The standard deviation σ controls how wide the distribution is; although for small σ the density looks like it becomes zero with enough distance from the mean, it never actually does. So also for negative values of t there is a positive likelihood that failure occurs. Furthermore, the failure rate $R'(t)/R(t)$ of the normal distribution is increasing over t. Due to these limitations, the normal distribution is not very often used in reliability engineering.

A more general approach is the Weibull distribution. Two variants are possible — the two-parametric and three-parametric Weibull distribution, where the two parametric is a special case of the three parametric.

The two-parametric Weibull distribution leads to the reliability function:

$$R(t) = e^{-\left(\frac{t}{T}\right)^{b}} \tag{1}$$

where T is the characteristic lifetime (defined by the condition $R(T) = 0.632$) and b is the shape parameter.

The three-parametric Weibull distribution has t_0 as a third parameter, which shifts the first occurrence of failure to the point t_0 by the substitution:

$$t \rightarrow \tilde{t} - t_0 \tag{2}$$

This substitution gives the reliability function:

$$R(t) = e^{-\left(\frac{t-t_0}{T-t_0}\right)^{b}} \tag{3}$$

In practice, the Weibull distribution can be used to model a wide variety of real-world scenarios, with the most famous one being the "bathtub curve." For this, three sections with individual parameters — t_0, T, and b — are defined, the first with a monotonous decreasing failure rate, the second with a constant failure rate, and finally a third section with increasing failure rate.

Determining the reliability of machine elements. There are currently no mechanical engineering standards that include the calculation of probability. A classic source for this calculation is Bertsche's book (Ref. 2), in which the possible processes have been described in great detail. Bertsche recommends the use of the 3-parameter Weibull distribution.

To simplify the writing of the equations, we define the lifetime L_p as the lifetime with reliability $R(L_p) = (100-p)$ (%). Both p and $R(t)$ are usually expressed in percent (%). To apply the Weibull distribution, several parameters are needed that depend on the type of component (gear, bearing, shaft). Bertsche tabulates the shape parameter b and a factor f_{tB}, that relates t_0 to the lifetime with 10% failure probability, $L_{10;}$ see Equation 5.

With these parameters, T and t_0 can be derived from the achievable life of the component, L_p, as follows (with failure probability p according to the calculation method from Table 1, b and f_{tB} from Table 2, according to Bertsche):

$$T = \left(\frac{L_p - f_{tb}\cdot L_{10}}{\sqrt[b]{-\mathrm{In}\,(1-p)}} + f_{tb}\cdot L_{10}\right) \tag{4}$$

$$t_0 = f_{tb}\cdot L_{10} \tag{5}$$

$$L_{10} = \frac{L_p}{(1-f_{tb})\cdot\sqrt[b]{\frac{\mathrm{In}\,(1-p)}{\mathrm{In}\,(0.9)}} + f_{tb}} \tag{6}$$

In Table 2 the parameter b has a wide range for breakage of shafts and tooth root. Bertsche comments in his book that for b, this is due to the confidence intervals of the statistical analysis (some of the test batches were relatively small), but also because the shape parameter b depends on the stress level: the higher the stress level, the larger the shape parameter.

For f_{tB}, however, it is mainly for gears with pitting as failure mode where the interval gets large. Here Bertsche states that this is due to a small number of tests available. He also voices the

Table 2 Factors for a Weibull distribution according to Bertsche (Ref. 2)

Shafts	0.7 to 0.9	1.1 to 1.9
Ball bearing	0.1 to 0.3	1.1
Roller bearing	0.1 to 0.3	1.35
Tooth flank	0.4 to 0.8	1.1 to 1.5
Tooth root	0.8 to 0.95	1.2 to 2.2

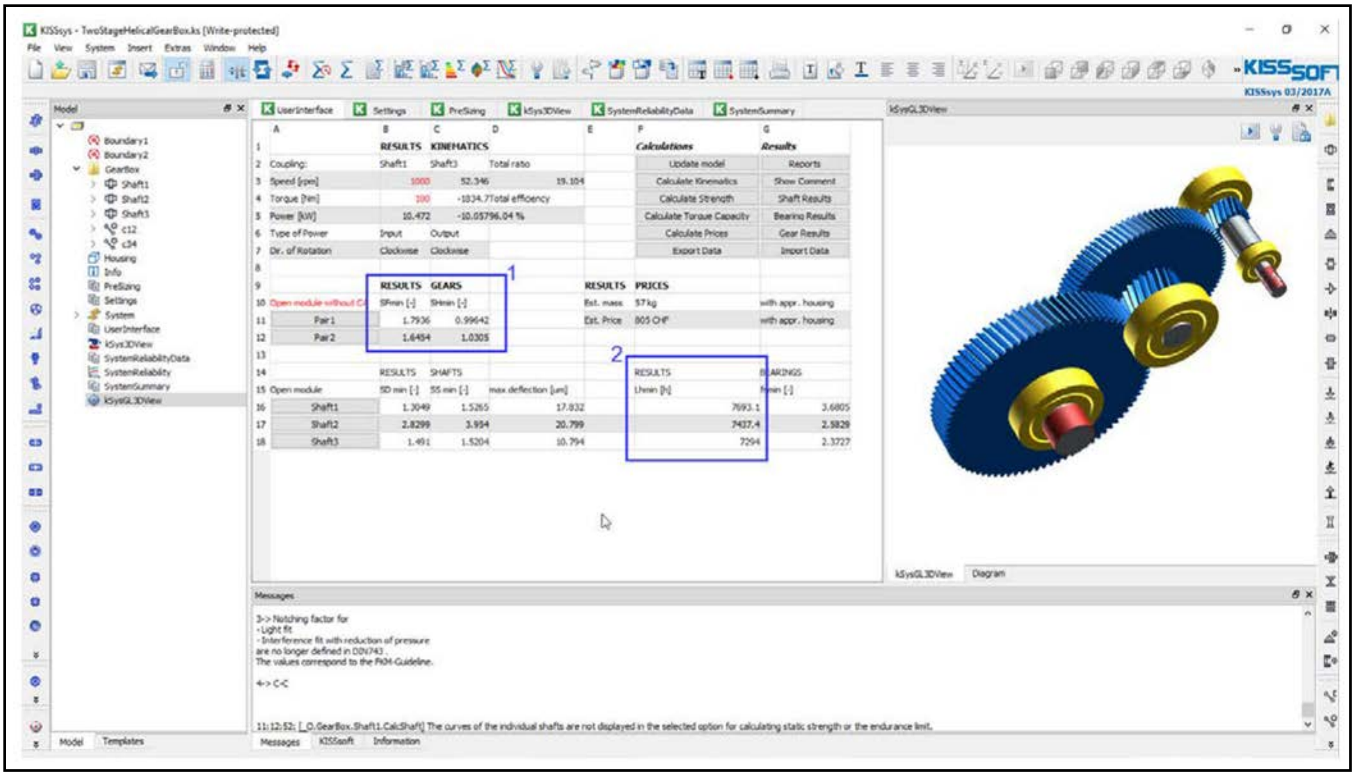

	A	B	C	D	E	F	G
1		RESULTS	KINEMATICS			*Calculations*	*Results*
2	Coupling:	Shaft1	Shaft3	Total ratio		Update model	Reports
3	Speed [rpm]	1000	52.346	19.104		Calculate Kinematics	Show Comment
4	Torque [Nm]	100	-1834.7	Total efficiency		Calculate Strength	Shaft Results
5	Power [kW]	10.472	-10.057	96.04 %		Calculate Torque Capacity	Bearing Results
6	Type of Power	Input	Output			Calculate Prices	Gear Results
7	Dir. of Rotation	Clockwise	Clockwise			Export Data	Import Data
8							
9		RESULTS	GEARS		RESULTS	PRICES	
10	Open module without C	SFmin [-]	SHmin [-]		Est. mass	57 kg	with appr. housing
11	Pair 1	1.7936	0.99642		Est. Price	805 CHF	with appr. housing
12	Pair 2	1.6454	1.0305				
13							
14		RESULTS	SHAFTS			RESULTS	BEARINGS
15	Open module	SD min [-]	SS min [-]	max deflection [um]		Lhmin [h]	fmin [-]
16	Shaft1	1.3049	1.5265	17.832		7693.1	3.6805
17	Shaft2	2.8299	3.954	20.799		7437.4	2.5829
18	Shaft3	1.491	1.5204	10.794		7294	2.3727

```
3-> Notching factor for
- Light fit
- Interference fit with reduction of pressure
are no longer defined in DIN743 .
The values correspond to the FKM-Guideline.

4-> C-C

11:12:52: [_O.GearBox.Shaft1.CalcShaft] The curves of the individual shafts are not displayed in the selected option for calculating static strength or the endurance limit.
```

Figure 4 **Example gearbox modelled in *KISSsys*.**

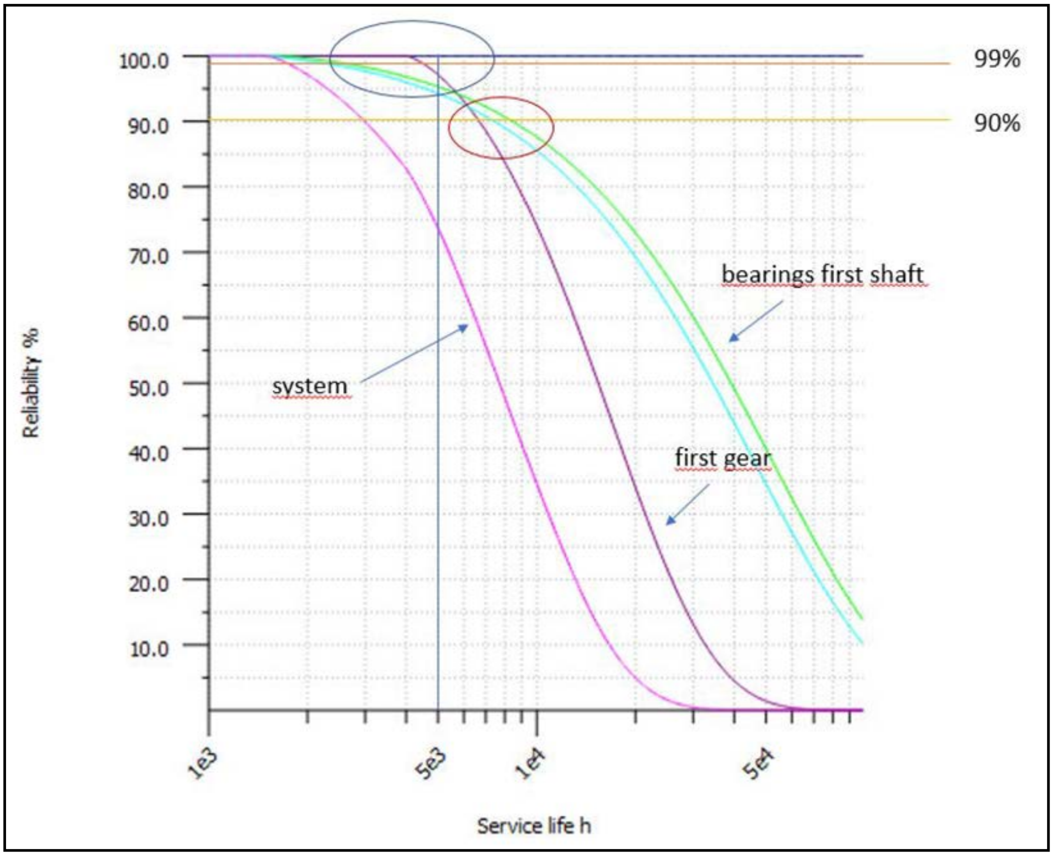

Figure 5 **Calculated reliability curves.**

hope that further tests could narrow this range down.

Equation (1) for $R(t)$ can now be used to display the progression of reliability over time (or number of cycles) as a graphic. The load cycle values t_0 and T can then be calculated after a service life calculation. Equations 4–6, using the achievable service life L_p, can be used for this purpose.

An example application. To illustrate the differences between the concept of safety factors and reliability, an example is shown. Figure 4 shows the model of a two-stage gearbox in *KISSsys* (Ref. 10). The design life is 5,000h. So, the critical component appears to be gear 1 with a flank safety factor of slightly below 1.0 (0.996) (see box "1"). The bearings have a calculated lifetime of above 7,000 hours (see box 2) and thus seem to be on the safe side.

However, looking at the graph in Figure 5 showing the reliability curves of some selected elements of the gearbox, the situation is more complex. In this graph the reliability was calculated according to the method of Bertsche (Ref. 2). The dark red curve shows the reliability of the flank for gear 1. For most probability levels, this curve is left of the two bearing curves shown, confirming the assessment from before. But this is only true for relatively low probabilities; the lower horizontal orange line is on the 90% probability level. Here, gear 1 indeed has the shorter lifetime. Still, this is above the required 5,000h design life, which is marked with the vertical blue line.

At 99% probability, the bearing life is much lower — about 3,000 hours. This is marked with the upper horizontal dark orange line. So, the more critical components are indeed the bearings. The curve for gear 1 crosses the 99% line left of the 5,000-hour bar, confirming the safety factor smaller than one.

Finally, the pink curve shows the reliability of the whole system. It is, by definition, always the left-most curve. The more components are considered, the further left this curve is moving. It is interesting to observe that for the system, the lifetime with a probability of 99% survival is about 1,800 hours, and for 90% reliability, it is about 3,000 hours. The probability of reaching the design life of 5,000 hours with this gearbox without failure is only about 73%.

Comparison of Bertsche with the Standards

Some standards, such as AGMA 2001-D04 (Ref. 7) or ISO 281 (Ref. 3), foresee factors to change the underlying failure probability of the calculation. It is thus a natural question of how well these factors compare to the approach of Bertsche.

Bearing lifetime per ISO 281. First, we look at ISO 281. As mentioned, bearings show a wide scattering of the results when lifetime tests are conducted. Therefore the approach for bearings is slightly different than the other methods. The method does not calculate effective stresses and a safety factor for a given lifetime, but directly a lifetime that is reached with a certain likelihood. So, it is easy to compare with the formulae in Bertsche.

In ISO 281 the factor a_1 is used to take different reliabilities into account (Table 3). The factor is directly multiplied to the lifetime L_{10} for 90% reliability, so it is straightforward to interpret (e.g. L_1 for 99% reliability equals to 0.25*L_{10}). To compare this factor with the values used by Bertsche, we calculate f_{tB} from a_1:

Table 3 Definition of a_1 in ISO 281

Reliability %	L_{nm}	a_1
90	L_{10m}	1
95	$L_{5m\cdot}$	0.64
96	L_{4m}	0.55
97	L_{3m}	0.47
98	L_{2m}	0.37
99	L_{1m}	0.25
99.2	$L_{0.8m}$	0.22
99.4	$L_{0.6m}$	0.19
99.6	$L_{0.4m}$	0.16
99.8	$L_{0.2m}$	0.12
99.9	$L_{0.1m}$	0.093
99.92	$L_{\ 0.08m}$	0.087
99.94	$L_{0.06m}$	0.080
99.95	$L_{0.05m}$	0.077

Equation 3

$$R(t) = e^{-\left(\frac{t-t_0}{T-t_0}\right)^b} \tag{7}$$

can be rearranged to:

$$\mathrm{In}\,(R(t)) = -\left(\frac{t-t_0}{T-t_0}\right)^b \tag{8}$$

With (Eq. 5), which relates t_0 to the lifetime with 10% failure probability L_{10} with the factor $f_{tB,}$

$$t_0 = f_{tb} \cdot L_{10} \tag{9}$$

$$\sqrt[b]{-\mathrm{In}\,(R(t))} = \frac{t-f_{tb}\cdot L_{10}}{T-f_{tb}\cdot L_{10}} \tag{10}$$

Solving for f_{tB} gives:

$$f_{tb} = \frac{\sqrt[b]{-\mathrm{In}\,(R(t))}\cdot T-t}{\left(\sqrt[b]{-\mathrm{In}\,(R(t))}-1\right)\cdot L_{10}} \tag{11}$$

Extracting L_{10} outside of the bracket in (Eq. 4) results in:

$$T = \left(\frac{\frac{t}{L_{10}}-f_{tb}}{\sqrt[b]{-\mathrm{In}\,(R(t))}}+f_{tb}\right)\cdot L_{10} \tag{12}$$

For the lifetime $t = L_{10}$ we have 10% failure probability, so the reliability is 90%:

$$t = L_{10} \Rightarrow R(t) = 0.9 \tag{13}$$

We set $t = L_{10}$ in (Eq. 12):

$$T = \left(\frac{1-f_{tb}}{\sqrt[b]{-\mathrm{In}\,(0.9)}}+f_{tb}\right)\cdot L_{10} \tag{14}$$

We now write the factor $a_1 = a_1\ (p)$ from Table 3 dependent on the probability p.

$$R(t) = p \Rightarrow t = L_p =: a_1(p)\cdot L_{10} \tag{15}$$

Injecting (Eq. 14) and (Eq. 15) in (Eq. 10) and sorting for f_{tB} gives:

$$f_{tb}\cdot\left(\frac{\sqrt[b]{-\mathrm{In}\,(p)}}{\sqrt[b]{-\mathrm{In}\,(0.9)}}-1\right) = \frac{\sqrt[b]{-\mathrm{In}\,(p)}}{\sqrt[b]{-\mathrm{In}\,(0.9)}}-a_1(p) \tag{16}$$

Finally, we find a relationship between $a_1\ (p)$ and f_{tB}:

$$f_{tb} = \frac{\sqrt[b]{\frac{-\mathrm{In}\,(p)}{-\mathrm{In}\,(0.9)}}-a_1(p)}{\sqrt[b]{\frac{-\mathrm{In}\,(p)}{-\mathrm{In}\,(0.9)}}-1} \tag{17}$$

Table 4 Definition of example gear set

Transmitted power (kW/hp)	[P]	26.099 / 35.000	
Speed gear 1 (1/min)	[n]	2950.000	
Pressure angle at normal section (°)	[alfn]	20.000	
Helix angle at reference circle (°)	[beta]	14.000	
Number of teeth	[z]	27	104
Face width (mm/in)	[b]	20.32 / 0.800	20.32 / 0.800

Table 5 Definition of K_R in AGMA 2001-D04 (Ref. 7)

Requirements of application	K_R[1]
Fewer than one failure in 10,000	1.50
Fewer than one failure in 1,000	1.25
Fewer than one failure in 100	1.00
Fewer than one failure in 10	0.85[2]
Fewer than one failure in 2	0.70[2, 3]

NOTES

[1] Tooth breakage is sometimes considered a greater hazard than pitting. In such cases a greater value of K_R is selected for bending.

[2] At this value plastic flow might occur rather than pitting.

[3] From test data extrapolation.

We can use this relationship to calculate the lifetime ratio $a_{Bertsche}(p) = L_\mathrm{p}/L_{10}$ for a given f_{tB}:

$$a_{Bertsche}(p) = \sqrt[b]{\frac{\mathrm{In}(p)}{\mathrm{In}(0.9)}} - f_{tb} \cdot \left(\sqrt[b]{\frac{\mathrm{In}(p)}{\mathrm{In}(0.9)}} - 1 \right) \quad (18)$$

Figures 6 and Figure 7 show the results. Bertsche proposes a range of $0.1 \leq f_{tB} \leq 0.3$. For a large range of the probability, this is fulfilled, only for reliabilities above 99.5%, f_{tB} drops below the lower limit. Figure 7 shows the lifetime ratios of ISO 281 over Bertsche. Until 99% probability, the ratio is close to 1, so both methods give nearly the same results. Then ISO 281 gets more conservative and for 99.95% reliability, the standard predicts about 50% of the lifetime compared to Bertsche.

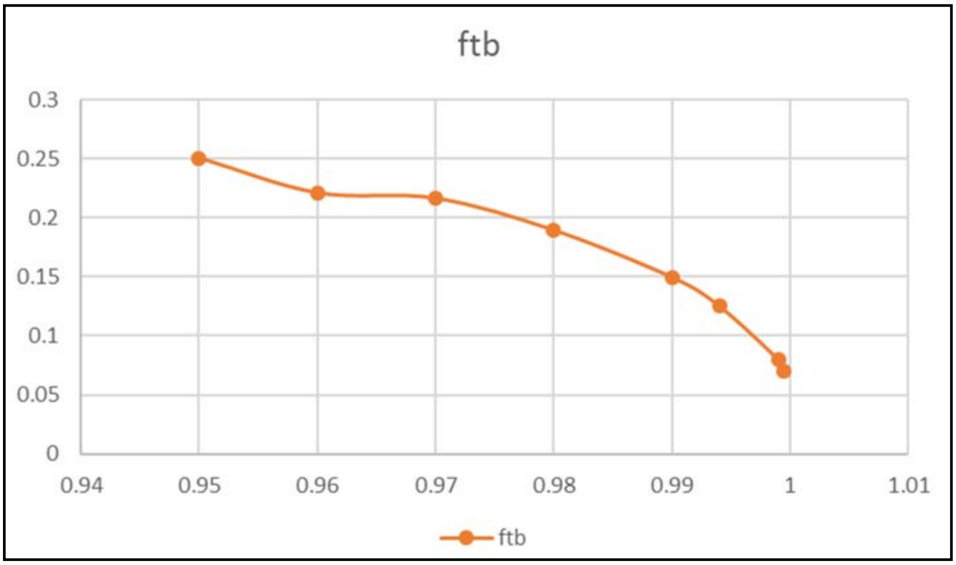

Figure 6 Calculated f_{tB} for changing reliabilities according to ISO 281.

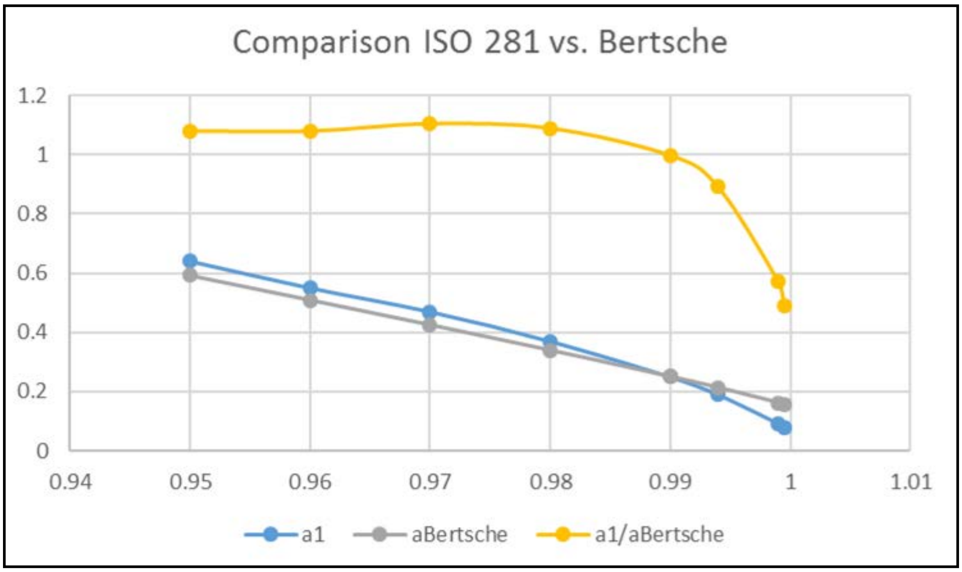

Figure 7 Comparison of a_1 and $a_{Bertsche}$.

So, for the most common range of requested reliability from 90% to 99%, both methods give similar results. For higher probabilities, ISO 281 is more conservative.

***Gear strength per AGMA** 2001-D04.* The second method we investigate is AGMA 2001-D04, "Fundamental Rating Factors and Calculation Methods for Involute Spur and Helical Gear Teeth" (Ref. 7). In the example given, we only focus on root fracture; the same statements can be made for flank failure (pitting).

The aforementioned method features a reliability factor K_R which reduces or increases the allowable root stress number s_t:

$$S_t = \frac{s_{at} Y_N}{S_F K_T K_R} \quad (19)$$

Table 5 shows the values of K_R for different failure probabilities. Since AGMA 2001 does not explicitly calculate an achievable lifetime (although for a given safety factor, the respective lifetime can be calculated using this standard), it is not possible, like for the bearings above, to directly compare the reliability factor with results from Bertsche. So here we use a different approach: we use a commercial software package (*KISSsoft*; Ref. 10) to calculate the achievable lifetime for a given gear set according to AGMA 2001 by varying the design life until we have a safety factor of 1.0. Then we

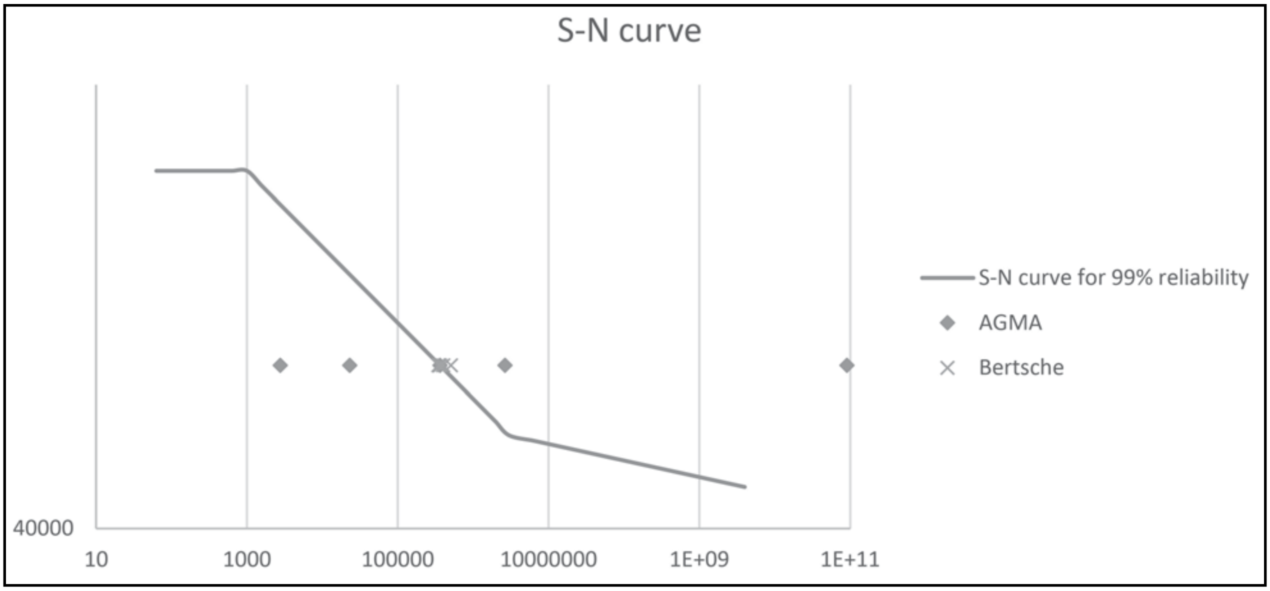

Figure 8 Calculated lifetimes for different probabilities according to AGMA (Ref. 7) and Bertsche (Ref. 2).

use these values to calculate the Bertsche parameters T and t_0. If both methods match, the parameters are nearly constant.

The gear set is defined in Table 4.

For a reliability of 99%, we get an achievable lifetime of 7.8 hours (failure of root on gear 2). The Bertsche parameters for this point are calculated as $T = 11.7$ hours and $t_0 = 7.6$ hours.

Now we switch to 90% probability, which means a reliability factor $K_R = 0.85$ is applied. The achievable lifetime increases to 57.5 hours. The Bertsche parameters are now $T = 77.4$h and $t_0 = 50.3$h. Obviously, AGMA and Bertsche use a different statistical model.

In a second experiment we calculated the lifetime for 90% reliability based on the Bertsche parameters for 99% reliability. This results in a lifetime of 8.7h. To find the corresponding value for $K_{R,}$ we solve (Eq.19) for K_R:

$$K_R = \frac{s_{at} Y_N}{S_F K_T s_t} \tag{20}$$

We change the allowable stress number in the software manually to reach the lifetime of 8.7h. Introducing this value into (Eq. 20), we find $K_{RBertsche} = 0.989$. Doing the same with a reliability of 99.9%, we find $K_{RBertsche} = 1.004$.

Figure 8 shows the resulting lifetimes for different probability levels from 50% to 99.99%, as defined in Table 5 for both AGMA and Bertsche, plotted into the respective S-N curve for 99% reliability. While the AGMA results seem very scattered, the results from Bertsche are in a very small interval. Both results, compared to the measurements in Figure 1, seem too extreme. This, however, cannot be generalized from a single example, so further investigation in this field would make sense to optimize the statistical models of the methods.

Summary

The reliability concept may be used to increase the transparency of the results of strength calculations of gearbox components. The method according to Bertsche is easily applicable, and the results seem reasonable. Compared to the reliability factor a_1 inside ISO 281, there is a very good match of both concepts. However, in comparison to the reliability factor K_R from AGMA 2001, there are large differences. It seems that AGMA exaggerates the effect of the probability level, whereas Bertsche underestimates it. But for a final evaluation, more detailed investigations would be necessary. Looking at the improved information for the engineer coming out of the reliability concept, further work in this field seems well justified.

References

1. Harris, T.A. *Rolling Bearing Analysis*, Edition 4, Wiley Intersience, New York, 2001.
2. Bertsche, B. *Reliability in Automotive and Mechanical Engineering*, Berlin, Heidelberg: Springer Verlag, 2008.
3. ISO 281:2007. Rolling Bearings — Dynamic Load Ratings and Rating Life.
4. ISO 6336:2006. Parts 1–6: Calculation of load capacity of spur and helical gears.
5. DIN 743:2012. Calculation of Load Capacity of Shafts and Axles.
6. DIN 3990:1987. Calculation of Load Capacity of Cylindrical Gears.
7. AGMA 2001-D04. Fundamental Rating Factors and Calculation Methods for Involute Spur and Helical Gear Teeth.
8. Kissling, U. "From the Single Component Safety Factor to the System Reliability Rating," *MPT 2017, Kyoto*, JSME.
9. Bronstein and Semendjajew. *Handbook of Mathematics*, 6th Edition, Harri Deutsch Verlag, 2005.
10. *KISSsoft/KISSsys*; Calculation Programs for Machine Design; *www.KISSsoft.AG.*
11. ISO 16269:2014. Statistical Interpretation of Data.

Dr. rer. nat. Stefan Beermann studied Mathematics and Computer Science in Karlsruhe. In 1996, he went to Zurich to join the gearbox company L. Kissling & Co. AG as product manager for the calculation software KISSsoft. In 1998 he switched to KISSsoft AG as one of its first employees. Today he is CEO of KISSsoft AG, together with the company's founder Dr. Ulrich Kissling.

Germany

OFFICIALLY RELEASES DIN ISO 1328-1:2018-3

Germany has officially released *DIN ISO 1328-1:2018-03*, and thereby has joined the United States, U.K., France and Japan in adopting *ISO 1328-1 Cylindrical gears — ISO system of flank tolerance classification — Part 1: Definitions and allowable values of deviations relevant to flanks of gear teeth*, without modification, as their national standard.

Now the gearing community has a single globally adopted standard for classification of gears by elemental measurements. This standard applies to gears from 5 to 1,000 teeth, diameters from 5 mm up to 15 meters, facewidths from 4 mm to 1.2 meters, normal modules from 0.5 to 70, and helix angles up to 45°. In other words, it applies to practically all cylindrical gears. Its stated goal is to provide "the gear manufacturer and the gear buyer with a mutually advantageous reference for uniform tolerances."

The last ISO TC60/WG2 meeting took place in Milan. Clockwise from the front of the doors are: Amir Aboutaleb (United States), John Rinaldo (United States), Heinz Roehr (DE, Germany), Ryohei Takeda (Japan), Michel Octrue (France), Elisabetta Fava (Italy), Michele Deni (Italy), Massimiliano Turci (Italy) and guest.

"From discussions with members of large companies (Siemens, ZF, Getrag) I got the impression that they really need and appreciate a new globally adopted standard. It makes the dialog between companies or branches of companies worldwide much easier if they can refer to the same rules and definitions. Otherwise there are always discussions about the interpretation of a parameter when the people are not familiar with it," said Heinz Roehr, a VDI committee member for the measurement of gears and gear drives, head of the DIN committee "Terminology and Tolerances," and a member of ISO/TC60 WG2 "Accuracy of Gears."

Formulas in the global standard are provided for:

- Single pitch tolerance, f_{pT}
- Total cumulative pitch (index) tolerance, F_{pT}
- Profile slope tolerance, $f_{H\alpha T}$
- Profile form tolerance, $f_{f\alpha T}$
- Total profile tolerance, $F_{\alpha T}$
- Helix slope tolerance, $f_{H\beta T}$
- Helix form tolerance, $f_{f\beta T}$
- Total helix tolerance, $F_{\beta T}$

There are also annexes covering runout, sector pitch deviation, adjacent pitch difference, and single flank composite testing. This standard not only provides formulas for tolerances, but also includes requirements on how the measured data is to be filtered and interpreted. In the past there was no guidance given on data filtering, and differences in filtering can result in different reported results. This latest edition of *ISO 1328-1*, along with the companion technical report *ISO/TR 10064-1*, should provide all those who measure gears with consistent results.

For the work on *ISO 1328-1:2013* it was very important that Roehr was also a member of VDI.

"Because we have VDI guidelines for the evaluation of modifications of segmented profiles and helices, I supplied the members of the committee with information about these strategies. So they found their way in *ISO 1328-1:2013* and have become an important part of the standard. It also helped that I took care that all definitions were absolutely precise without room for interpretation," Roehr added.

The group is currently working on a tolerance standard for the composite inspection of gears based on (ISO) 2015-2 as well as turning the AGMA 2002 Tooth Thickness Specification and Measurement into an ISO standard.

(*www.iso.org*)

Mahr

APPOINTS DON FOISY DIRECTOR OF OPERATIONS

Mahr Inc. recently announced that **Don Foisy** has been promoted to director of operations to support continued company growth. In his new position, Foisy will be responsible for overseeing the engineering, manufacturing, planning and facilities departments. With seven years of experience at Mahr, Foisy's strong managerial skills and mechanical engineering expertise will help to further enhance the company's standards of operational excellence and commitment to high quality.

"I look forward to the opportunity to work with our entire operations team as we strive to perfect our internal processes to help us meet our company's expanding goals," said Foisy. "We want to foster new ideas and innovative technologies to improve our efficiency in providing market-leading precision metrology solutions. Our focus will continue to be the delivery of high quality products, on-time to our customers to support their growing needs."

He joined the Mahr team in 2011 in the position of design engineering supervisor and was later promoted to engineering manager. With more than 17 years of industry experience, Foisy previously served as a mechanical engineer at John Crane and as a product engineering manager at Dresser-Masoneilan. He has a bachelor's degree in mechanical engineering from New England Institute of Technology. (*www.mahr.com*)

Röhm Products of America

OFFERS COMPREHENSIVE CHUCK REPAIR AND REBUILD SERVICES

To better serve its customers, Röhm Products of America has made significant investments in its ability to offer comprehensive chuck repair and rebuild services at its Suwanee, Georgia-based headquarters, as well as onsite at its customers' manufacturing facilities across the country. In doing so, the company creates a one-stop shop for all chuck service needs.

"When we moved to our new headquarters in 2015," said Adis Malkoć, manager of Röhm's Service Center. "We dedicated a lot of space for our service team, along with new 2-ton and 10-ton cranes for the biggest repair/rebuild jobs. With this investment, we've created a turnkey approach that has been very popular with our customers. We offer the quickest way for shops to install, maintain and repair their workholding devices."

Röhm's engineering staff possesses nearly 50 years of combined experience with the fixturing, equipment and processes necessary for the precision repair and rebuilding of even the largest sized chucks. These same service engineers also provide new customers with installation assistance along with guidance in proper product use and in the development of an optimal preventative maintenance schedule. They also conduct training sessions for products currently in use to keep operator skills and knowledge current.

"It's hard for shops to maintain the level of expertise our specialized team has," noted Service Engineer Doug Thompson. "But after our training, we can ensure that manufacturers have the know-how to keep fixtures in working order until they need to be sent back for periodic rebuilding."

The Röhm Service Center provides rebuild quotes and services that extend the life of valuable products. Most parts needed for these rebuild processes are in stock at the company's Georgia facility, though large, complex or custom fixtures may require parts from the company's German factory. These scheduled rebuilds can also identify worn parts before they fail completely, which results in significant savings for those manufacturers that take preventative maintenance seriously. (*www.rohm-products.com*)

Kitagawa North-Tech

ANNOUNCES NEW REGIONAL SALES MANAGER

Kitagawa North-Tech, Inc. recently announced that **Mike Johnston** has joined the company as regional sales manager. Mr. Johnston's sales territory for Kitagawa NorthTech will include Pennsylvania, Ohio and Indiana of the Great Lakes regions of the USA. He is supporting Kitagawa's offering of workholding which includes standard power chucks, advanced chucks, automated workholding (AJPS), engineered rotational and prismatic workholding solutions, turning and grinding line of steady rests, hydraulic cylinders, grippers and rotary tables.

Johnston will also sell and represent Kitagawa NorthTech's inhouse repair, rebuild and preventative maintenance services. Johnston adds, "Kitagawa NorthTech's Machine Tool accessories such as their Tri-Kote grease for lubricating power chucks and their digital grip force analyzer software and kit for measuring grip force are unique products that every machine shop should use for everyday chuck maintenance, as if you do not know your grip force you cannot optimize your machine tool to produce the maximum amount of parts safely."

Johnston will be servicing and supporting a wide range of customers for the company including: end-users, OEMs, machine tool distributors and cutting tool distributors for the Kitagawa workholding and chuck offering. With over 30 years of metalworking industry experience, Johnston has an extensive and broad background. Throughout his career in metalworking and machining, he has worked in several capacities including: CNC programming, design engineering, applications engineering, machine tool sales and accessories sales, as well as owned a machine shop focused on machining parts for the Medical industry. Most recently Johnston was a regional sales manager for workholding manufacturer ATS Systems.

Johnston resides in Euclid, Michigan and will be report out of Kitagawa NorthTech's headquarters and full-service manufacturing facility for the Americas based in Schaumburg, IL. The Kitagawa NorthTech facility features in-house design, engineering, manufacturing and repair services for workholding.

In addition, Kitagawa North-Tech, Inc. recently announced that **Edward Borsos** has joined the company also as a regional sales manager. Borsos has over 30 years of machining and metalworking industry experience. He will be responsible for supporting and developing channel partners and end-users selling Kitagawa's standard chucks, advanced chucks and engineered rotational and prismatic workholding solutions. Borsos has extensive experience in automotive and oil and gas, as well as general turning and milling workholding applications.

Borsos began his career as a toolmaker and machinist and worked in various supervisory positions at metalworking machine shops and later transitioned into technical workholding sales for MSCI Industrial Supply. In his most recent position he worked in regional sales management for Rohm, German-based workholding company before joining Kitagawa NorthTech.

Borsos will help support and manage projects for the custom engineered solutions business. Kitagawa NorthTech's engineered workholding solutions are supported by an in-house applications engineering team committed to developing custom workholding for turning and prismatic applications. In addition to designing and engineering custom solutions, Kitagawa NorthTech utilizes their in-house design, manufacturing, inspection and testing facility to manufacturer, modify and test components and workholding systems for their customers.

Borsos resides in Waterford, Michigan and will be report out of Kitagawa NorthTech's headquarters and full-service manufacturing facility for the Americas based in Schaumburg, IL. Upon joining the company, Boros adds, "I am excited to join a company with such a rich history in workholding. Kitagawa has always been the gold standard of chucks in the workholding industry. In addition, Kitagawa NorthTech's custom engineered workholding capabilities offer customers superior part-specific machining solutions for turning and prismatic applications."

(*www.kitagawa.us*)

12th International Congress and Expo

CTI Symposium USA

Automotive Transmissions, HEV and EV Drives

14 – 17 May 2018, Novi, MI

www.transmission-symposium.com/usa

PART OF
CTI
AUTOMOTIVE
WEEK
USA

Keynote Speaker

Plenary Speakers Include

Dan Nicholson

Vice President,
Global Propulsion Systems,
General Motors, USA

Denise Gray

President and
Chief Executive Officer,
LG Chem Power Inc., USA

Dr V. Anand Sankaran

Director,
Electrified Powertrain Engineering,
Ford Motor Company, USA

Prof. Dr Uwe Dieter Grebe

Executive Vice President, Global Business
Development, Sales & International
Operations, AVL List GmbH, Austria

Jeremy Holt

President,
Means Industries, USA

Dr Johannes-Joerg Rueger

Executive Vice President,
Robert Bosch GmbH, Germany

Specials

- 2-Day Introductory Seminar
- Pre-Event Networking Reception
- Networking Night on 16 May 2018
- Exhibition
- CTI Test Drive

> **Excellent convergence of leading thinkers who are transforming the future.** Steve Wesolowski, Dana Inc.

> **'Woodstock' for transmissions engineers. The premier get together event.** George Pethon, Allison Transmission

Sponsors

MAGNA

SCHAEFFLER

ad index

DO YOU HAVE SURPLUS GEAR MACHINERY FOR SALE OR AUCTION?

You need to talk to Goldstein Gear Machinery LLC (GGM), of which Michael Goldstein was President and primary buyer and seller at his former company, Cadillac Machinery Co., Inc.

For large departments or whole plants, 100% of the SALE proceeds goes to the owner

GGM is the only one experienced gear machinery expert to get you the highest value. Gear equipment is not like general purpose machinery; they have unique features and capabilities, which only an expert can describe and know to photograph, especially Gleason mechanical bevel equipment, of which GGM is the leading expert.

GGM has over 55 years of experience buying/selling and auctioning gear machinery, with a reputation for knowledge, experience and capability second to none. GGM, and Michael's prior company, Cadillac Machinery, were in a joint venture with Industrial Plants Corp (IPC) in Industrial Plants Ltd (UK) (IPC-UK) and Michael was the primary auction evaluator and organizer for over 10 years. As he tracks every gear auction, worldwide, he has records of what every gear machine is sold for.

Get experience and knowledge working for you

MACHINERY DEALERS NATIONAL ASSOCIATION

www.gearmachineryexchange.com

April 26–28—AGMA/ABMA Annual Meeting 2018 Naples, Florida. The 2018 Annual Meeting combines the expert knowledge of the gear and bearing industries with the latest emerging technologies that influence manufacturers and suppliers. More than 300 executives will gather this April to experience the information-packed week full of top-tier speakers. Members will be connected to innovation and opportunities in the industry with potential to strengthen business connections and relationships. Join AGMA & ABMA for an event that is tailored directly for its members to address trends, successes and future possibilities. For more information, visit *www.agma.org*.

April 30–May 3—OTC 2018 Houston, Texas. The Offshore Technology Conference (OTC) is where the world's energy professionals meet to exchange ideas and opinions to advance scientific and technical knowledge for offshore resources and environmental matters. OTC is the largest global event for the oil and gas sector featuring approximately 2,000 exhibitors and attendees from across the globe. The event provides excellent opportunities for global sharing of technology, expertise, products, and best practices. OTC brings together industry leaders, investors, buyers, and entrepreneurs to develop markets and business partnerships. Technical highlights include updates on world-class projects, offshore renewable energy, the digital revolution, safety and risk management and more. For more information, visit *2018.otcnet.org*.

May 1–3—AGS Manufacturing Training Series – Introduction to Gear Process Engineering Naperville, Illinois. The intensive 3-day course is designed to provide attendees with a comprehensive overview of the fundamentals involved in successful processing of gears for manufacturing. Finding qualified gear process engineers is a common challenge in the gear manufacturing industry and companies are often faced with the need to train internal resources on their own. However, this can be a very long process and can put a strain on existing engineering staff. By utilizing the AGS training experience, trainees can acquire a comprehensive overview of gear processing from leading industry experts; resulting in a skilled process engineer much faster and for far less cost. Upon completing the course, attendees will have processed sample gears, and will fully understand the core principles - preparing them for further on-the-job refinement of their skills. Attendees will also receive an in-depth training manual for future reference on key topics. For more information, visit *www.arvinglobalsolutions.com*.

May 7–10—AWEA Windpower 2018 Chicago, Illinois. Windpower 2018 is the wind industry's premier North American event with wind energy professionals from all over the world gathering in one place. It's the most effective way for attendees to expand their knowledge base and business network. With competitive pricing and stable policy in place, the wind industry is booming. Now the industry can focus on the future and the other drivers that will propel the industry forward through the 2020s. The program will feature speakers with "disruptive" and innovative ideas that will continue to strengthen wind energy's value proposition and challenge the current way we do business. Attendees will hear about how technology advances will continue to lower LCOE, and learn lessons from other industries that are more mature or have experienced similar rapid growth. They will also receive updates on: state policy support, transmission infrastructure efforts, and emerging and growing offtake trends. For more information, visit *www.awea.org*.

May 7–10—AISTech 2018 Philadelphia, Pennsylvania. This event will feature technologies from all over the world that help steel producers to compete more effectively in today's global market. AISTech 2018 provides perspective on the technology and engineering expertise necessary to power a sustainable steel industry. More than 7,000 people are expected to attend AISTech 2018. Along with over 500 exhibiting companies, AISTech 2018 allows attendees to meet face-to-face with key individuals involved in the production and processing of iron and steel. The comprehensive conference schedule includes topics on metallurgy, safety, material handling, energy, maintenance and reliability, lubrication and more. For more information, visit *www.aist.org*.

May 7–11—NPE 2018 Orlando, Florida. NPE2018 provides exclusive access to the innovations, people, processes, science and ideas that are shaping the future of plastics. Attendees will build connections, exchange ideas and explore the largest concentration of machinery, tools, technology and professional training available in today's plastic industry. On the show floor, attendees will meet with the 2,000+ of the world's leading plastic manufacturers and suppliers to gather important information and insights on the latest equipment, products and materials for every phase of plastics production. Focus areas include 3D/4D printing, moldmaking, material science, medical parts, processors and more. For more information, visit *www.npe.org*.

May 14–16—SAE Fundamentals of Modern Vehicle Transmissions Seminar Durham, North Carolina. Starting with a look at the transmission's primary function—to couple the engine to the driveline and provide torque ratios between the two—this updated and expanded seminar covers the latest transmission systems designed to achieve the most efficient engine operation. Current designs, the components and subsystems used, their functional modes, how they operate, and the inter-relationships will be discussed. For more information, visit *www.sae.org/learn/content/99018/*.

May 14–17—CTI Symposium USA Novi, Michigan. This event, organized by the German Car Training Institute (CTI), focuses on the latest technical innovations in automotive transmissions, hybrid and alternative drivetrains with experts and suppliers from the United States, Asia and Europe. The symposium will examine current debates on economics, politics and the environment. Topics will be examined from the perspective of technology, customers and the context of market success. Keynote speakers include Dan Nicholson, vice president, global propulsion systems, General Motors, USA, Dr. V. Anand Sankaran, director, electrified powertrain engineering, Ford Motor Company, Dr. Johannes-Joerg Rueger, executive vice president, Robert Bosch GmbH and more. For more information, visit *www.transmission-symposium.com/usa*.

May 22–24—Advanced Methods and Best Practices for Gear Process Engineering Naperville, Illinois. The intensive three-day course is a follow-up to "An Introduction to Gear Process Engineering" conducted by Arvin Global Solutions (AGS). It is designed to provide attendees with a solid understanding of the methods and best practices for the successful processing of gears for manufacturing. In this course, the attendees will learn: minimizing and compensating for heat treat distortion with machining methods, critical quality procedures to include in the process, expert tips and tricks to review and refine a process for achieving optimal productivity and cost savings and much more. For more information, visit *www.arvinglobalsolutions.com*.

The Greatest Show & Tell on Earth

It's Perfectly Acceptable to Bring Work Home with You for Maker Faire

Matthew Jaster, Senior Editor

If you consider yourself a manufacturer, engineer, gearhead, inventor or simply a technophile, then you should consider a trip to Maker Faire this year. Maker Faire is a family-friendly showcase of invention, creativity, and resourcefulness. The event is described by its creators as "part science fair, part county fair and part something entirely new."

Bottom line, it's an eye-popping, cerebral celebration of the Maker Movement — individuals who create and market DIY products that are recreated and assembled using unique supplies and materials typically developed in garages or basements with limited manufacturing resources. It can be argued that the gadgets, robots, drones, simple machines and wearable devices created at Maker Faire events are somewhat responsible for bringing engineering mainstream.

The Statistics Don't Lie

Maker Faire celebrated 221 Faires in 2017 and engaged more than 1.58 million attendees globally in 45 countries around the world. The 12th annual Maker Faire Bay Area welcomed some 1,200 Makers and 125,000 attendees. World Maker Faire New York, the East Coast flagship event, has grown in eight years to 750+ Makers and 90,000 attendees.

"Eight years in with our partner, the New York Hall of Science, bringing World Maker Faire to the East Coast, and the enthusiasm and engagement from the maker community is still strong," said Dale Dougherty, co-founder of Maker Faire and CEO of Maker Media. "It's a testament to the maker culture and people wanting to connect around something that satisfies their deeper curiosity for exploring and problem-solving, and putting their talents and ingenuity to work. They know they will find these connections and opportunities at Maker Faire."

All photos courtesy of Maker Faire.

Unique Tech Trends

So what types of projects have been displayed at Maker Faire events?

Users can create their own robots and motion control using Arduino, an open-source electronics platform based on easy-to-use hardware and software. Arduino boards are able to read inputs - light on a sensor, a finger on a button, or a Twitter message - and turn it into an output - activating a motor, turning on an LED, publishing something online. You can tell your board what to do by sending a set of instructions to the microcontroller on the board. (*www.arduino.cc/en/Guide/Introduction*)

Kinetic Steam Works, a Bay Area collective dedicated to steam powered kinetic art and education, came together in 2005 to explore, restore and share the artifacts of clockwork modernity. KSW is a small group of industrial artists building with steam that created a project where large wooden gears were used to drive a 110-year-old automatic pencil sharpener. (*www.youtube.com/watch?v=CS6v8sQ34sQ&feature=youtu.be*)

Fablab O Shanghai presented its "Dishu Machine" a robot capable of making large paintings of Chinese poetry using water on the ground. The machine is a composition of 3D printed and laser cut materials and employs a combination of stepper motors, a water pump, Arduino Uno × CNC Shield and a custom G-code transcoder. (*http://archive.fabacademy.org/archives/2017/fablabshangai/students/190/week9a.html*)

The Future of Engineering & Manufacturing

While these unique and clever projects might entice our readers to sit in the garage for the next three weeks and invent something, the truth is that 50 percent of Maker Faire attendees bring their children. This is the key takeaway from an event like Maker Faire. We need the next generation of engineers, manufacturers and scientists to get their hands dirty and create the technologies of the future. This passion for STEM activities can start right here.

To find the next Maker Faire event near you, visit *https://makerfaire.com/map/*.